UNIVERSITY OF TASMANIA

Improved miniaturised solid phase extraction

by

Esme Candish PhD

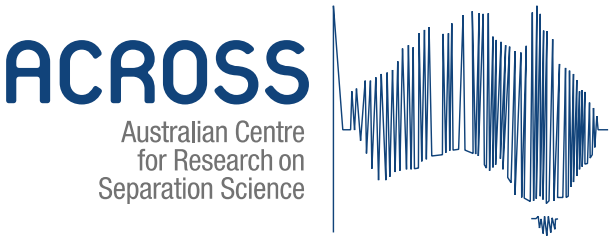

School of Physical Sciences
University of Tasmania
June 2015

Declaration

This thesis contains no material which has been accepted for a degree or diploma by the University or any other institution, except by way of background information and duly acknowledged in the thesis, and to the best of the my knowledge and belief no material previously published or written by another person except where due acknowledgement is made in the text of the thesis, nor does the thesis contain any material that infringes copyright.

The publishers of the papers in this thesis hold the copyright for that content, and access to the material should be sought from the respective journals. The remaining non published content of the thesis may be made available for loan and limited copying and communication in accordance with the Copyright Act 1968.

The research associated with this thesis abides by the international and Australian codes on human and animal experimentation, the guidelines by the Australian Government's Office of the Gene Technology Regulator and the rulings of the Safety, Ethics and Institutional Biosafety Committees of the University

Esme Candish
June 2015

Acknowledgements

Throughout my PhD candidature I have been assisted, advised and guided by my three supervisors Prof. Emily Hilder, A/Prof. Robert Shellie and Dr. Andrew Gooley. I am very grateful to them for their support throughout the project and for providing me with the means to learn, conduct experiments and publish my work. I would like to acknowledge the support of SGE Analytical Science and Trajan Scientific and Medical for providing me with funding, unique networking opportunities as well as opportunities to gain experience by attending conferences to meeting interesting scientists.

I offer special acknowledgement to all the friends that I have made during this roller coaster of a journey. I am very grateful to Han-Jürgen Wirth for research guidance, support and friendship throughout my candidature. I am especially thankful to Artchie Kazarian for continued love, support, food and the occasional hard words of perspective. A super duper special thanks to my very bestest friends Tim (TJ) Causon and Ryan Nai, Mari Egeness, Eli Fornells Vernet (1/2 of Smeli), Joan Marc Cabot Canyelles, Amin Khodabandeh, Anton Peristyy, Daniel Gostoettenmayr, Naama Karu and Laura Parsley for support, chats and laughs. Also to the students, post docs and staffs in ACROSS and the Department of Chemistry for offering their assistance and friendships throughout my candidature. Thank you for making my working life an enjoyable one. Everything is and was awesome!

Last but not least, I would like to thank my family for the constant support that they have given me.

Statement of co-authorship

The following people and institutions contributed to the publication of work undertaken as part of this thesis:

Esme Candish, School of Physical Sciences, UTAS = Candidate

Robert A. Shellie, School of Physical Sciences, UTAS = Author 1

Hans-Jürgen Wirth, Trajan Scientific and Medical = Author 2

Andrew Gooley, Trajan Scientific and Medical = Author 3

Emily F. Hilder, School of Physical Sciences, UTAS = Author 4

Peter A. Dawes, EPrep Pty. Ltd. = Author 5

Marion Gaborieau, Molecular Medicine Research Group, UWS =Author 6

Thomas Rodemann· Central Science Laboratory, UTAS = Author 7

Author details and their roles:

Paper 1 <Recent advances in the diverse selectivity's, formats and applications of organic porous polymer monoliths for sample preparation>

Located in chapter 1

Candidate was the primary author (65%) with author 1 (15 %). Author 3 and 4 (10% respectively) assisted with refinement and presentation.

Paper 2, < A simplified approach to direct SPE-MS >

Located in chapter 2

Candidate was the primary author (65%) with author 2 (5%). Author 3, 4 and 5 (10% respectively) contributed to the idea, and its formalisation and development. Author 2, 2, 4 assisted with refinement and presentation

Paper 3, <A comprehensive evaluation of highly crosslinked poly(divinyl benzene) and hypercrosslinked polymer monoliths for solid phase extraction>

Located in chapter 3

Candidate was the primary author (70%) with author 2 (15%). Author 1,3,5 (5% respectively) contributed to the idea, and its formalisation and development. Author 1, 3, 4 assisted with refinement and presentation

Paper 4, < Surface modified monolithic poly(divinyl benzene) restricted access adsorbents and their application for miniaturized solid phase extraction>

Located in chapter 4

Candidate was the primary author (70%) with author 4 (15%). Author 1 (10%) and author 3 (5%) contributed to the idea and its formalisation and development. Author 6, 7 provided assistance with specialised instrumentation. Author 1, 3 4, 6 assisted with refinement and presentation

We the undersigned agree with the above stated "proportion of work undertaken" for each of the above published (or submitted) peer-reviewed manuscripts contributing to this thesis:

Signed:

Signed:

Emily Hilder
Supervisor
School Of Physical Science
University of Tasmania

John Dickey
Head of School
School of Physical Science
University of Tasmania

Date: 14/06/2015

List of publications and presentations

1. Candish. E., Shellie, R. A. Gooley, A., & Hilder, E. F. 2013. Recent advances in the diverse selectivity's, formats and applications of organic porous polymer monoliths for sample preparation. *J. Chrom. A. Submitted* (Chapter 1)

2. Candish. E. Gooley, A., Wirth, H-J., Dawes, P. A., Shellie, R. A. & Hilder, E. F. 2012. A simplified approach to direct SPE-MS. *J. Sep. Sci*. 35, 2399–2406. (Chapter 2)

3. Candish, E. Gooley, A., Shellie, R. A. & Hilder, E. F. 2014. A comprehensive evaluation of highly crosslinked poly(divinyl benzene) and hypercrosslinked polymer monoliths for solid phase extraction. *J. Chrom. A. Submitted* (Chapter 3)

4. Candish, E. Shellie, R. A. Gooley, A., Gaborieau, M., Rodemann, T., & Hilder, E. F. Hydrophilic monolithic poly(divinyl benzene) restricted access adsorbents and their application for miniaturized solid phase extraction. *J. Chrom. A. In preparation* (Chapter 4)

5. Candish. E. Gooley, A., Shellie, R. A. & Hilder, E. F. 2014. Eliminating chromatography? Screening metabolites with µSPE-MS. *G.I.T. Laboratory Journal, Europe,* 18(3-4), 32-34.

6. Candish. E. Gooley, A., Wirth, H-J., Shellie, R. A. & Hilder, E. F. 2014. Rapid sample preparation using miniaturized solid phase extraction (oral presentation*). 5th Australia New Zealand Micro and nanofluidics symposium.* Hobart. Australia.

7. Candish. E. Gooley, A., Wirth, H-J., Shellie, R. A. & Hilder, E. F. 2014. Rapid sample preparation using miniaturized solid phase extraction (oral presentation*). 13th Hyphenated Techniques in Chromatography.* Bruges. Belgium.

8. Candish. E. Gooley, A., Wirth, H-J., Dawes, P. A., Shellie, R. A. & Hilder, E. F. 2012. Rapid sample preparation protocols using microextraction by packed

sorbent (oral presentation). *14th International Symposium on Extraction Technologies.* Messina. Italy.

9. Candish. E. Gooley, A., Wirth, H-J., Shellie, R. A. & Hilder, E. F. 2015. Miniaturized solid phase extraction for rapid sample preparation (poster presentation). *ASMS Conference on Security and Forensic Applications of Mass Spectrometry*. Clearwater. USA.

10. Candish. E. Hon, W. B. Gooley, A., Wirth, H-J., Shellie, R. A. & Hilder, E. F. 2014. Microsample preparation devices for filtration, digestion and extraction of whole blood (poster presentation). 62nd ASMS Conference on Mass Spectrometry and Allied Topics. Baltimore. USA.

11. Candish. E. Gooley, A., Wirth, H-J., Shellie, R. A. & Hilder, E. F. 2013. High surface area polymer monoliths as adsorbents for solid phase extraction (poster presentation). 40th HPLC. Hobart. Australia.

12. Candish. E. Gooley, A., Wirth, H-J., Dawes, P. A., Shellie, R. A. & Hilder, E. F. 2013. At-line approach to direct solid phase extraction - mass spectrometry (poster presentation). 61st ASMS Conference on Mass Spectrometry and Allied Topics. Minneapolis. USA.

13. Candish. E. Gooley, A., Wirth, H-J., Dawes, P. A., Shellie, R. A. & Hilder, E. F. 2013. At-line approach to direct solid phase extraction - mass spectrometry (poster presentation). 24th Biannual Conference Australia and New Zealand Society for Mass Spectrometry. Parkville. Victoria.

14. Candish. E. Gooley, A., Wirth, H-J., Dawes, P. A., Shellie, R. A. & Hilder, E. F. 2011. Rapid sample preparation and direct validation of codeine urinary metabolites using eVol-MEPS (poster presentation). 11th Asia Pacific International Symposium on Microscale Separations and Analysis. Hobart, Australia

Abstract

The thesis focuses on the development of miniaturised solid phase extraction (SPE) technologies for the rapid and effective processing of complex biological samples prior to mass spectrometry (MS) analysis.

The first section focuses on the format and operation of miniaturised solid phase extraction devices. The existing technology was queried and improved for a more efficient operation. The miniaturised SPE technology, microextraction by packed sorbent (MEPS), was explored as a representative format due to ease of operation. A superior format of MEPS was developed that incorporates a two-way valve in the syringe barrel for efficient sample and solvent introduction to the adsorbent bed. Controlled directional flow (CDF)-MEPS allows fluid to be introduced directly into the syringe barrel, bypassing the adsorbent bed entirely. Matching extraction workflows demonstrated a reduction in carryover from 65% for conventional MEPS to only 1% for CDF-MEPS. The developed technology was directly hyphenated with electrospray ionisation (ESI)-MS and sharp, concentrated sample bands were revealed.

The second section of this thesis explores the concept of organic polymer monolith adsorbents for improved miniaturised SPE. Polymer monoliths are widely described as adsorbents for SPE but appropriate characterisation of physical characteristics is rarely explored to probe any observed advantages and disadvantages over alternative adsorbents. Fabrication of large surface area adsorbent involved a high percentage of the crosslinking monomer, divinyl benzene (DVB), or the hypercrosslinking of pre-formed polymer. Frontal analysis studied the adsorption of probes; anisole, phenol and cortisone. Extraction performance was compared with conventional polymer particulate adsorbents. The polymer monolith adsorbents demonstrated a clear advantage for the

small probes, as a high extraction performance (high recovery) could be achieved independent of flow rate. Limited retention of cortisone was seen for both polymer monolith adsorbents as the surface area was predominantly provided by micropores inaccessible to the larger probe cortisone.

The size exclusion mechanism of the microporous large surface area poly(DVB) was exploited as it presented a physical barrier restricting proteins from accessing the adsorbent's internal surface. A hydrophilic layer of poly(ethylene glycol) methacrylate (PEGMA) was grafted to the residual vinyl groups of the poly(DVB) and their suitability as restricted access materials was explored. PEGMA monomers with glycol chain lengths of M_n 360 and 950 were studied. The external hydrophilic layer was delicately balanced to prevent protein binding while preserving the hydrophobic capacity and rapid analyte mass transfer. Sharp breakthrough curves confirmed that both hydrophobic capacity and rapid analyte mass transfer were maintained for poly(DVB)-*g*-PEGMA$_{950}$, while the adsorbent displayed a substantial reduction in protein binding. Ibuprofen was extracted from human plasma (diluted 20% v/v), using both poly(DVB) and poly(DVB)-*g*-PEGMA$_{950}$. The extracts were analysed by at-line ESI-MS. The sample from prepared with the biocompatible poly(DVB)-*g*-PEGMA$_{950}$ provided extracts with reduced protein content resulting in a more sensitive and improved at-line ESI-MS analyses.

Table of content

List of abbreviations

Acronym	Representation
AAm	acylamide
AIBN	2,2'-azo-bis-isobutironitrile
APPBA	3-acrylamidophenylboronic acid
ATR-FTIR	attenuated total reflectance fourier transform infrared
BAEE	N-α-benzoyl-L-arginine ethyl ester
BET	Brunauer, Emmett and Teller
BIN	barrel insert needle
BMA	butyl methacrylate
BSA	bovine serum albumin
CIM®	convective interactive media
CDF	controlled directional flow
cMWNT	carboxylated multi-wall carbon nanotube
CP-MAS NMR	cross-polarization magic angle spinning nuclear magnetic resonance
DART	direct analysis real time
DCE	1, 2-dichloroethane
DVB	divinyl benzene
EDA	ethylene dimethacrylate
EDMA	ethylene glycol dimethacrylate
ESI	electrospray ionization
GMA	glycidyl methacrylate
GlyMA	glycerol monomethacrylate
HEMA	2-hydroxyethyl methacrylate
HPLC	high performance liquid chromatography
HSA	human serum albumin
IMER	immobilised enzyme reactor
ISEC	inverse size exclusion chromatography
LLE	liquid-liquid extraction
MS	mass spectrometry
META	[2-(methacryloyloxy)ethyl] trimethylammonium chloride
MBA	N,N′ methylenebisacrylamide

Acronym	Representation
MAA	methacrylic acid
MALDI	matrix assisted laser desorption ionisation
MEPS	microextraction by packed sorbent
MYO	myoglobin,
NAS	N-acryloxysuccinimide
NLDFT	non-localized density functional theory
PE	polyethylene
PEG	poly(ethylene glycol)
PEGDA	poly(ethylene glycol) diacrylate
PEGMA$_{360}$	poly(ethylene glycol) methacrylate M_n 360
PEGMA$_{950}$	poly(ethylene glycol) methyl ether methacrylate M_n 950
PETRA	pentaerythritol triacrylate
PDMS	polydimethylsiloxane
RAM	restricted access material
SEM	scanning electron microscopy
SPE	solid phase extraction
SBSE	stir bar sorptive extraction
SPME	solid phase microextraction
Sty	styrene
TEGMA	triethylene glycol dimethacrylate
TOF	time of flight
UV	ultraviolet
VAL	4,4-dimethyl-2-vinyl azlactone
VBC	4-vinylbenzyl chloride
VLP	N-vinylpyrrolidone

Preface

The analysis of exogenous and endogenous compounds and their respective metabolites in biological matrices such as urine, serum, plasma, whole blood or saliva is a necessity for many fields of science. These fields, which include drug development, forensic analysis and the monitoring of therapeutics medications, drugs of abuse and diagnostic biomarkers, require qualitative and often quantitative determination of a broad range of target analytes. A typical pre-analytical workflow first involves sample collection, next the sample must be prepared for analysis, typically some type of separation and detection, and finally the data must be interpreted. The last decade has seen a number of improvements in the analytical phase of the workflows but it has been the improvements in mass spectrometry (MS) instrumentation where the impact has been most significant. MS enables highly selective and sensitive analyses with sensitivities routinely lower than parts per billion (ppb) [1]. For assays targeting only a small number of pre-defined analytes it becomes feasible to eliminate the bench-top chromatograph from the analytical workflow to facilitate a rapid analytical outcome.

Eliminating the bench-top chromatograph from the analytical workflow also permits the potential to realise at-line analysis using MS instrumentation with the longer term objective of point-of-test analysis with portable or fieldable formats of MS instrumentation such as the 908 Devices M908 and Microsaic 4000 MID. Bringing the laboratory to a patient for point-of-care testing and diagnostics either, within a clinic or even at a patient's home, initiates customised healthcare scenarios; such as rural and remote communities [2]. However, the matrix components of complex biological samples remain the "Achilles' Heel" of an MS analysis [3]. Matrix components complicate data, foul analytical instruments, and significantly suppress ionisation,

reducing assay sensitivity and selectivity. Highly effective sample preparation becomes critical for fast and accurate on-site MS analysis to be achieved, but the required combination of technologies to couple sample preparation with MS analysis has not yet been achieved. Sample preparation technologies must be developed that are, not only reliable but reproducible and simplified, particularly in the decentralised laboratory environment.

The basic principle of sample preparation is to selectively enrich the analyte in a single liquid or a solid phase for manipulation. Solid-liquid approaches are generally more robust due to the practicalities of operation. A solid phase can be packed into various embodiments (columns, cartridges, disks) and the liquid phase can be percolated through the solid phase adsorbent bed. Today, the exhaustive solid phase extraction (SPE) cartridge formats are universally adopted as one of the most reliable and robust sample preparation processes available, Agilent's BondElut®, Water's Oasis® and Phenomenex's Strata® are standard consumables in many laboratories. However, they are largely incompatible with on-site analysis as the workflow(s) are time intensive, highly laborious and often require significant volumes of harmful organic solvent [4]. To circumvent the limitations of traditional SPE one logical extension is to miniaturise the whole SPE process; modern analytical instruments are certainly sensitive and selective enough to enable routine ppb analysis.

One successful implementation of miniaturised SPE is in the field of proteomics where peptides generated from pure proteins are concentrated using SPE pipette tips, here a small mass of sorbent material is encased in a disposable polypropylene pipette tip. Peptide digests are easily manipulated with a standard laboratory autopipette, peptides are extracted from the salty digest solution and eluted in volumes less than 1 µL directly

onto a targets plate for matrix assisted laser desorption ionisation time of flight MS (MALDI-TOF) [5, 6]. This technique was universally adopted and subsequently many laboratories went on to develop their own particular version of this miniatuirised SPE pipette tip technology [7-9].

Despite successful adoption by MALDI-TOF MS laboratories, interfacing the pipette tip SPE embodiment directly with electrospray ionisation (ESI) remains a practical challenge and additional hardware is required [10, 11]. An alternative format for miniaturised SPE is microextraction by packed sorbent (MEPS) [12]. This technology originally described the addition of standard SPE adsorbents into the barrel of an analytical syringes but was subsequently modified in the commercial embodiment where the adsorbent was embedded in a modified analytical syringe needle that houses approximately 2-4 mg of the SPE adsorbent (**Figure 1**). The modified needle can be inserted into a conventional analytical syringe to realise the extraction, washing and elution steps of an SPE method. The stainless steel needle format enables clean sample effluent to be efficiently infused into an ESI source using a simple zero dead volume union. Unlike the pipette tip based SPE, which is single use extraction technology, MEPS has been developed to be reusable.

Figure 1. The modified syringe needle and the MEPS device.

Using a miniaturised SPE approach can maximise the efficiency of the extraction and obtaining a sensitive assay becomes possible if a high analyte recovery and low sample

carryover are achieved. In the pursuit of high analyte recovery and increased assay sensitivity the vast majority of the MEPS publications demonstrate considerable effort to optimise each component of the sample preparation workflow [13-16]. Unfortunately, miniaturised exhaustive SPE technologies, such as MEPS, present significant operational shortcomings that necessitate these lengthy extraction optimisation protocols (relative to the time required for the extraction). The shortcomings stem from the fundamental format of the technology that dictates the mode of operation. For traditional SPE devices the fluid makes only a single pass of the adsorbent bed; fluid is applied to the top of the adsorbent bed and percolated through the device using positive pressure or vacuum. The operation of miniaturised MEPS SPE embodiment is distinctly different as the flow of fluid is bi-directional. To aspirate, the plunger is withdrawn creating a negative pressure drawing the fluid into the device and through the adsorbent bed. To dispense the plunger is pushed down, resulting in the fluid making a second pass through the adsorbent bed prior to being expelled out the needle. The principles of normal partitioning equilibrium ultimately dictate a diminished recovery that reduces the sensitivity of the assay. The high amount of analyte remaining on the adsorbent bed must be eliminated for reuse and extensive washing protocols must be developed to reuse the adsorbent bed. These precautionary steps have been largely successful but they add steps to both the sample preparation and the optimisation workflows, increasing the sample preparation time [17].

A second constraint of miniaturised SPE technology is backpressure limitations of the devices that necessitate use of a highly permeable adsorbent bed. Conventionally, large diameter porous particulate adsorbents on the order of 40-100 µm are employed to provide adequate bed permeability [18]. This is problematic because large diameter particles lead to slow diffusion-driven mass transfer as the liquid phase moves though

the interstitial voids between the packed particles. Analyte mass transfer is slow and considerable time is required for the analyte to interact with the adsorbent bed. If equilibrium is not achieved the reduced assay efficiency is exposed by a diminished recovery and a high sample carryover, this occurrence is common when using higher flow rates. Unfortunately, reducing the flow rate can dramatically increase the time required for analysis. To overcome these limitations extensive protocols can be developed which involve optimising the operational flow rate [19]. If miniaturised MEPS SPE is to be routinely adopted, adsorbents that present structural morphologies more suited towards rapid and highly efficient sample preparation are required.

There are four essential design considerations underlying the development of new SPE adsorbent phases. First, as mentioned above is the interaction between the adsorbent bed and analyte should be efficient and largely independent of the operational flow rate enabling high-throughput without compromising assay sensitivity [20]. Second, the adsorbent should be highly permeable to enable the fast flow of fluid through the bed for rapid and high through-put sample processing, Third, the adsorbent should retain a high capacity for the analyte(s) of interest and a large, interactable surface is critical for achieving maximum sensitive assay [20]. Finally, the application of highly complex biological sample matrices to the adsorbent bed should not foul the cartridge as this subsequently diminishes sample preparation performance [21].

The unique structural architecture of porous organic polymer monoliths (known hereafter as polymer monoliths) is highly appealing for SPE. Structurally, the material is composed of a porous interconnected network of fused microglobules. The microglobules possess a highly crosslinked non-porous core therefore any interactable surface is accessible by a small diffusion distance which enables high flow rates without

compromising the extraction efficiency [22]. In addition, the presence of the precipitant or the pore forming solvent in the polymerisation mixtures inherently provides the resultant adsorbents with macroporous (>50 nm) cavities or voids for highly permeable fluid flow [23]. Consequently, polymer monoliths have been extensively explored as adsorbents for sample preparation [24-26] .

While polymer monoliths satisfy two of the qualifying criteria for SPE adsorbents the surface area of these materials is generally substantially smaller than particulate materials and monolithic silica adsorbents, where surface areas of 300-1000 $m^2 g^{-1}$ are common. In addition, the approaches to fabricate large surface area polymer monolithic adsorbents typically incorporate highly hydrophobic monomers. The hydrophobic adsorbent beds are often subject to non-specific protein interactions that lead to adsorbent fouling and reduced sample preparation efficiency. If these materials are to be adopted into routine analysis these shortcomings must be addressed, the performance must be understood and superiority over existing alternatives clearly demonstrated.

Scope of this thesis

The goal of this thesis is to develop a sample preparation approach capable of being interfaced directly with MS analysis for at-line analysis. For this to be realised the inherent problems of miniaturised SPE formats must be overcome to provide a technology which does not require extensive optimisation protocols. Three distinctly separate limitations must be addressed to realise the goals of this dissertation. First, the device itself must be redesigned to address the flow path of not only the sample but the wash and elution buffers. Second, the extraction efficiency must be independent of the extraction flow rate. This necessitates that the adsorbent bed must be carefully re-

designed to meet this requirement. Finally, for improved assay sensitivities biocompatible absorbents will be developed to improve the extraction of target analytes from complex biological matrices such as plasma or whole blood.

The first chapter of this thesis evaluates the broad potential of polymer monoliths for miniaturised sample preparation to reveal the limitations and necessary future developments of this field. The second chapter of this thesis deals with improving the miniaturised SPE device to provide a suitable format for polymer development. The approach investigates the incorporation of a simple “push-pull” valve into the syringe to provide control over the application of the fluid to the adsorbent bed. The technology will be implemented for at-line ESI-MS applications. The third chapter examines the adsorbent bed for fast and efficient extractions. Polymer monoliths, which display large surface area, will be investigated and characterised to evaluate their suitability for high capacity extractions. The final chapter investigates approaches to fabricate high capacity biocompatible adsorbents for more efficient sample preparation of highly complex biological fluids.

References

[1] Hopfgartner, G., Bourgogne, E. *Mass Spectrom. Rev.* 2003, *22*, 195–214.

[2] Tirimacco, R. *Clin Biochem Rev* 2010, *31*, 75–80.

[3] Taylor, P. J. *Clin Biochem* 2005, *38*, 328–334.

[4] Pawliszyn, J. *Anal. Chem.* 2003, *75*, 2543–2558.

[5] Gobom, J., Nordhoff, E., Mirgorodskaya, E., Ekman, R., Roepstorff, P. *J. Mass Spectrom.* 1999, *34*, 105–116.

[6] Pluskal, M. G. *Nat. Biotechnol.* 2000, *18*, 104–105.

[7] Zhang, Y., Kang, X., Chen, L., Pan, C., Yao, Y., Gu, Z.-Z. *Anal. Bioanal. Chem.* 2008, *391*, 2189–2197.

[8] Miyazaki, S., Morisato, K., Ishizuka, N., Minakuchi, H., Shintani, Y., Furuno, M., Nakanishi, K. *J. Chromatogr. A* 2004, *1043*, 19–25.

[9] Altun, Z., Skoglund, C., Abdel-Rehim, M. *J. Chromatogr. A* 2010, *1217*, 2581–2588.

[10] Henion, J. D., Kurz, T. U.S. Patent No. 8,546,752. 2013.

[11] Huang, Y.-Q., You, J.-Q., Yuan, B.-F., Feng, Y.-Q. *Analyst* 2012, *137*, 4593.

[12] Abdel-Rehim, M. *J. Chromatogr. B* 2004, *801*, 317–321.

[13] Chaves, A. R., Leandro, F. Z., Carris, J. A., Queiroz, M. E. C. *J. Chromatogr. B* 2010, *878*, 2123–2129.

[14] Gonçalves, J., Mendes, B., Silva, C. L., Câmara, J. S. *J. Chromatogr. A* 2012, *1229*, 13–23.

[15] Kaur, R., Rani, S., Malik, A. K., Aulakh, J. S. *J. Sep. Sci.* 2014, *37*, 966-973.

[16] Mendes, B., Silva, P., Mendonça, I., Pereira, J., Câmara, J. S. *Talanta* 2013, *116*, 164–172.

[17] Miyaguchi, H., Iwata, Y. T., Kanamori, T., Tsujikawa, K., Kuwayama, K., Inoue, H. *J. Chromatogr. A* 2009, *1216*, 4063–4070.

[18] Poole, C. F., Gunatilleka, A. D., Sethuraman, R. *J. Chromatogr. A* 2000, *885*, 17–39.

[19] Prieto, A., Schrader, S., Möder, M. *J. Chromatogr. A* 2010, *1217*, 6002–6011.

[20] Simpson, N. J. K. *Solid-Phase Extraction*; CRC Press, 2000.

[21] Li, Y., Lee, M. L. *J. Sep. Sci.* 2009, *32*, 3369–3378.

[22] Svec, F., Tennikova, T. B., Deyl, Z. *Monolithic Materials*; Elsevier, 2003.

[23] Buchmeiser, M. R. *Polymer* 2007, *48*, 2187–2198.

[24] Svec, F. *J. Chromatogr. B* 2006, *841*, 52–64.

[25] Potter, O. G., Hilder, E. F. *J. Sep. Sci.* 2008, *31*, 1881–1906.

[26] Namera, A., Nakamoto, A., Saito, T., Miyazaki, S. *J. Sep. Sci.* 2011, *34*, 901–924.

1. Literature review: recent advances and future perspectives for the design and application of porous organic polymer monoliths for sample preparation

1.1. Introduction

Increasing importance is being placed on the processes of preparing a crude sample for analysis since sample preparation often influences identification, confirmation and quantification of the analyte. Sample preparation is a umbrella term used to describe the procedures of modifying a sample from its original format to one that is suitable for analysis [1]. There are three primary objectives of sample preparation; (1) extraction of analytes from interfering matrix components for enhanced assay selectivity, (2) enrichment of low concentration analytes to increase assay sensitivity and (3) conversion of the analyte to a form that is suitable for analysis, such as a chromatographic separation and detection. Sample preparation processes are generally considered the most labour-intensive, time-consuming and error-prone steps in analytical workflows, often consuming more than 80% of the total analysis time [2-4].

The basic principle of sample preparation is to localise (and enrich) the analyte in a single liquid or a solid phase for manipulation. Solid-liquid approaches are generally considered more robust due to the practicalities of operation and the ability to automate [2]. A solid phase can be packed into various embodiments (columns, cartridges, disks, pipette tips) and the liquid phase can be percolated through the solid phase adsorbent bed. The morphology of the adsorbent phase can play an integral role in the sample preparation efficiency. In this context efficiency is defined as recovery, enrichment

factor, or percentage of analyte conversion. Particulate-based adsorbents are routinely employed but upper pressure limitations of sample preparation devices necessitates the use of large diameter porous particulate adsorbents on the order of 40-100 µm to provide adequate bed permeability [5]. This is problematic because the vast majority of the interactable surface of these large diameter particles is provided by the internal network of pores; this leads to slow diffusion-driven mass transfer as the liquid phase moves though the interstitial voids between the packed particles. Considerable time is required to achieve equilibrium between the analyte and the adsorbent bed and flow rates that are not optimal often result in reduced assay efficiency. When the assay is miniaturised or the sample is limited the pursuit of highly efficient sample preparation is increasingly important for assay sensitivity.

Considerable attention has been placed on the development of adsorbents that present structural morphologies more suited towards rapid and highly efficient sample preparation. Of the contenders porous monoliths are perhaps the most widely investigated, these adsorbents can be fabricated from either silica or organic polymer based materials. However, the ease of synthesis and diversity of functionality of the organic polymer monoliths has lent them more towards sample preparation than the silica counterparts [6, 7]. Consequently, the discussion will focus solely on organic polymer monoliths henceforth referred to as polymer monoliths. The benefits of polymer monoliths and their advantageous physical properties are described herein.

1.2. Polymer monoliths

Polymer monoliths were first introduced as an alternative to particulate-based chromatographic stationary phases for high performance liquid chromatography (HPLC) in the late 1980’s when Hjerten pondered the possibility of designing a single

piece of continuous sorbent bed *in situ* using bulk polymerisation [8]. Significant pioneering work undertaken by Svec and Fréchet in the 1990's further laid the foundation for introduction and development of polymer monoliths in separation science [9, 10]. Visually these materials appear as a macroporous (pores > 50 nm) series of interconnected clustered microglobules (typically 100s of nanometers in diameter) cross-linked together as a single rigid piece **(Figure 1.1)**. Polymer monoliths have been predominantly explored as stationary phases for HPLC [11, 12], and have also been widely explored for use in sample preparation [4], micro-mixing [13] and solid phase chemistry [14]. Despite intense investigation, there is limited demonstrable evidence of polymer monoliths having advantages over particulate-based stationary phases. The chromatographic performance of polymer monoliths is compromised by the degree of bed heterogeneity, an intrinsic limitation of free radical polymerisation, and this is particularly problematic for fast-diffusing low molecular weight compounds [15, 16]. Performance of sample preparation is less sensitive to a heterogeneous bed structure, so exploration of polymer monoliths for this purpose is a justifiable pursuit.

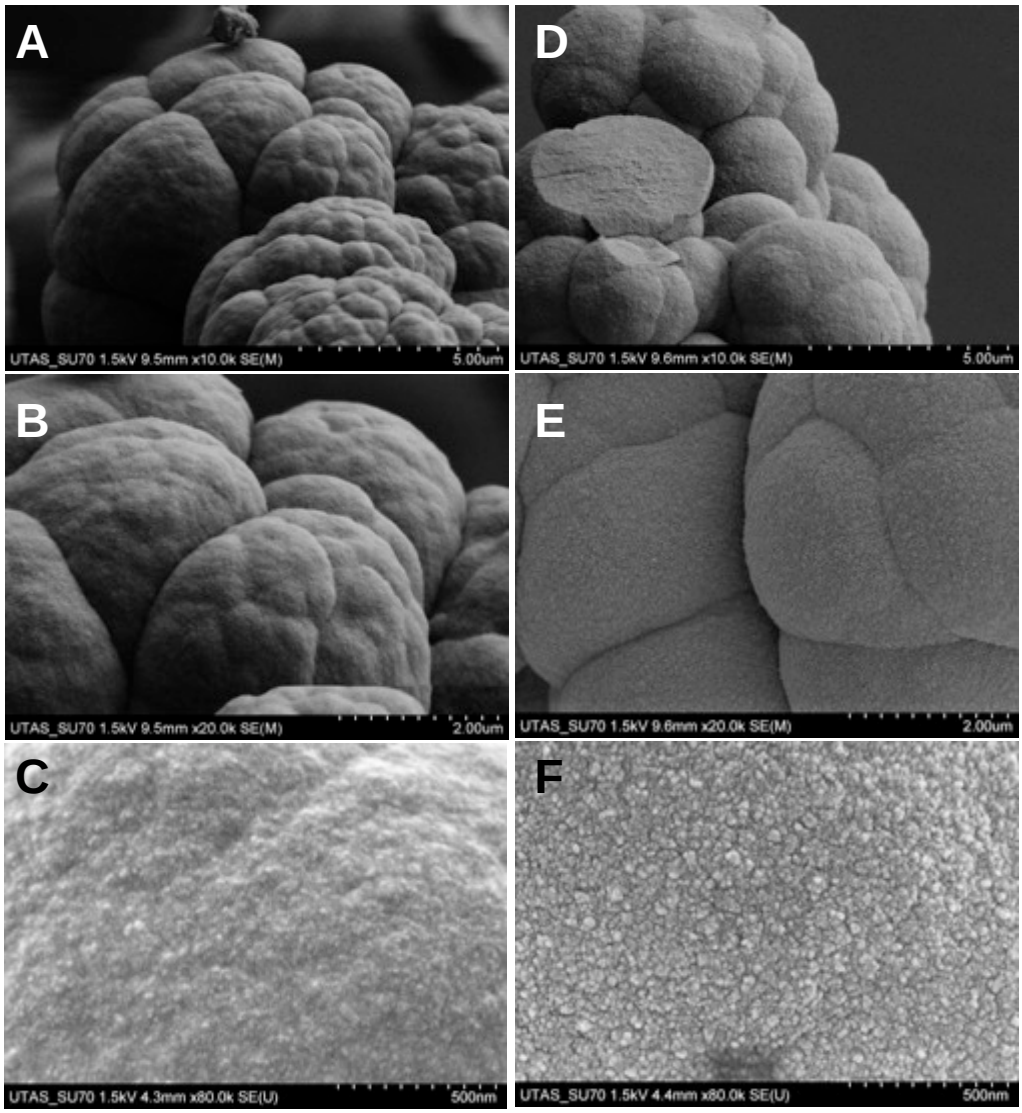

Figure 1.1. The SEM of poly(4-vinylbenzyl chloride-*co*-styrene-*co*-divinyl benzene) with a small surface area (A-C) and poly(divinyl benzene) adsorbent containing a textured structure and a large surface area (D-F). Top) 10 000 x magnification. Middle) 20 000 x magnification. Bottom) 80 000 x magnification.

The structural morphology of polymer monoliths presents a number of unique features that enable rapid and efficient sample preparation. First, the macroporous structure is highly permeable, allowing fast fluid flows while maintaining low backpressures. Second, the polymeric microglobules possess non-porous highly crosslinked cores for improved solute mass transfer kinetics. Unlike particulate adsorbent where the interactable surface area or active ligands are deep inside the particle, the surface of a polymer monolith adsorbent is accessible by a small diffusion distance, which enables high flow rates without compromising efficiency [17].

Svec and Fréchet described the first use of polymer monoliths for a sample preparation in 1996 for the digestion of proteins using a poly(glycidyl methacrylate-*co*-ethylene glycol dimethacrylate) (GMA-*co*-EDMA) adsorbent to which trypsin was covalently immobilized [18]. The proteolytic activity of the polymer monolith with immobilised trypsin was compared to 10 µm poly(GMA-*co*-EDMA) particles with trypsin immobilised thereon. Trypsin activity was greater using the polymer monolith adsorbent since the immobilised enzyme was more accessible to the relatively large molecular weight analyte (cytochrome c - ~12 kDa). Later, a large surface area (400 m^2 g^{-1}) polymer monolithic adsorbent was prepared from a high percentage of the crosslinking monomer divinyl benzene (DVB) and used for the extraction of phenolic compounds from water samples [19]. These first demonstrations of polymer monoliths for sample preparation set the scene for steady expansion. A wide variety of sample preparation applications and platforms have been described [20]. The current literature review focuses on the most recent developments and trends in the design and application of polymer monoliths for sample preparation. This includes a discussion on the structural requirements, adsorbent selectivity considerations, and provides an overview of formats currently explored.

1.3. Structural requirements of adsorbents sample preparation

1.3.1 Extraction and pre-concentration of low molecular weight compounds

Sample preparation of low molecular weight compounds centres on SPE principles for purification and pre-concentration of analytes in complex matrices. A large interactable surface is critical for achieving a high extraction capacity. However, the surface area of polymer monoliths is generally substantially smaller than particulate materials and monolithic silica adsorbents, where surface areas of 300-1000 m^2 g^{-1} are common. Typically, particulate materials and monolithic silica adsorbents possess a high degree of mesoporosity (2 to 50 nm) that accounts for the vast majority of the surface area available for interaction. In contrast, polymer monoliths generally display very small surface areas (< 20 m^2g^{-1}) and low adsorption capacity, as they are largely absent of any mesopores or micropores (0.3 to 2 nm).

Approaches to increase the surface area of a polymer monoliths structure must be explored. Producing an adsorbent with an increased number of small diameter microglobules increases the surface area. Approaches for achieving this goal include high temperature polymerisation, or increased concentrations of the solvating porogen (microporogen) [21, 22]. Unfortunately, these approaches can limit permeability as the void size between the globules (macropores size) is reduced. For these reasons it is generally accepted that there is a trade-off between the surface area and permeability [21] and this places substantial limitation on the applicability of polymer monoliths for SPE.

Several approaches exist for preparation of polymer monoliths with bimodal porous structure. These materials are highly macroporous while exhibiting micro - and mesoporous features [23]. Several SPE adsorbents have been produced with surface

areas as high as 650 m^2 g^{-1} [24-26] by incorporating a high degree of internal crosslinking from an elevated percentage of crosslinking monomer [27, 28]. An alternative approach involves augmenting the surface area through extensive post-crosslinking of a pre-formed polymer using a Davankov reaction [29]. Here a preformed poly(Styrene-*co*-DVB) (Sty) adsorbent is reacted using Friedel-Craft's alkylation to produce structural bridges between neighbouring phenyl groups. Dramatically increased surface area up to 900 m^2 g^{-1} has been described using this approach [30-32]. As both approaches provide adsorbents with large surface areas their superiority for high capacity extractions is often assumed. A detailed characterisation is still necessary to support these assumptions.

Researchers often choose to characterise their newly developed materials by the macropore size, determined by mercury intrusion porosimetry and surface areas obtained by BET N_2 adsorption/desorption. While the macropore size distribution is routinely reported graphically, the BET isotherm is rarely provided. This is unfortunate as the isotherms provide considerable detail regarding pore structure, size and even some insight into shape. While nitrogen is routinely explored as the adsorbate in these studies, investigation using alternative gases such as argon, carbon dioxide or even benzene could reveal additional information about the pore size, shape and pore size distribution. The use of argon at 87K and carbon dioxide at ambient temperature could reveal the presence of ultramicropores (< 1 nm) in large surface area polymer monoliths [33]. The use of benzene as a comparison to nitrogen or argon could provide interesting information regarding pore accessibility given the larger cross-sectional area of benzene. In addition, benzene may swell the polymer monolith and provide pore information in the swollen state [33]. Exploring non-local density functional theory the more accurate approach to estimate pore size and pore size distribution, will also

generate a better understanding of the polymer monolith adsorbents and help identify the features that promote highly efficient extraction.

However, while there are considerable benefits of a detailed characterisation in the dry state the short-comings of these techniques has long been lamented for not adequately reflecting the performance under operational conditions (solvated state) [34]. Characterisation in the solvated state is time consuming and often avoided, but it is critical to truly understand the performance, and it can no longer be ignored. If these materials are to be adopted into routine analysis the performance must be understood and superiority over existing alternatives clearly demonstrated.

1.3.2 Sample preparation of high molecular weight compounds

Polymer monoliths represent an ideal structure for sample preparation of high molecular weight species. A highly porous architecture largely devoid of small pores enables convective mass transfer to efficiently transport high molecular weight species through the adsorbent bed [35]. Due to sample complexity and typically low concentration of high molecular weight analytes, selective extractions based on molecular recognition are often necessary. Adsorbent developments commonly focused on covalently attaching biorecognition ligands or nanoparticles to preformed reactive polymer monoliths. The alternative approach is to introduce affinity monomers or nanoparticles directly into the polymerisation mixture, which often yields adsorbents with widely different macroporous properties. Despite broad claims of enhanced performance, the experimental designs used in many literature reports makes it difficult to disentangle the specific benefits of molecular recognition agents from changes in macroporosity to observed performance benefits. Yang *et al.* the utilised a porogenic template to enable the systematic study of the effects of incorporating a functional monomer for boronate

affinity extraction of glycoproteins from a bovine serum albumin (BSA) solution, using poly(3-acrylamidophenylboronic acid-*co*-ethylene dimethacrylate) (APPBA-*co*-EDA) [36]. The metal-organic gel porogenic template was fabricated at 45 to 80°C to produce templates of different size. Porogenic templates are attractive as they provide a unique opportunity to adjust the pore size independently from composition of the polymerisation mixture.

1.4. Sample preparation formats using polymer monoliths

Polymer monolith polymerisation takes place within a mould that dictates the adsorbent shape. Consequently, polymer monoliths present flexible opportunities to develop unique formats for sample preparation. Polymerisation can be initiated using a range of methods including thermal [10], ultraviolet (UV) [37], redox [38], γ-radiation [39], or electron beam [40]. To date the investigations of adsorbent beds for sample preparation has been largely limited to UV or thermal initiation. Alternative approaches to induce polymerisation of sample preparation adsorbents remain largely unexplored and this presents exciting possibilities for researchers to probe unique and obscure formats.

Potter and Hilder discussed the use of polymer monoliths for sample preparation [41], highlighting formats for on-line sample preparation, where the polymer monolith adsorbent is directly coupled with HPLC and MS for sample clean up, or with CE for pre-concentration. On-line sample preparation approaches facilitate high-throughput, improve assay reproducibility and reduce human error. Despite this, the formats and operations of on-line sample preparation have seen little advance in the last five years. Research has primarily focused around opportunities to develop adsorbents for targeted applications through the exploration of adsorbent functionality. The operational

challenges, particularly for CE, have proved difficult to overcome and many researchers have focused on alternative approaches for analyte pre-concentration.

One area of on-line sample preparation where polymer monoliths have seen noteworthy advances is the development of microfluidic lab-on-a-chip technologies that aim to integrate all aspects of the analytical workflow into a single device. While considerable advances have been seen in this field, complex samples pose a considerable challenge, and they are often processed and purified off-line prior to analysis. Efforts are now being focused to incorporate sample preparation onto the device. Polymer monoliths present attractive practicalities as they can be formed directly into the microchannel of such devices. Implementing a UV mediated irradiation polymerisation enables the polymer monolith to be photopatterned in a desired location without the need of frits to hold the sorbent in place [42]. To date only a handful of researchers have explored the potential of polymer monolith adsorbents beds for chip-based sample preparation.

Coupling microfluidic devices to mass spectrometry (MS) provides a route to highly sensitive and selective analysis [43]. Commercial platforms (e.g. Chip Cube, IonKey) have been developed for microchip-based separations but these currently lack the flexibility required for high throughput microscale sample preparation. Harrison and coworkers reported a series of works aiming to integrate fractionation, pre-concentration, tryptic digestion and desalting into a single chip-based platform for proteomics [44]. Electrokinetic pumping drives fluid flow through the device, thus it is necessary to incorporate a charged monomer to maintain appropriate fluid flow over the adsorbent bed. In their first example the channel walls were coated with the polycationic coating and zones of poly([2-(methacryloyloxy)ethyl] trimethylammonium chloride-*co*-BMA-*co*-EDMA) (META), and were fabricated *via* a co-polymerisation.

Proteins were extracted based on hydrophobic interactions (maximum capacity of 11.5 mg mL^{-1} for cytochrome c). Immobilised proteins were digested by flushing with a trypsin solution, and substantial improvements in digestions were achieved (15 min compared with 24 h for the solution based assay). By extension devices with multiple channels were fabricated for fractionation (6-8 channels) for elution into a single exit port for detection [45]. The importance of the META (0.45 %) was authenticated in this multiplexed device, the cationic monomer enabled the flow of sample to be controlled preventing any cross-contamination between channels. The 6-channel device was used to demonstrate the channel-to-channel reproducibility where the recovery of model proteins varied by only 8 % RSD. Further work demonstrated a 36-channel device where electrokinetic pumping was generated by native silanol groups on the channel wall, hence incorporation of the negatively charged monomer (2-acrylamido-2-methylpropane sulfonic acid) maintained fluid flow over the adsorbent bed [46].

Wheeler and co-workers offered a simplified format to circumvent any challenges of microchannel fabrication wherein a digital microfluidic device involves *in situ* fabrication of a 2 mm poly(butyl acrylate-*co*-1,3- butanediol diacrylate-*co*-lauryl acrylate) adsorbent disk directly on an insulated electrode (**Figure 1.2**) [47]. Extraction was implemented by sequentially driving the solvent and sample from five individual wells over the polymer monolith disk by application of an electrostatic force. The device showed highly promising results for the recovery of fluorescamine-labeled angiotensin IV when compared with C18 ZipTips® with 93 ± 14% and 92 ± 5% respectively. The effectiveness was further explored by assessing the ability to desalt a peptide solution for off-line nano electrospray ionisation (ESI)-MS, angiotensin II solution prepared in 100 mM NaCl. The signal of a non-extracted sample was completely suppressed, whereas desalting with the device ensured a strong signal at the

corresponding *m/z*. The work has been further extended to strong cation-exchange extraction of proteins and peptides [48]. While the microfluidic formats appear highly promising current work has been limited to model proteins in aqueous solution and a demonstration of device utility and compatibility with real complex samples (spiked or otherwise) is necessary. Preparation of highly complex samples using microfluidic platforms is non-trivial and we are eagerly waiting for this to be demonstrated.

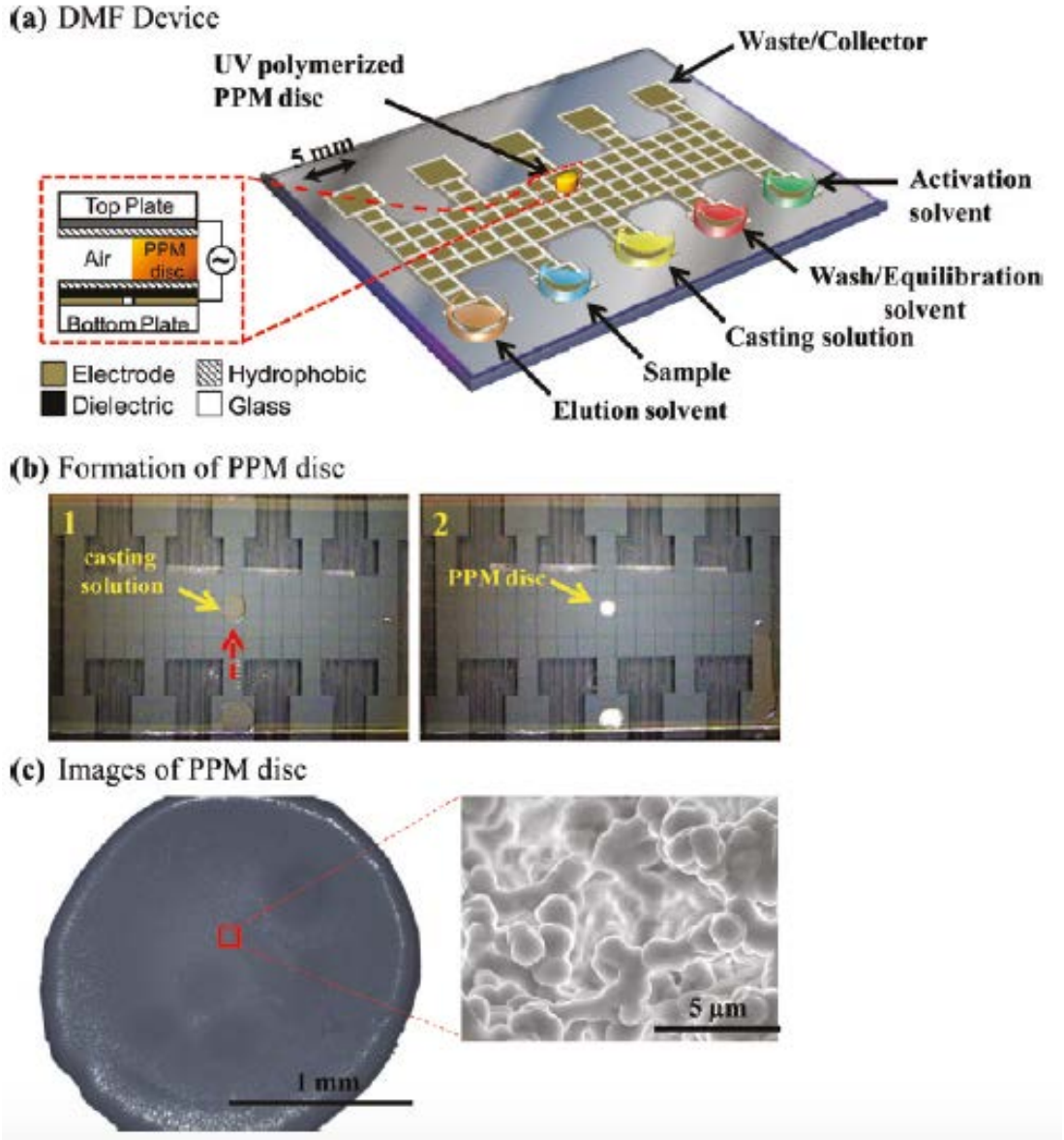

Figure 1.2. The digital microfluidic device for SPE using polymer monolith disks. Reprinted with permission from ref. [47] Copyright 2011 American Chemical Society.

Adaption of off-line sample preparation tools into routine laboratories is more realistic than emerging on-line formats and new devices for off-line sample preparation have received substantial attention in the last five years. In-tube flow through devices have received the largest amount of attention of all off-line formats investigated. Feng and co-workers introduced polymer monolith microextraction in which the adsorbent is fabricated in a wide-bore capillary (0.2 – 2 cm × 0.53 mm i.d), which is subsequently attached *via* a pinhole connection to a 1 mL plastic syringe to drive the extraction [49]. This format has been investigated using a wide variety adsorbents to suit targeted applications including antibiotics in chicken and antidepressants in human plasma [49, 50]. The primary advantage of this format is the cost effective manufacture from general laboratory consumables as well as the use of a conventional laboratory syringe pump to drive extraction [49]. Pietrzynska *et al.* reported a robust flow through extraction device where the adsorbent was prepared in stainless steel needle for subsequent attachment to a 10 mL syringe [51]. Miniaturised flow through extraction devices are frequently described as solid phase microextraction (SPME) in the literature. As Potter and Hilder [41] stated the term SPME is strongly associated with the equilibrium partitioning governed extractions described by Pawliszyn [52] and therefore should not be used in the context of exhaustive extraction technologies.

While dispensing fluid over a polymer monolith is not generally problematic, fluid aspiration is challenging due to the restriction created by the polymer monolith adsorbent bed. Filling the syringe with fluid prior to attaching the extraction capillary has typically circumvented this limitation. Regrettably, this introduces several handling steps that are difficult to automate. Consequently, workflows are labour intensive making them unsuitable for routine analysis. Unfortunately, this means that such formats cannot be considered as anything other than a tool for polymer monolith

development. We believe the solution is to engineer a device combatable with a wide range of adsorbent permeability.

Mugo *et al.* increased adsorbent surface to volume ratio while preserving permeability by employing an extruded multichannel silica optical fibers for porous layer open tubular microextraction (**Figure 1.3**) [53]. The intention of this work was to fabricate a 1 µm thick layer of poly(Sty-*co*-DVB) on the walls of each of the 168 channels to permit fast extraction kinetics while still maintaining a high surface area for an increased extraction capacity. Unfortunately, the authors were unable to reproducibly form the polymer monolith in all of the 168 channels. Although a polymer monolith layer formed in some channels, others were either completely filled or remained empty. Nevertheless, the use of multichannel optical fiber for improved sample preparation is an exciting concept that warrants further investigation.

Micropipette tip devices are an alternative format for flow through sample preparation, in which a short adsorbent bed is cast in a polypropylene pipette tip. There are a number of attractive features about this format, namely polypropylene pipette tips span a broad size range. In addition, they are inexpensive consumables making them amenable to single use application. Further, they can be introduced to any lab equipped with an auto pipette. Equally, micropipette tips are readily automated with robotic liquid handling devices that facilitate simultaneous extraction of 8 to 96 samples. Prior to 2010 Abdel Rehim *et al.* demonstrated 96 array poly(BMA-*co*-EDMA) micropipette tips for high throughput sample preparation in the pharmaceutical industry [54]. Permeability of the adsorbent bed is particularly critical in this format as there is little scope to introduce sample and solvent into the pipette tip above the adsorbent bed. Developers have often chosen to introduce a flow-channel through the adsorbent bed to achieve unrestricted

fluid flow. One may assume that this would be detrimental for extraction efficiencies but Xie *et al.* found that increasing the diameter flow channel (from 250 - 760 µm) improved analyte recovery [55]. The alternative is to develop a micropipette format for the extraction of large biomolecules where a highly macroporous architecture is preferred. Examples include affinity supports where incorporated ligands or nanoparticles provide highly specific interaction sites for the analyte while the polymer monolith itself merely acts as a scaffold [56-59].

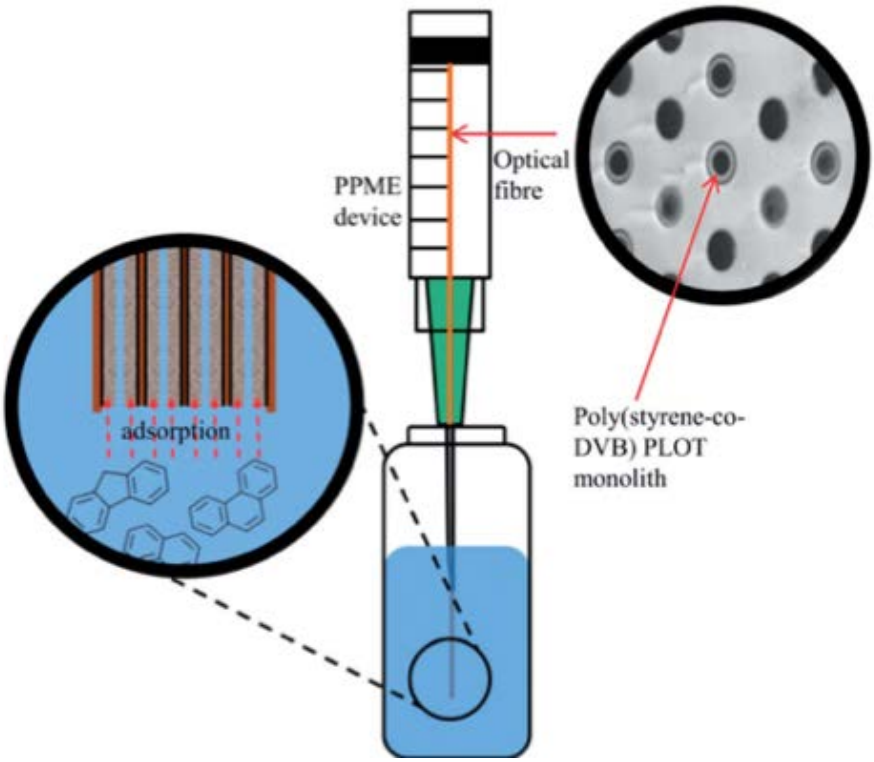

Figure 1.3. Multichannel porous layer open tubular poly(Sty-co-DVB) polymer monolith devices. Reproduced from ref. [53] with permission from The Royal Chemical Society.

A unique device was prepared by Peroni *et al.*, where hydrophobic poly(Sty-*co*-DVB) and poly(BMA-*co*-EDMA) adsorbents were employed to phase separate the solvents of

a liquid-liquid extraction (LLE) [60]. Phase separation was realised by flushing the LLE sample through a chamber, a capillary (3 mm × 0.53 mm i.d) containing the polymer monolith was inserted perpendicular to fluid flow. Solvents were separated by pressurising the chamber; the non-polar organic solvent migrated through the pores of the hydrophobic adsorbent while water was completely excluded from the capillary and directed to waste. The poly(Sty-*co*-DVB) macropore size was varied over a range of 0.9 to 14.7 µm and, as expected, 14.7 µm was most suitable as it enabled the highest flow of the organic solvent, *n*-hexane. The phase separator was employed for the LLE extraction of polyaromatic hydrocarbons in wastewater where recoveries of 93 - 114% were achieved.

While flow through extraction devices require highly permeable adsorbent beds, polymer monolith stir bar sorptive extraction (SBSE) presents operational flexibility over a wide range of macropore sizes. SBSE involves a layer of polymer monolith deposited over a magnetic rod (10 mm × 1.2 mm) encased in vinylised glass tubing [61]. Alternatively the polymer monolith may be adhered by physical absorption to a stir bar encased in a metal spring [25]. The stir-bar is directly exposed to the stirred (300-600 ppm) sample matrix and then manually rinsed to remove matrix contaminants. Finally, the analytes are desorbed by stirring in a desorption buffer [62]. As polymer monoliths can be brittle and prone to damage, Huang *et al.* inserted an *ex situ* formed polymer monolith adsorbent in a magnetic holder (**Figure 1.4**) to minimise the physical damage induced by high-speed collisions with the walls of the extraction vessel [63].

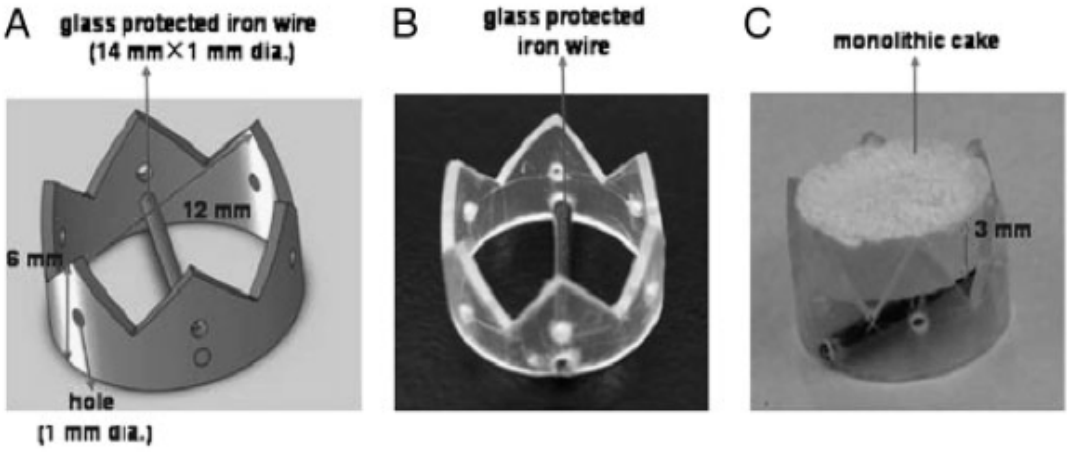

Figure 1.4. SBSE, the protective housing to encase the polymer monolith disk. Reproduced from ref. [63] Copyright 2011 from Wiley.

Recently, Takahashi *et al.* prepared an epoxide polymer monolith disk for the enrichment of polar organic compounds, followed by thermal desorption in an on-line chamber attached to gas chromatography-MS [64]. Rather than using the polymer monolith itself to agitate the solution the disks were submerged in an aqueous sample and subjected to sonication. Pyrolysis analysis of the epoxide polymer monolith from 100 - 700°C revealed that the material began to decompose at 300°C, so 250°C was selected for thermal desorption. The epoxy polymer monolith was demonstrated for the extraction from red wine where the adsorbent demonstrated selectivity towards the polar elements in the sample.

Hilder *et al.* has demonstrated the use of planar hydrophilic polymer monolith as a storage medium for dried blood spot sampling [65]. The poly(HEMA-*co*-EDMA) adsorbents were prepared on a flexible backing polymer fibre material, a format suited to automation [66]. By developing a material with a macropore size greater than 7 µm whole blood was able to soak instantly into the adsorbent. The performance of the flat

poly(HEMA-*co*-EDMA) was compared with a commercially available cellulose based adsorbents and a glass fiber-based adsorbent. Spot size variability was compared for samples with hematocrit levels from 20 to 80%. Additionally, analyte diffusion across the spot was assessed to determine the feasibility sampling the same spot multiple times. In both cases the polymer monolith afforded superior performance over the commercially available counterparts. The polymer monolithic adsorbents also present further opportunities to introduce functionality for improved sample stability, selective extraction and elimination of matrix components.

1.5. Diverse functionalities

The polymer monolith surface functionality plays an important role in interactions between the analyte and the adsorbent. There are a number of approaches to introduce functionality to a polymer monolithic adsorbent, with each approach having distinct advantages and disadvantages. Co-polymerisation is by far the most common methodology to impart functionality. It is the simplest approach as the functional monomer(s) is directly incorporated into the polymerisation mixture. Unfortunately, depending on monomer reactivity the functional group may be buried within the non-porous microglobules of the bulk scaffold, and will be inaccessible for analyte interaction. Careful consideration of the reactivity of the functional and crosslinking monomers can uncover adsorbents with accessible functionality. To date this has not adequately been explored and it would be encouraging to see these considerations demonstrated. A more practical disadvantage is the need to re-optimise the conditions of polymerisation for every particular monomer to maintain suitable scaffold porosity. Changes in porosity occurring through functional monomer incorporation also means it

can be challenging to truly assign any performance improvements solely to surface functionality.

An alternative approach is to directly functionalise the pre-formed polymer through a post-polymerisation modification. While this approach for adsorbent production is more involved, the structural integrity is largely maintained so the net process is beneficial. There are two general post-polymerisation modification routes; the first exploits the reactivity of the functional monomer such as GMA or 4,4-dimethyl-2-vinylazlactone (VAL) for covalent attachment of the desired functionality (both non-specific and affinity ligands). However, post-polymerisation modification reactions can be time consuming and a range of functional ligands available for attachment are limited to those with complementing chemistry. The second approach involves a thin layer of reactive polymer chains UV photografted onto the surface of the preformed polymer. Again this post-polymerisation modification approach is limited to compatible monomers [67]. Adsorbents decorated with functionalised nanoparticles have recently gained status for use in sample preparation as can they provide increased points of interaction with unique chemistry [68, 69]. Nanoparticles can be introduced by direct embedding in the polymer monolith structure or by covalent immobilisation. These approaches deliver the same advantages and drawbacks as functional monomer incorporation [70, 71]. Functionalised adsorbents, which have been discussed for both non-specific and specific interactions, are listed in **Tables 1-4**.

1.5.1. Non-specific interactions

The popularity of polymer monolith adsorbents for SPE can be in part attributed to the diverse range of functional monomers commercially available for exploration [6, 72, 73]. This presents endless opportunities to tailor the surface chemistry of the adsorbent

to suit the desired application. **Table 1.1** and **Table 1.2** summarise the incorporation of functional monomers and nanoparticles into polymer monolith SPE adsorbents as discussed in this section of the review.

Polymer monolithic adsorbents are suitable materials for SBSE, for which, until recently polydimethylsiloxane (PDMS) was the only available adsorbent. PDMS is highly retentive for apolar analytes, but retention can be limited when polar moieties are displayed. Subsequently, the diverse range of functional monomers has facilitated development of polymer monolith SBSE adsorbents that provide hydrophilic and ion exchange functionality [74]. Huang and coworkers fabricated a range of SBSE for polar and mid-polar analytes using a hydrophobic crosslinker (EDMA or DVB) with the hydrophilic functional monomers vinylpyridine, vinylamidazole, and vinylpyrrolidone (VLP) [75, 76, 62]. Here, a high concentration of the crosslinking monomer was utilised (>85% of the monomer concentration), which can provide an abundance of small pores, and avail a large surface area for analyte interaction. The extraction mechanism for polymer monolith SBSE is adsorption rather than equilibrium partitioning, and comparison with commercial PDMS exhibited impressive improvements in the extraction capacity of polyaromatic amines and steroid sex hormones [75, 76, 62]. The dramatic increase in the surface-to-volume ratio of the polymer monolith adsorbent compared to PDMS likely contributes substantially to the increased capacity.

Bratkowska *et al.* utilised poly(VLP-*co*-DVB) to simulate OASIS® HLB, to promote more efficient surface contact with aqueous samples [25]. Large surface area adsorbents (650 $m^2 g^{-1}$) were employed for the extraction of personal care products from waste water and impressive performance improvements were achieved when comparing with PDMS. These performance gains were attributed to increased surface area, and to

interactions with the functional and crosslinking monomers (π-π interactions). To further probe retention mechanisms a series of adsorbents were fabricated; poly(HEMA-*co*-pentaerythritol triacrylate) (PETRA) a hydrophilic adsorbent with a small surface area, poly(HEMA-*co*-DVB) a hydrophobic adsorbent with a large surface area, and poly(poly(ethylene glycol) methacrylate-*co*-PETRA) (PEGMA) a non-porous polymer that swells considerably in solvent. Surprisingly, the swollen non-porous poly(PEGMA-*co*-PETRA) polymer monolith provided comparable recoveries to the poly(HEMA-*co*-DVB) polymer monolith, which the authors rationalised by the high number of polar sites [77]. When compared with new commercially available EG Slicone Twister® and Acrylate Twister® polar stir-bars, the polymer monolith afforded higher recoveries over a wider range of analytes [78].

Preparation of polymer monoliths as adsorbents for SPE based on ion exchange interactions has been extensively investigated. However, polymer particulate-based ion exchange or mixed mode (reversed phase/ion exchange resins) resins inherently possess a higher ion exchange capacity as recipes permit a greater concentration of functional monomer which provide more points of interaction and subsequently greater capacities [69]. Adsorbents fabricated from poly(methacrylic acid-*co*-DVB) (MAA) (25% MAA:75% DVB) provided a large interactable surface area (500 m^2 g^{-1}). Attempts were made to exploit the carboxylic acid functionality for cation exchange extraction of amines, but despite the presence of MAA, better recoveries were obtained for deprotonated analytes [24]. Caution must be taken when comparing the high accessible surface area and the capacity of functional groups available for interaction. Many researchers quote the dry state surface area obtained by nitrogen adsorption but there are far fewer examples of ion exchange capacity of the materials being provided. Where ion exchange capacity has been demonstrated it appears there is a lack of convention in the

experimental design that makes it difficult to draw comparisons between materials. It is clear that there is a considerable challenge around the development of polymer monoliths which possess a higher density of functional groups but unless a standard approach is adopted to adequately benchmark the ion exchange capacities, the task of improving these materials become more onerous as we continue to work blindly. Both a sound understanding of the mechanistic properties of these polymer monolith adsorbents and creativity in their synthesis is the key overcoming these challenges.

Table 1.1. Polymer monoliths adsorbents incorporating functional monomers for sample extraction and preconcentration based on non-specific interactions

Monomer Type	Functionality	Application	Embodiment	Ref.
poly(META-*co*-BMA-*co*-EDMA)	hydrophobic	protein immobilisation	microchip	[44]
poly(AMPS-*co*-BMA-*co*-EDMA)	hydrophobic	protein immobilisation	microchip	[46]
poly(butyl acrylate-*co*-1,3- butanediol diacrylate-*co*-lauryl acrylate)	hydrophobic	protein immobilisation	microchip	[47]
poly(GMA-*co*-EDMA)	strong cation exchange	protein immobilisation	microchip	[48]
poly(MAA-*co*-EDMA)	hydrophobic	antidepressants in urine and plasma	capillary - syringe driven	[49]
poly(MAA-*co*-EDMA)	hydrophobic	antibiotics in chicken	capillary - syringe driven	[50]
poly(Sty-*co*-DVB)	hydrophobic	phenolics in water	stainless steel needle - syringe driven	[51]
poly(Sty-*co*-DVB)	hydrophobic	polyaromatic hydrocarbons	multichannel fiber optic capillary - syringe driven	[53]
poly(Sty-*co*-DVB) and poly(BMA-*co*-EDMA)	hydrophobic	phase separator	capillary - on-line	[60]
poly(VLP-*co*-EDMA)	hydrophobic	steroid sex hormones in waste water	SBSE	[75]

Monomer Type	Functionality	Application	Embodiment	Ref.
poly(vinylamidazole-*co*-DVB)	hydrophobic	polar aromatic amines in water	SBSE	[62]
poly(vinylpyrrolidone-*co*-DVB)	hydrophobic	apolar and polar organic compounds and heavy metal ions	SBSE	[76]
poly(VLP-*co*-DVB)	hydrophobic	personal care products in river water	SBSE	[25]
poly(PEGMA-*co*-PETRA)	hydrophilic	polar analytes	SBSE	[77]
poly(HEMA-*co*-DVB)	hydrophilic	polar analytes	SBSE	[77]
poly(HEMA-*co*-PETRA)	hydrophilic	polar analytes	SBSE	[77, 78]
diglycidyl ether of bisphenol A	hydrophilic	polar organic compounds in aqueous media	thermal extraction disk	[64]
poly(HEMA-*co*-EDMA)	hydrophilic	pharmaceuticals in dried blood spot	flat sheet	[65]

Thabano *et al*. developed an approach to improve the ion-exchange capacity of a poly(MAA-*co*-EDMA) adsorbent by directing the orientation of the carboxylic acid group to the pore surface [79]. The intention of the work was to employ 80 nm silica nanoparticles to template small macroporous cavities into the microglobule surface to improve surface area. The silica nanoparticles were removed from the adsorbent scaffold by etching. While scanning electron micrograph images provided no visual indication of a templated surface, the adsorbent displayed a 10-fold increase in ion-exchange capacity. The authors suggested this is due to a re-orientation of the carboxylic acid groups caused by hydrogen bonding to silica nanoparticles in the porogenic solvent, making them more accessible to the surface. This work provides an exciting insight to the development of novel porogenic solvent compositions that ameliorate the problem of the monovinyl monomer functionality being buried in the bulk polymer. Fabrications of materials using approaches to orient the location of the functional group afford exciting possibilities and warrant further investigation

Alternatively, nanoparticles have been incorporated into the adsorbent structure in an attempt to overcome the low density of reactive functional groups of polymer monoliths. In a series of works Jia and coworkers have studied the incorporation of graphene nanosheets, graphene oxidide, γ-alumina and β-cyclodextrin / nanocuprous oxide into methacrylate adsorbents [80-84]. The effect of directly embedding the hydrophobic graphene nanosheets and β-cyclodextrin / nanocuprous oxide nanoparticles into poly(BMA-*co*-EDMA) was studied to determine the influence on the extraction of glucocorticoids from cosmetics and pesticides [81, 85, 84]. Direct incorporation of nanoparticles into the polymerisation mixture influences microglobule formation, and often decreased globule size, providing a structure different from the control adsorbent [86]. When the nanoparticles possess a similar retention mechanism to the bulk polymer

it can be difficult to truly ascertain whether the improved performance results from the nanoparticles themselves, or by way of altered porous architecture of the adsorbent. Covalent attachment of nanoparticles to the pore surface using the reactive poly(GMA-*co*-EDMA) adsorbent is an alternative fabrication methodology. The GMA epoxide group (oxirane) was reacted with diethylamine to provide amine surface chemistry for covalent attachment of graphene oxide and subsequently graphene nanosheets. The extraction of sarosine, a urine-derived prostate cancer biomarker, was demonstrated. However, an assessment with a wider variety of more commentary probes is necessary to truly ascertain the reason of any performance improvements [80].

Zhou *et al.* presented a unique approach to evenly disperse carboxylated multi-wall carbon nanotubes (cMWNT) into the poly(MAA-*co*-EDMA) adsorbent as seen in **Figure 1.5** [87]. The initiated thermal polymerisation was stopped after 20 min and a solution of cMWNT was added, after which polymerisation was continued until 24 h. The oligomers formed during the first 20 min facilitated even distribution of the cMWNT through the polymer. BET surface area of poly(MAA-*co*-EDMA-cMWNT) adsorbent increased from 14 m^2 g^{-1} to 86 m^2 g^{-1} without a dramatic reduction in permeability. The adsorbents displayed a substantial improvement in the cation-exchange retention of basic proteins measured by frontal elution chromatography. The amount of basic proteins hemoglobin and cytochrome c loaded on the column increased from 0.26 mg mL^{-1} and 0.26 mg mL^{-1} respectively for poly(MAA-*co*-EDMA) to 6.4 mg mL^{-1} and 6.1 mg mL^{-1} for the poly(MAA-*co*-EDMA-cMWNT). The utility of the adsorbent was demonstrated for the effective enrichment of the basic protein, hemoglobin, from whole human blood.

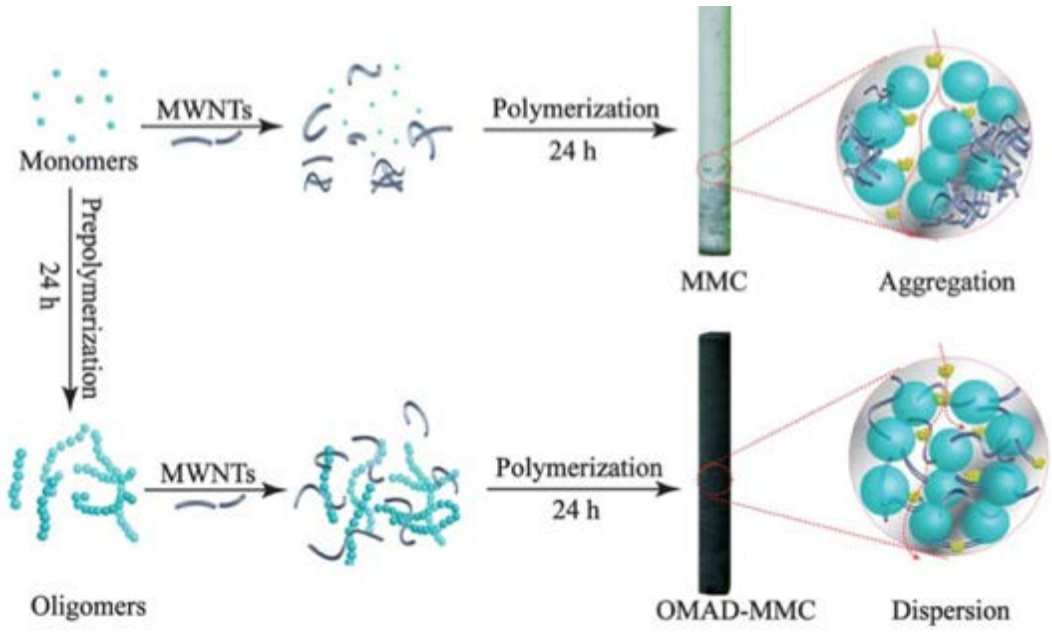

Figure 1.5. Oligomer stabilised distribution of carbon nanotubes through a poly(MAA-*co*-EDMA) adsorbent. Reproduced from ref. [87] with permission from The Royal Chemical Society.

Xie *et al.* investigated approaches to increase the capacity of the poly(EDMA) adsorbent by directly embedding 60 µm Oasis® HLB particles into the adsorbent [55]. Here, the polymer monolith largely assumes the role of a support scaffold for the large surface area 60 µm particles which improved the capacity by approximately 50%. While this may increase the capacity of the adsorbent bed, any improvements in mass transfer are lost since analyte diffusion distance requires considerable time for the analyte to partition in and out of the large particle to reach the interaction sites.

A vast number of additional articles published in this area outline a detailed investigation to reveal the optimal extraction conditions, recoveries, and limits of detection, which are typically compared with benchmark metrics gathered from the literature. Unfortunately, this type of comparison does not accurately probe the performance of the adsorbent materials themselves. To truly benchmark the developed

polymer monolith adsorbents it is necessary to provide a direct comparison with alternative technologies by analysing all extracts under identical chromatographic and detection conditions, but this is time consuming and therefore rarely undertaken. Researchers must place greater emphasis on investigating mechanistic aspects rather than superficial exploration of the application of functional monomers if the field is to genuinely advance.

Table 1.2. Polymer monoliths incorporating nanoparticles for sample preparation based on non-specific interactions

Monomer Type	Particle	Approach	Functionality	Application	Embodiment	Ref.
poly(MAA-*co*-EDMA)	silica nanoparticle	template	weak cation exchange	neurotransmitters in aqueous solution	capillary – on-line	[79]
Poly(BMA-co-EDMA)	graphene nanosheets	embedded	hydrophobic	glucocorticoids in waste water	capillary - syringe driven	[81]
Poly(GMA-co-EDMA)	graphene nanosheets & graphene oxide	covalent attachment	hydrophobic	sarcosine in urine	capillary-syringe driven	[80]
Poly(BMA-co-EDMA)	β-cyclodextrin / nanocuprous oxide	embedded	hydrophobic	polychlorinated biphenyls in water	capillary - syringe driven	[84]
poly(N-isopropylacrylamide-*co*-MBA)	γ-alumina	embedded	hydrophobic	synthetic food dyes in soft drinks	capillary - syringe driven	[82]
poly(N-isopropylacrylamide-*co*-GMA-*co*-MBA)	γ-alumina	covalent attachment	hydrophobic	sudan dyes in wine	capillary - syringe driven	[83]
poly(MAA-*co*-EDMA)	cMWNT	embedded	cation exchange	proteins in blood	stainless steel column	[87]
poly(EDMA)	60 µm OASIS HLB	embedded	hydrophobic	pharmaceuticals in human plasma	pipette tip	[55]

1.5.2. Affinity interactions

Highly specific sample preparation typically utilises affinity interactions based on a three-dimensional chemical and spatial recognition between an immobilised ligand and the target analyte. The use of polymer monoliths as adsorbents for affinity chromatography is prevalent throughout the literature and a number of recent reviews detail the array of specific affinity ligands and applications [88-90]. As such, only a brief discussion on the current trends to fabricate affinity adsorbents for sample preparation will follow, the summary of this section is tabluted in **Table 1.3**.

Boronic acid functionality has been exploited to selective extract analytes possessing 1,2 and 1,3-*cis*-vicinal diol moieties (saccharides, nucleosides, and glycoproteins) through the reversible formation of cyclic aromatic esters. Recent examples involved the co-polymerisation of a poly(4-vinyl phenylboronic acid-*co*-EDMA) adsorbent for the extraction of catecholamines [26]. A high concentration of crosslinking monomer provided a large interactable surface (239 m^2 g^{-1}) and a maximum adsorption capacity of approximately 14 mg g^{-1} for epinephrine. The capacity of this adsorbent was not appreciably greater than poly(APPBA-*co*-EDA), which displayed only a small surface area material (20 m^2 g^{-1}) and an adsorption capacity of 8.2 mg g^{-1} for the large biomolecule ovalbumin. As suggested above, it can be problematic to prepare adsorbents with a high density of functional groups available for interaction. An alternative approach is molecularly imprinted polymers, templated structures which comprises three-dimensional recognition cavities for analytes or classes of analytes of specific shape and functionality. The inherent disadvantages of these materials are well known, namely they suffer poor extraction kinetics and it can be difficult to completely remove the template molecule. This has largely limited molecularly imprinted polymer

monoliths as a topic of academic interest. Recent developments have been application-focused and are therefore not discussed in this literature review [91-93].

The fabrication of adsorbents for highly selective macromolecule extractions almost exclusively involves a co-polymerisation with GMA to provide a location for the covalent attachment of bioligands. The well characterised poly(GMA-*co*-EDMA) adsorbents possess the oxirane functionality that can react with the nucleophilic amino groups of many affinity ligands. However, as the reaction kinetics are slow this approach is generally avoided. The most common approach (**Figure 1.6**) is to react the oxirane group with the nucelophilic ethylenediamine followed by introducing a difunctional spacer ligand (glutaraldehyde), and covalent attachment of the affinity ligand [18]. The glutaraldehyde spacer not only provides a point of attachment but also limits interactions between the adsorbent surface and the affinity ligand, which maintains its structural integrity and therefore function. Some of the most elegant work in this field has been demonstrated for the commercially available Convective Interactive Media (CIM®) disks manufactured by BIA Separations (Ljubljana, Slovenia) [94, 95].

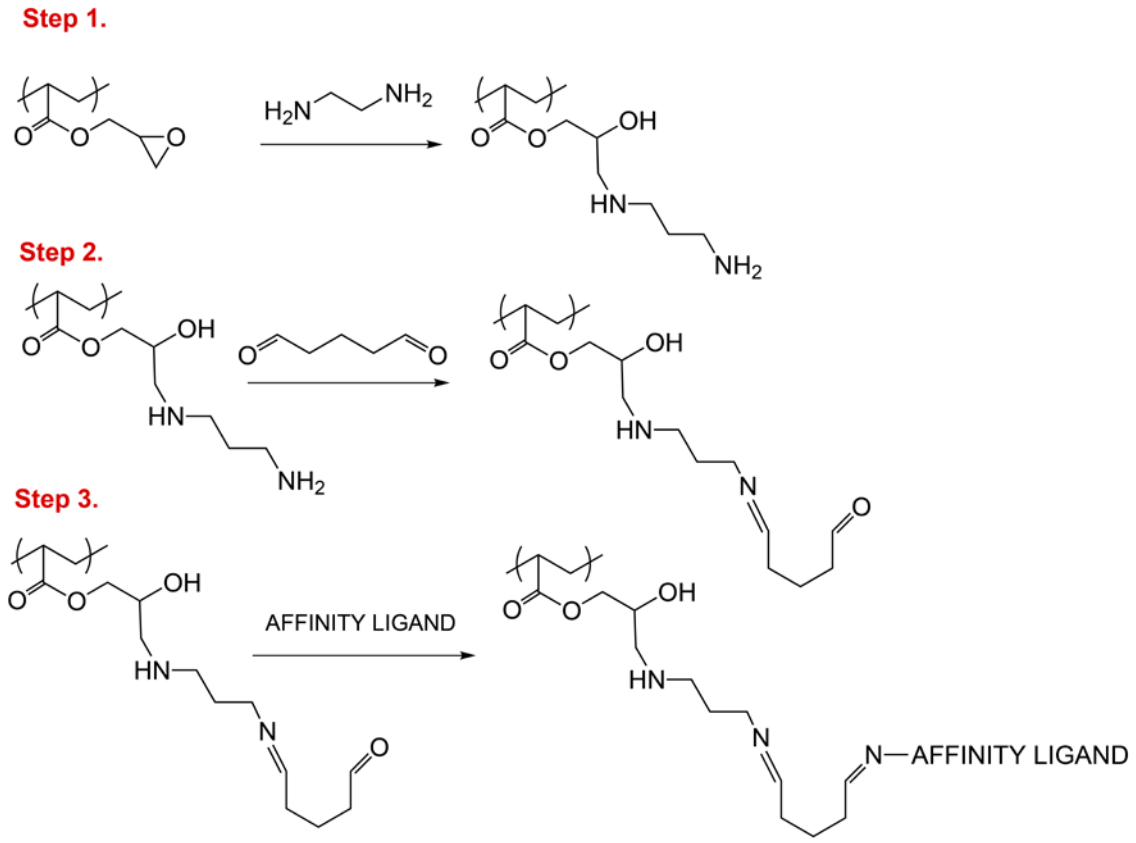

Figure 1.6. A commonly employed reaction scheme used for the immobilisation of affinity ligands and enzymes to poly(GMA-*co*-EDMA). The three-step reaction involves the amination of GMA's oxirane ring for the attachment of the difunctional glutaraldehyde linker. The affinity ligand or enzyme can then be covalently bound to the glutaraldehyde moieties.

An alternative approach employed the reactive monomer glyceryl monomethacrylate (GlyMA). This monomer possesses 1,2-diol functionality typically obtained through a hydrolysis ring opening reaction of the oxirane group of GMA. A poly(GlyMA-*co*-EDMA) adsorbent was prepared and the 1,2-diol was oxidised to an aldehyde for the immobilisation of the lectin family of affinity ligands: wheat germ agglutinin, concanavalin A and *Ricinus communis* agglutinin-I. Three polymer monolith affinity columns were placed in series for the selective extraction of glycoproteins from human serum [96]. While, the use of GlyMA simplifies adsorbent fabrication, GMA cannot be

substituted directly with the hydrophilic GlyMA as drastically different pore forming solvents are necessary to retain a highly porous architecture and optimisation processes can be tedious. The use of a pore templating porogenic solvent may overcome this disadvantage.

An exciting approach to introduce the affinity ligand to the porous surface of a hydrophilic poly(PEGMA-*co*-triethylene glycol dimethacrylate) (TEGMA) was demonstrated using electron beam irradiation induced polymerisation and grafting [56]. The hydrophilic poly(PEGMA-*co*-TEGMA) adsorbent scaffold was selected to prevent non-specific protein interactions. However, since hydrophilic adsorbents can be prone to shrinkage, hydrophilic silica particles were incorporated into the polymerisation mixture, to limit shrinkage and facilitate efficient attachment to walls a polypropylene pipette tip housing. The graft solution, of poly(allyamine), was evenly dispersed throughout the adsorbent bed using centrifugation to yield a pore surface modified with amine functionality. Next, lectin cocanavalin A was immobilised to the surface using a glutardialdehyde spacer/linkage ligand in a reaction that only required 1.5 h. The selective function of the adsorbent material was demonstrated using a mixture of the glycosylated protein ovalbumin and BSA, then analysed using matrix-assisted laser desorption/ionisation (MALDI)-MS. This polymer monolith outperformed commercial AffinSpin ConA adsorbent, with recoveries of 75% and 42% respectively, despite the polymer monolith cocanavalin A adsorbent possessing 5% less of the affinity ligand. The improved performance was attributed to the polymer monolith structures and the high accessibility of the binding sites.

Instead of utilising affinity ligands Krenkova *et al.* developed a series of polymer-nanoparticle hybrids for the selective extraction of phosphopeptides to facilitate

sensitive MS analysis. The first approach reported the hydrophilic poly(HEMA-*co*-EDMA) adsorbent embedded with 50 nm rod shaped hydroxyapatite nanoparticles for extraction based on immobilised metal affinity chromatography interactions (**Figure 1.7A**) [86]. Again, hydrophilic poly(HEMA-*co*-EDMA), fabricated in-capillary, was specifically selected to limit non-specific protein interactions. The capacity of the polymer-monolith hybrid was 14.6 mg g^{-1} of hydroxyapatite, which is comparable to the commercially available hydroxyapatite adsorbents. The utility of the poly(HEMA-*co*-EDMA-hydroxyapatite) was demonstrated to isolate the phosopeptides from a tryptic digest of the α- and β-caseins. Direct MALDI-MS analysis (with no extraction) yielded a spectrum dominated by highly-abundant non-phosphorylated peptides. In contrast, the extraction spectrum for the β-casein digest displayed a significant increase for the three phosphopeptides, while the more complex sample of digested α-casein displayed 10 enriched phosophopeptides. Another approach was demonstrated by electrostatically immobilising 20 nm iron oxide particles on the pore surface of a poly(GMA-*co*-EDMA) adsorbent in-capillary for selective isolation of phosphopeptides using interactions based on metal oxide affinity chromatography [97]. The process of fabrication involved a reaction with the oxirane moieties of GMA with diethylamine followed by a further alkylation with iodoethane to generate a quaternary amine for particle immobilisation. The binding capacity was measured with adenosine-5-triphosphate and determined to be 86 mmol mL^{-1}. For both α- and β-casein the poly(GMA-*co*-EDMA-iron oxide) outperformed poly(HEMA-*co*-EDMA)-hydroxyapatite adsorbent by isolating the 3 phosphopeptides for β-casein and 13 for α-casein. The work was extended to the format of pipette tips but the described process of preparing the poly(GMA-*co*-EDMA-iron oxide) adsorbents was not compatible with the polypropylene pipette tips. A redesigned poly(HEMA-*co*-EDMA) adsorbent was photografted with META to provide the amine functionality for iron oxide immobilisation [59]. Again the polymer monolith with

electrostatically bound iron oxide outperformed the directly embedded hydroxyapatite adsorbent. Both polymer monolith-nanoparticle hybrids showed improved results over the commercially available TiO tip, although it must be acknowledged that the optimum reaction conditions where not used for the TiO tip. It would be exciting to extend this work and showcase these materials for use with more complex samples and phosphorylated samples less abundant than the caseins.

Alwael *et al.* took a different approach where gold nanoparticles were immobilised on the surface of a poly(EDMA) polymer monolith to anchor the affinity ligand *Erythrina cristagalli* lectin (ECL) for the selective extraction of galactosylated glycoproteins [58]. A complex multistep fabrication first involved polymerisation of the poly(EDMA) scaffold which was then photografted with the reactive monomer VAL [98]. VAL presents a superior alternative to GMA as the azalactone readily reacts with a variety of functionalities (thiols, amines and alcohols) facilitating efficient immobilisation of nanoparticles and bioligands [99]. Gold nanoparticles were electrostatically immobilised on VAL (**Figure 1.7B**). The bifunctional linker di(N-hydroxysuccinimide ester) was introduced to the gold nanoparticle surface to provide a stable covalent attachment with the *Erythrina cristagalli* lectin. Finally, to prevent non-specific binding, tris(hydroxymethyl)amino-methane was used to block both the remaining succinimidyl groups and any bare gold adsorption sites. In spite of the complex fabrication, di(N-hydroxysuccinimide ester) readily interacts with any bio-recognition molecules thus presenting the possibility of a universal scaffold with unlimited applications. The adsorbent function was demonstrated with a complex mix of proteins where it displayed a high selectivity towards the glycoproteins containing a terminal galactose (desialylated transferrin and desialylated thyroglobulin) where recovery of the desialylated transferrin was > 86%. Finally, the adsorbent was applied to an *Escherichia*

coli cell lysate sample spiked with galactosylated glycoproteins to successfully demonstrate matrix tolerance.

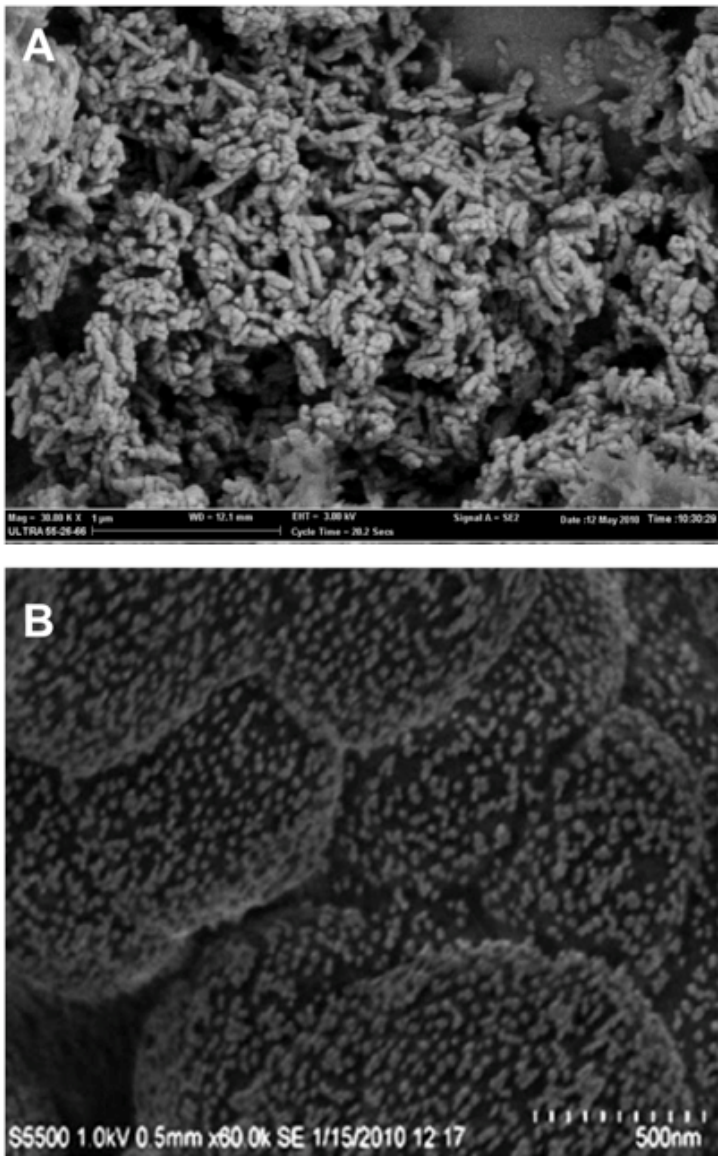

Figure 1.7. Polymer monolith-nanoparticle hybrids, (A) poly(HEMA-*co*-EDMA) directly embedded with hydroxyapatite nanoparticles. Reprinted with permission from ref. [86] Copyright 2010 American Chemical Society. (B). poly(EDMA)-*g*-VAL with covalently attached gold nanoparticles. Reproduced from ref. [58] with permission from The Royal Chemical Society.

Table 1.3. Polymer monoliths adsorbents based on affinity interactions

Monomer Type	Ligand/Nanoparticle	Functionality	Application	Embodiment	Ref.
poly(APPBA-*co*-EDA)		boronate affinity	glycoprotein	stainless steel column	[36]
poly(4-vinyl phenylboronic acid-*co*-EDMA)		boronate affinity	catecholamines	microchip	[26]
poly(GlyMA-co-EDMA)	wheat germ agglutinin, concanavalin A and *Ricinus communis* agglutinin	lectin affinity	glycoprotein	stainless steel column	[96]
poly(PEGMA-*co*-TEGMA)-*g*-poly(allyamine)	cocanavalin A	lectin affinity	glycoprotein	plastic pipette	[56]
poly(HEMA-*co*-EDMA)	hydroxyapatite	immobilised metal affinity	phosphopeptide	capillary and pipette tip	[86]
poly(GMA-*co*-EDMA)	iron oxide	metal oxide affinity	phosphopeptide	capillary	[97]
poly(HEMA-*co*-EDMA)-*g*-META	iron oxide	metal oxide affinity	phosphopeptide	pipette tip	[59]
poly(EDMA)-*g*-VAL	gold nanoparticles, di(N-hydroxysuccinimide ester), *Erythrina cristagalli* lectin	lectin affinity	galactosylated glycoproteins spiked *Escherichia coli* cell lysate	pipette tip	[58]

1.6. Immobilised enzyme reactors for protein digestion.

Polymer monolith immobilised enzyme reactors (IMER) is an area of sample preparation receiving considerable attention to facilitate rapid streamlined workflows. The highly porous architecture provides an idea structure of the immobilisation of enzyme macromolecules, e.g. the endoproteinase trypsin (23 kDa). Fabrication of IMER devices has been extensively reviewed in the last five years for the vast majority support materials [100-102]. The discussion here will be focused on the current movement of fabricating monoliths for IMER. For a summary of the materials discussed in this section please see **Table 1.4**.

Development of biocompatible adsorbents resistant to protein fouling is one major area of interest for IMER scaffolds. Proteins and peptides, in particular the serum albumins, can adsorb non-specifically to surfaces through hydrophobic, hydrogen bonding and ion-exchange interactions and despite extensive washing protocols they can be difficult to remove. Protein fouling caused by the non-specific adsorption leads to considerable disadvantages, active sites can be blocked limiting the re-usability of the IMER device and the carryover of protein and peptide residues can make quantitative proteome analysis challenging. As the introduction of hydrophilic surface functionality can eliminate much of the non-specific adsorption various approaches to prepare hydrophilic adsorbents have been investigated. Hydrophilic materials can be decisive in preserving the proteolysis activity, whereas hydrophobic materials are not favorable. Again, a wide variety of commercially available monomers provides numerous opportunities to realise an adsorbent with the ideal surface chemistries for IMER.

IMERs fabricated from crosslinked GMA are by far the most popular choice for protease immobilisation. Krenkova *et al.* conducted an extensive study to eliminate non-specific binding on these materials. Starting with in-capillary poly(GMA-*co*-EDMA), the adsorbent was sequentially modified to improve hydrophilicity (**Figure 1.8**) [103]. The oxirane moieties were first hydrolysed to generate the diol surface functionality, but even in 20% acetonitrile the bed appeared to visibly adsorb a substantial amount of the fluorescently labeled BSA. A surface layer of PEGMA was photografted on the adsorbent to improve hydrophilicity [98]. The PEGMA surface demonstrated reduced BSA fouling with just 5% acetonitrile. For covalent endoproteinase attachment (trypsin and endoproteinase LysC) a second layer of functional monomer VAL was photografted to the adsorbent. Unlike GMA, the nucleophilic enzyme is covalently bound to the open azalactone surface in a matter of minutes. Digestion of cytochrome c could be achieved in just 1.5 min using a trypsin IMER, while the large globular protein BSA required only 4.5 min digestion time, with a sequence coverage of 93 and 80% respectively. The utility of trypsin and endoproteinase LysC IMERs was also assessed for the 150 kDa protein polyclonal human IgG. While the trypsin IMER provided sequence coverage comparable the solution digestion the endoproteinase LysC was much lower and here the only advantage was the improved reaction kinetics (6 min digestion). However, if the device reproducibly cleaves a series of unique marker peptides that can be assigned using multiple reaction monitoring MS the low sequence coverage is of little consequence.

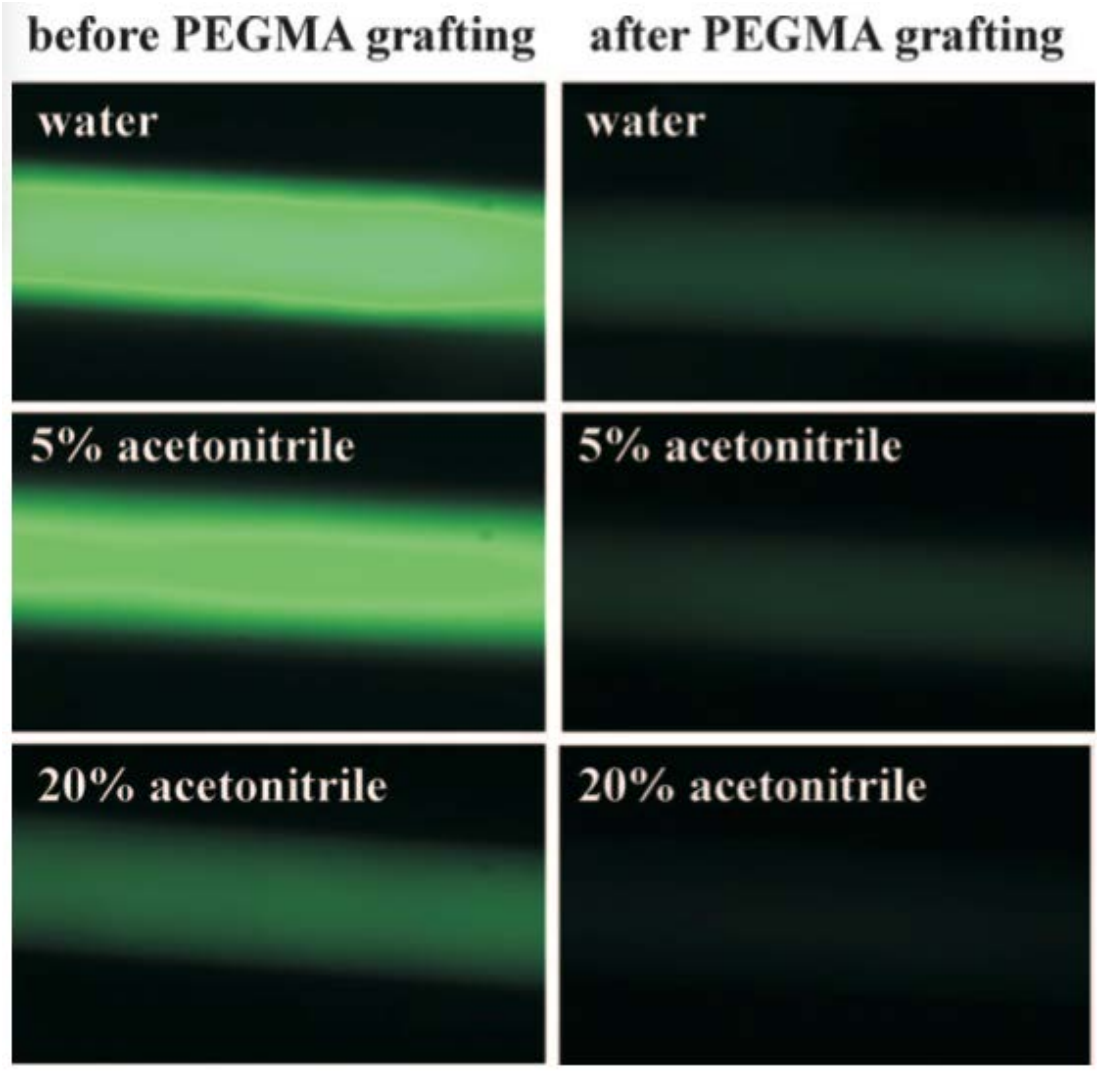

Figure 1.8. The non-specific protein binding with fluorescently labeled BSA poly(GMA-*co*-EDMA) adsorbent sequentially modified to improve the hydophilicity of the surface, on the left the oxirane moiety has been modified to provide a diol and on the right the surface has been photografted with PEGMA. Reprinted with permission from ref. [103] Copyright 2009 American Chemical Society.

Krenkova *et al.* extended this platform for the immobilisation of peptide-N-glycosidase F for the deglycosylation of model proteins [104]. The analysis of deglycosylation product from human IgG was compared for IMER and the in solution assay using off-line MALDI and no observable difference in the reaction products were displayed (**Figure 1.9**). The IMER was integrated into an on-line system comprising on-line

glycan release followed by chromatographic separation and detection with ESI-MS. This enabled sample preparation and analysis to be achieved in only 5.5 min, which is inconceivable for the solution-based assay.

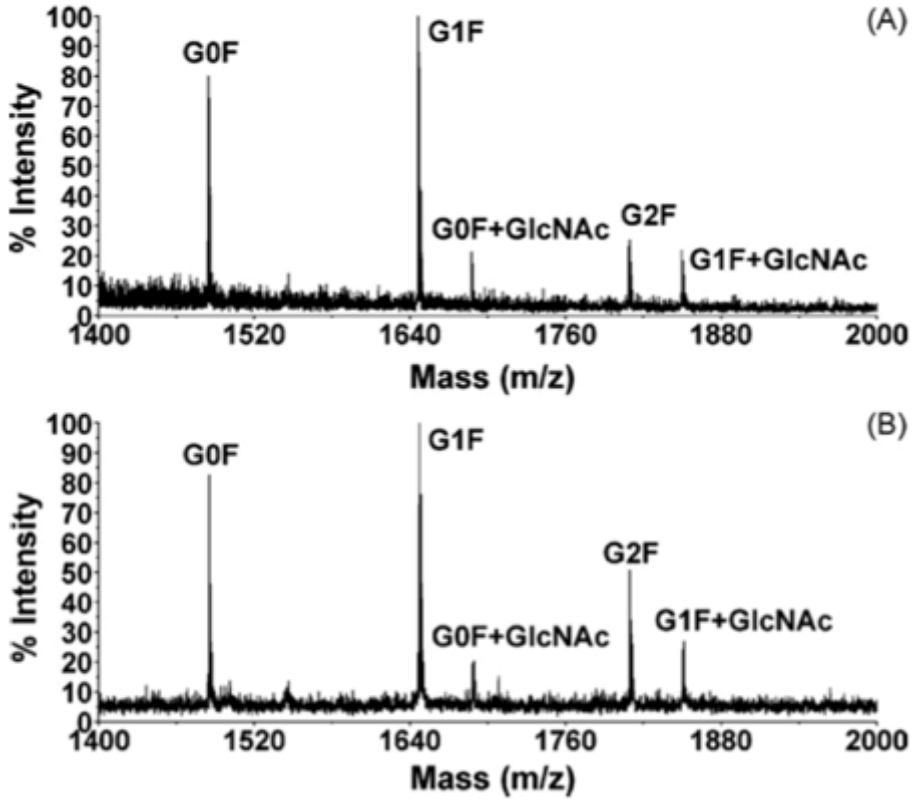

Figure 1.9. The identical MALDI mass spectrum of the N-linked glycans released from hIgG using: (A) PNGase F immobilised on the poly(GMA-co-EDMA) adsorbent (B) soluble PNGase F. Reprinted ref. [104] Copyright 2009 with permission from Elsevier.

In a simplified fabrication process the hydrophilic poly(N-acryloxysuccinimide-*co*-poly(ethylene glycol) diacrylate) (NAS-*co*-PEGDA) adsorbent was fabricated in a microfluidic platform. The succinamide reactivity was exploited to achieve single step trypsin immobilisation in just 4 h [105]. Non-specific binding was also assessed in this approach using fluorescently labeled BSA. When compared with a diol functionalised poly(GMA-*co*-EDMA), the poly(NAS-*co*-PEGDA) displayed much lower fouling. A particulate C_{18} packed electrospray emitter was attached to the microfluidic platform to

interface the digest directly with MS. Again the effectiveness of the device was demonstrated by comparison with a solution-based digestion. Depending on the flow rate the digestion could be achieved in 12-71 sec with a sequence coverage of 61% for myoglobin (MYO). In a commendable move the authors then demonstrated the utility of their platform for the analysis of a randomly selected RPLC fraction of *Escherichia coli* extracts and in three consecutive runs 28 proteins could be identified repeatably.

As the covalent attachment of the enzyme can be time consuming, Gao *et al.* demonstrated an interesting approach to introduce the enzyme to the poly(AAm-*co*-N,N′ -methylenebisacrylamide) (MBA) adsorbent [106]. Trypsin was reacted with NAS under mild polymerization conditions to introduce vinyl functionality to the enzyme itself. The vinylised trypsin was included directly to the polymerisation mixture and crosslinked with the poly(AAm-*co*-MBA). Polymerisation using the initiators tetramethylethylenediamine and ammonium persulfate was investigated at room temperature to prevent enzyme denaturation. Proteolytic activity was assessed using N-α-benzoyl-L-arginine ethyl ester (BAEE) as the model substrate and enzyme encapsulation did not appear to inhibit the enzyme's function. The 49 s digests for MYO and BSA provided sequence coverage of 94 and 29 percent respectively. The utility of the IMER was demonstrated in off-line mode by the digestion of weak anion exchange/RPLC fractions of the real proteome sample, a human liver extract and 16 unique peptides corresponding to 3 proteins could be identified.

Calleri *et al.* presented an important systematic study involving poly(GMA-*co*-diethylene glycol dimethacrylate) IMERs, specifically investigating the effects of adsorbent porosity and the introduction of the hydrophilic monomers GlyMA and acrylamide (AAm) with diol and amine functionalities respectively [39]. The trypsin

was bound to the adsorbents and the digestion yields were studied by using BAEE as a model peptide. A three-fold improvement in catalytic activity was demonstrated when the poly(GMA-*co*-EDMA) displayed increased porosity suggesting greater access of the substrate to the site of the immobilised enzyme. A stronger affinity between the BAEE substrate and the enzyme for GlyMA / AAm absorbents was demonstrated due to improved protein-surface contacts. However, for proteins the authors found that surface hydrophilicity may be detrimental to the affinity between enzyme-substrate as reduced interactions with the hydrophobic proteins was seen.

Almost two decades since the first demonstration of polymer monolith IMER newly developed adsorbents are still compared to in-solution digestion and the time saving advantages reported accordingly; this seems a redundant study as these benefits are well established. Credibly, Hahn *et al.* compared the performance of a relatively hydrophobic poly(GMA-*co*-DVB) IMER fabricated in pipette tips against commercially available IMER tips from two vendor sources [57]. The poly(GMA-*co*-DVB) IMER outperformed commercially available tips from both vendors (based on monolithic silica) for the model proteins α-casein, MYO and BSA with sequence coverage of 83, 89 and 78 respectively. The robustness of the poly(GMA-*co*-DVB) was confirmed by the digestion of α-casein in milk and as well as for the highly abundant proteins (human serum albumin, apolipoprotein A II and IgG) in human serum and for both these applications the sequence coverage for the developed IMER were comparable to the in solution digestion. Researchers must undertake more systematic studies such as the one of Hahn *et al.* to compare newly developed adsorbents IMER to alternative IMERs as only this will truly drive this technology forward and demonstrate the superiority of polymeric monolithic IMER.

Table 1.4. Polymer monoliths adsorbents for IMER

Monomer Type	Enzyme	Application	Embodiment	Ref.
poly(GMA-*co*-EDMA)-*g*-PEGMA & VAL	trypsin and endoproteinase LysC	digestion of model proteins	capillary	[103]
poly(GMA-co-EDMA)-*g*-PEGMA & VAL	peptide-N-glycosidase F	deglycosylation of model proteins	capillary	[104]
poly(NAS-*co*-PEGDA)	trypsin	digestion proteins extracted from fraction of *Escherichia coli*	capillary	[105]
poly(AAm-*co*-MBA)	trypsin covalently linked to NAS	digestion of model proteins	capillary	[106]
poly(GMA-*co*-diethylene glycol dimethacrylate) co-polymerised with GlyMA & AAm	trypsin	digestion of model proteins	capillary	[39]
poly(GMA-*co*-DVB)	trypsin	α-casein in milk and human serum albumin, apolipoprotein A II and IgG in plasma	pipette tips	[57]

1.7. Concluding remarks

Polymer monoliths have now been demonstrated as SPE substrates and IMERs for close to two decades and a wide range of chemistries and functionalities have been explored in detail. Despite extensive investigations the number of commercially available sample preparation products based on organic polymer monoliths remains limited. It is clear that these materials present ideal adsorbents for sample preparation of biological macromolecules as their porous properties enable more efficient mass transfer through the bed, while the well established chemistries enable effective immobilisation of affinity ligands and nanoparticles. Numerous examples have been detailed through this review where these adsorbents, when compared with alternative materials, have a distinct advantage due to the pore structure of the polymer monolith enabling improved accessibility of biological macromolecule analytes to the active sites on the adsorbent bed. In many cases the improved performance was demonstrated regardless of the polymer monoliths possessing a lower polymer immobilised density of the functional ligand. For these reasons, it is well established that polymer monolith adsorbents are ideal for the preparation and purification of biological macromolecules. Exciting possibilities now emerge to investigate these materials in different formats that facilitate both the high throughput sample preparation and analysis. However, the integration of polymer monolith adsorbents into routine laboratories will not be realised if we continue to rely solely on further polymer development. The answer lies in engineering suitable formats and devices to complement these polymer monolithic adsorbents.

IMER displays some of the most appealing performance benefits, but in spite of the innovative and attractive developments in adsorbents and devices this field has stagnated. It is clear that the adequate demonstration of polymer monolith IMER

requires comparison not only with alternative materials but between polymer monolith adsorbents themselves. In addition, any developed technologies have solely focused on enzymatic digestion, as it is the most time-consuming component of the workflow. However, to achieve efficient digestion most proteins must first be reduced and alkylated and these process still occur in solution, which can be time consuming. It may prove interesting to immobilise these chemistries, particularly for on-line and lab-on-a-chip proteomic workflows.

In contrast, both the structure and the inability to effectively prepare adsorbents with a high density of functional groups for interaction have limited the success of polymer monoliths for SPE of low molecular weight species. Regardless, a vast number of publications have been demonstrated but often the only advantage of the polymer monolith is the ease of fabrication and the wide variety of functional monomers available for exploitation. In fact, in this review alone over 20 different types of functional monomer are discussed. It is clear that conventional polymer monoliths do not possess the ideal structure for SPE. While efficient analyte interactions can be achieved, the small surface area available for interaction limits their suitability. While it is possible to fabricate polymer monoliths with large surface areas, little work has been undertaken to identify and optimise the exact pore structure characteristics that provide improved capacities. Developing polymer monoliths with improved structural characteristics and a high density of functionality remains a practical challenge and innovation is required to drive this technology forward.

1.8. References

[1] Smith, R. M. *J. Chromatogr. A* 2003, *1000*, 3–27.

[2] Chen, Y., Guo, Z., Wang, X., Qiu, C. *J. Chromatogr. A* 2008, *1184*, 191–219.

[3] Costa, R. *Crit. Rev. Anal. Chem.* 2014, *44*, 299–310.

[4] Saunders, K. C., Ghanem, A., Boon Hon, W., Hilder, E. F., Haddad, P. R. *Anal. Chim. Acta* 2009, *652*, 22–31.

[5] Poole, C. F., Gunatilleka, A. D., Sethuraman, R. *J. Chromatogr. A* 2000, *885*, 17–39.

[6] Namera, A., Nakamoto, A., Saito, T., Miyazaki, S. *J. Sep. Sci.* 2011, *34*, 901–924.

[7] Nema, T., Chan, E. C. Y., Ho, P. C. *J. Pharmaceut. Biomed. Anal.* 2014, *87*, 130–141.

[8] Hjerten, S., Liao, J. L., Zhang, R. *J. Chromatogr. A* 1989, *473*, 273–275.

[9] Tennikova, T. B., Svec, F., Belenkii, B. G. *J. Liq. Chromatogr.* 1990, *13*, 63–70.

[10] Svec, F., Fréchet, J. M. J. *Anal. Chem.* 1992, *64*, 820–822.

[11] Arrua, R. D., Causon, T. J., Hilder, E. F. *Analyst* 2012, *137*, 5179–5189.

[12] Arrua, R. D., Talebi, M., Causon, T. J., Hilder, E. F. *Anal. Chim. Acta* 2012, *738*, 1–12.

[13] Mair, D. A., Schwei, T. R., Dinio, T. S., Svec, F., Fréchet, J. M. J. *Lab Chip* 2009, *9*, 877–883.

[14] Deverell, J. A., Rodemann, T., Smith, J. A., Canty, A. J., Guijt, R. M. *Sensor. Act. B-Chem.* 2011, *155*, 388–396.

[15] Guiochon, G. *J. Chromatogr. A* 2007, *1168*, 101–168.

[16] Nischang, I., Brüggemann, O., Svec, F. *Anal. Bioanal. Chem.* 2010, *397*, 953–960.

[17] Svec, F., Tennikova, T. B., Deyl, Z. *Monolithic Materials*; Elsevier, 2003.

[18] Petro, M., Svec, F., Fréchet, J. M. J. *Biotechnol. Bioeng.* 1996, *49*, 355–363.

[19] Xie, S., Svec, F., Frechet, J. M. *Chem. Mater.* 1998, *10*, 4072–4078.

[20] Svec, F. *J. Chromatogr. B* 2006, *841*, 52–64.

[21] Viklund, C., Svec, F., Fréchet, J. M. J., Irgum, K. *Chem. Mater.* 1996, *8*, 744–750.

[22] Svec, F., Fréchet, J. M. J. *Chem. Mater.* 1995, *7*, 707–715.

[23] Svec, F. *J. Chromatogr. A* 2012, *1228*, 250–262.

[24] Bratkowska, D., Fontanals, N., Cormack, P. A. G., Borrull, F., Marcé, R. M. *J. Chromatogr. A* 2012, *1225*, 1–7.

[25] Bratkowska, D., Marcé, R. M., Cormack, P. A. G., Borrull, F., Fontanals, N. *Anal. Chim. Acta* 2011, *706*, 135–142.

[26] Cakal, C., Ferrance, J. P., Landers, J. P., Caglar, P. *Anal. Chim. Acta* 2011, *690*, 94–100.

[27] Sýkora, D., Peters, E. C., Svec, F. *Macromol. Mater. Eng.* 2000, *275*, 42–47.

[28] Lubbad, S. H., Buchmeiser, M. R. *J. Chromatogr. A* 2010, *1217*, 3223–3230.

[29] Davankov, V. A., Tsyurupa, M. P. *React. Polym.* 1990, *13*, 27–42.

[30] Urban, J., Svec, F., Fréchet, J. M. J. *Anal. Chem.* 2010, *82*, 1621–1623.

[31] Urban, J., Svec, F., Fréchet, J. M. J. *J. Chromatogr. A* 2010, *1217*, 8212–8221.

[32] Maya, F., Svec, F. *Polymer* 2013, 1–7.

[33] Landers, J., Gor, G. Y., Neimark, A. V. *Colloid. Surface. A* 2013, *437*, 3–32.

[34] Nischang, I. *J. Chromatogr. A* 2013, *1287*, 39–58.

[35] Peters, E. C., Svec, F., Fréchet, J. M. J. *Adv. Mater.* 1999, *11*, 1169–1181.

[36] Yang, F., Lin, Z., He, X., Chen, L., Zhang, Y. *J. Chromatogr. A* 2011, *1218*, 9194–9201.

[37] Peterson, D. S., Rohr, T., Svec, F., Frechet, J. M. *Anal. Chem.* 2003, *75*, 5328–5335.

[38] Yao, K., Yun, J., Shen, S., Wang, L., He, X., Yu, X. *J. Chromatogr. A* 2006, *1109*, 103–110.

[39] Calleri, E., Temporini, C., Gasparrini, F., Simone, P., Villani, C., Ciogli, A., Massolini, G. *J. Chromatogr. A* 2011, *1218*, 8937–8945.

[40] Svec, F. *J. Chromatogr. A* 2010, *1217*, 902–924.

[41] Potter, O. G., Hilder, E. F. *J. Sep. Sci.* 2008, *31*, 1881–1906.

[42] Rohr, T., Ogletree, D. F., Svec, F., Frechet, J. M. *Adv. Funct. Mater.* 2003, *13*, 264–270.

[43] Wang, X., Yi, L., Mukhitov, N., Schrell, A. M., Dhumpa, R., Roper, M. G. *J. Chromatogr. A* 2015, *1382*, 98–116.

[44] Hua, Y., Jemere, A. B., Harrison, D. J. *J. Chromatogr. A* 2011, *1218*, 4039–4044.

[45] Hua, Y., Jemere, A. B., Dragoljic, J., Harrison, D. J. *Lab Chip* 2013, *13*, 2651.

[46] Wang, Z., Jemere, A. B., Harrison, D. J. *Electrophoresis* 2012, *33*, 3151–3158.

[47] Yang, H., Mudrik, J. M., Jebrail, M. J., Wheeler, A. R. *Anal. Chem.* 2011, *83*, 3824–3830.

[48] Mudrik, J. M., Dryden, M. D. M., Lafrenière, N. M., Wheeler, A. R. *Can. J. Chem.* 2014, *92*, 179–185.

[49] Wei, F., Fan, J., Zheng, M.-M., Feng, Y.-Q. *Electrophoresis* 2010, *31*, 714–723.

[50] He, H.-B., Lv, X.-X., Yu, Q.-W., Feng, Y.-Q. *Talanta* 2010, *82*, 1562–1570.

[51] Pietrzyńska, M., Voelkel, A., Bielicka-Daszkiewicz, K. *Anal. Chim. Acta* 2013, 1–21.

[52] Arthur, C. L., Pawliszyn, J. *Anal. Chem.* 1990, *62*, 2145–2148.

[53] Mugo, S. M., Huybregts, L., Mazurok, J. *Anal. Methods* 2014, *6*, 1291.

[54] Altun, Z., Skoglund, C., Abdel-Rehim, M. *J. Chromatogr. A* 2010, *1217*, 2581–2588.

[55] Xie, W., Mullett, W., Pawliszyn, J. *Bioanalysis* 2011, *3*, 2613–2625.

[56] Reichelt, S., Elsner, C., Prager, A., Naumov, S., Kuballa, J., Buchmeiser, M. R. *Analyst* 2012, *137*, 2600.

[57] Hahn, H. W., Rainer, M., Ringer, T., Huck, C. W., Bonn, G. K. *J. Proteome Res.* 2009, *8*, 4225–4230.

[58] Alwael, H., Connolly, D., Clarke, P., Thompson, R., Twamley, B., O'Connor, B., Paull, B. *Analyst* 2011, *136*, 2619.

[59] Krenkova, J., Foret, F. *Anal. Bioanal. Chem.* 2013, *405*, 2175–2183.

[60] Peroni, D., Vanhoutte, D., Vilaplana, F., Schoenmakers, P. J., de Koning, S., Janssen, H.-G. *Anal. Chim. Acta* 2012, *720*, 63–70.

[61] Huang, X., Yuan, D. *J. Chromatogr. A* 2007, *1154*, 152–157.

[62] Huang, X., Qiu, N., Yuan, D., Lin, Q. *J. Chromatogr. A* 2009, *1216*, 4354–4360.

[63] Huang, X., Chen, L., Lin, F., Yuan, D. *J. Sep. Sci.* 2011, *34*, 2145–2151.

[64] Takahashi, T., Odagiri, K., Watanabe, A., Watanabe, C., Kubo, T., Hosoya, K. *J. Sep. Sci.* 2011, *34*, 2925–2932.

[65] Hilder, E. F. *Aust. J. Chem.* 2011, *64*, 843–843.

[66] Hilder, E. F., Hon, W. B. U.S. Patent Application. No. 012766. 2014.

[67] Rohr, T., Hilder, E. F., Donovan, J. J., Svec, F., Frechet, J. M. *Macromolecules* 2003, *36*, 1677–1684.

[68] Hilder, E. F., Svec, F., Fréchet, J. M. J. *J. Chromatogr. A* 2004, *1053*, 101–106.

[69] Hutchinson, J. P., Hilder, E. F., Shellie, R. A., Smith, J. A., Haddad, P. R. *Analyst* 2006, *131*, 215–221.

[70] Connolly, D., Currivan, S., Paull, B. *Proteomics* 2012, *12*, 2904–2917.

[71] Krenkova, J., Foret, F., Svec, F. *J. Sep. Sci.* 2012, *35*, 1266–1283.

[72] Xu, L., Shi, Z.-G., Feng, Y.-Q. *Anal. Bioanal. Chem.* 2010, *399*, 3345–3357.

[73] Camino-Sánchez, F. J., Rodríguez-Gómez, R., Zafra-Gómez, A., Santos-Fandila, A., Vílchez, J. L. *Talanta* 2014, *130*, 388–399.

[74] Gilart, N., Marcé, R. M., Borrull, F., Fontanals, N. *TRAC Trend. Anal. Chem.* 2014, *54*, 11–23.

[75] Huang, X., Lin, J., Yuan, D., Hu, R. *J. Chromatogr. A* 2009, *1216*, 3508–3511.

[76] Huang, X., Qiu, N., Yuan, D., Huang, B. *Talanta* 2009, *78*, 101–106.

[77] Gilart, N., Marcé, R. M., Cormack, P. A. G., Fontanals, N., Borrull, F. *J. Sep. Sci.* 2014, *37*, 2225–2232.

[78] Gilart, N., Cormack, P. A. G., Marcé, R. M., Borrull, F., Fontanals, N. *J. Chromatogr. A* 2013, *1295*, 42–47.

[79] Thabano, J. R. E., Breadmore, M. C., Hutchinson, J. P., Johns, C., Haddad, P. R. *J. Chromatogr. A* 2009, *1216*, 4933–4940.

[80] Tong, S., Zhou, X., Zhou, C., Li, Y., Li, W., Zhou, W., Jia, Q. *Analyst* 2013, *138*, 1549.

[81] Tong, S., Liu, Q., Li, Y., Zhou, W., Jia, Q., Duan, T. *J. Chromatogr. A* 2012, *1253*, 22–31.

[82] Li, W.-J., Zhou, X., Tong, S.-S., Jia, Q. *Talanta* 2013, *105*, 386–392.

[83] Li, W., Zhou, X., Ye, J., Jia, Q. *J. Sep. Sci.* 2013, *36*, 3330–3337.

[84] Zheng, H., Liu, Q., Jia, Q. *J. Chromatogr. A* 2014, *1343*, 47–54.

[85] Qi, R., Jiang, H., Liu, S., Jia, Q. *Anal. Methods* 2014, *6*, 1427–1434.

[86] Krenkova, J., Lacher, N. A., Svec, F. *Anal. Chem.* 2010, *82*, 8335–8341.

[87] Zhou, C., Du, Z., Li, G., Zhang, Y., Cai, Z. *Analyst* 2013, *138*, 5783.

[88] Arrua, R. D., Alvarez Igarzabal, C. I. *J. Sep. Sci.* 2011, *34*, 1974–1987.

[89] Sproß, J., Sinz, A. *J. Sep. Sci.* 2011, *34*, 1958–1973.

[90] Li, H., Liu, Z. *TRAC Trend. Anal. Chem.* 2012, *37*, 148–161.

[91] Li, J., Zhai, H., Chen, Z., Zhou, Q., Liu, Z., Su, Z. *J. Sep. Sci.* 2013, *36*, 3608–3614.

[92] Su, Z., Zhai, H., Chen, Z., Zhou, Q., Li, J., Liu, Z. *Anal. Bioanal. Chem.* 2013, *406*, 1551–1556.

[93] Szumski, M., Grzywiński, D., Prus, W., Buszewski, B. *J. Chromatogr. A* 2014, *1364*, 163–170.

[94] Mönster, A., Hiller, O., Grüger, D., Blasczyk, R., Kasper, C. *J. Chromatogr. A* 2011, *1218*, 706–710.

[95] Brgles, M., Clifton, J., Walsh, R., Huang, F., Ručević, M., Cao, L., Hixson, D., Müller, E., Josic, D. *J. Chromatogr. A* 2011, *1218*, 2389–2395.

[96] Selvaraju, S., Rassi, El, Z. *J. Sep. Sci.* 2012, *35*, 1785–1795.

[97] Krenkova, J., Foret, F. *J. Sep. Sci.* 2011.

[98] Stachowiak, T. B., Svec, F., Fréchet, J. M. J. *Chem. Mater.* 2006, *18*, 5950–5957.

[99] Coleman, P. L., Walker, M. M., Milbrath, D. S., Stauffer, D. M., Rasmussen, J. K., R Krepski, L., Heilmann, S. M. *J. Chromatogr. A* 1990, *512*, 345–363.

[100] Calleri, E., Ambrosini, S., Temporini, C., Massolini, G. *J. Pharmaceut. Biomed. Anal.* 2012, *69*, 64–76.

[101] Safdar, M., Sproß, J., Jänis, J. *J. Chromatogr. A* 2014, *1324*, 1–10.

[102] Krenkova, J., Svec, F. *J. Sep. Sci.* 2009, *32*, 706–718.

[103] Krenkova, J., Lacher, N. A., Svec, F. *Anal. Chem.* 2009, *81*, 2004–2012.

[104] Krenkova, J., Lacher, N. A., Svec, F. *J. Chromatogr. A* 2009, *1216*, 3252–3259.

[105] Liang, Y., Tao, D., Ma, J., Sun, L., Liang, Z., Zhang, L., Zhang, Y. *J. Chromatogr. A* 2011, *1218*, 2898–2905.

[106] Gao, M., Zhang, P., Hong, G., Guan, X., Yan, G., Deng, C., Zhang, X. *J. Chromatogr. A* 2009, *1216*, 7472–7477.

Candish. E. Gooley, A., Wirth, H-J., Dawes, P. A., Shellie, R. A. & Hilder, E. F. 2012. A simplified approach to direct SPE-MS. J. Sep. Sci. 35, 2399–2406

3. Polymer monoliths with large surface area for solid phase extraction: a comprehensive evaluation of their suitability

3.1. Introduction

Polymer monoliths have been extensively explored as an alternative to particulate materials for chromatography and sample preparation due to the unique features of their structural morphology. These adsorbents can be tailored to present a highly permeable macroporous structure, permitting fast fluid flows while maintaining low backpressures. Further, the polymeric microglobules possess non-porous highly crosslinked cores therefore any interactable surface is accessible by a small diffusion distance [1]. Consequently, these materials can provide improved solute mass transfer kinetics. Despite these attractive features bed heterogeneity has limited the realisation of these materials as genuinely competitive materials for high efficiency chromatographic applications [2]. Unlike chromatographic separations, sample preparation seeks binary analyte interactions (on/off; retained/unretained); thus is less sensitive to the heterogeneous adsorbent structure. Polymer monoliths have the potential to offer genuine benefit in the sample preparation domain.

Typically, polymer monoliths have a lower extraction capacity than particles, the capacity of an adsorbent bed is strongly related to the surface area available for interaction, thus a greater surface area affords improved assay sensitivity. Whereas surface areas of up to 1000 $m^2 g^{-1}$ are common for polymer particles, polymer monoliths generally display very small surface areas (< 20 $m^2 g^{-1}$). While micro (0.3 to 2 nm) and mesopores (2 to 50 nm) have been suggested in polymer monolith structures their quantity is substantially lower than for particulate adsorbents. Approaches to prepare a

polymer monolith with a bimodal porous structure and an associated large surface area can be divided into two distinct categories; the first approach is to incorporate a high degree of internal crosslinking in the polymer network. Increased crosslinking at an early stage in the polymerisation results in a large number of swollen nuclei that aggregate to form the globular structure typical of a polymer monolith [3]. Voids between aggregated nuclei deliver micro- and mesoporosity that drive up the surface area of the polymer monolith [3]. Increased crosslinking has been demonstrated using an elevated percentage of crosslinking monomer [4-6] and by prematurely terminating the polymerisation reaction [7-9]. Polymer monoliths, which contain a high concentration of the crosslinking monomer divinyl benzene (DVB), possess surface areas as large as 490 m^2g^{-1} [10]. The second approach to generate a large surface area polymer monolith is through extensive post-crosslinking of a pre-formed polymer using a Davankov reaction [11]. The reactive monomer 4-vinylbenzyl chloride (VBC) can be incorporated into the precursor polymer to act as an internal electrophile, followed by a Friedel-Craft's alkylation to produce structural bridges between neighboring phenyl groups for increased surface porosity [12, 13]. Urban *et al.* recently applied this method to polymer monoliths and demonstrated the increased surface area of a polymer monolith precursor from 29 m^2 g^{-1} to 663 m^2 g^{-1} [14, 15]. This was extended by Maya *et al.* who used an external crosslinker to prepare polymer monoliths with surface areas as great as 900 m^2 g^{-1} [16]. Given the large obtainable surface areas of these polymer monoliths their superiority for SPE is often assumed. Despite these assumptions the suitability of large surface area polymer monoliths for SPE still remains inconclusive and a detailed characterisation is necessary uncover any cause-effect relationships that may provide benefits or disadvantages for SPE.

In this study large surface area polymer monoliths were investigated and a detailed investigation of their physical properties was performed to accurately determine the adsorbents' suitability for SPE applications. Two classes of polymer monoliths (the first prepared from a high concentration of crosslinking monomer and the second using a hypercrosslinking reaction) were selected as representative approaches for the fabrication. The resulting polymer monoliths were investigated using frontal analysis with the probe analytes anisole, phenol and cortisone to explore *adsorption behavior*, *capacity* and *surface area*. In addition, the *porous properties* of these materials were characterised by mercury intrusion porosimetry, scanning electron microscopy (SEM) and argon adsorption/desorption to any unravel links between physical characteristics and extraction performance. Additionally, we have benchmarked the performance of the polymer monolith adsorbents against commercially available polymer particulate adsorbents. This information may help in promoting better understanding polymer monolith morphologies and could be of assistance in further tailoring their physical properties as SPE adsorbents.

3.2. Experimental section

3.2.1 Chemicals and materials

DVB (containing 80% 1,3-DVB + 1,4-DVB and 20% -ethyl-3-vinyl benzene + 1-ethyl-4-vinyl benzene), (97%), Styrene (Sty) (99%), VBC (99%), 1-dodecanol, toluene, benzophenone (99%), 1,2 dichloroethane (DCE) (anhydrous 99.8%), ferric chloride, anisole, cortisone, and phenol were all purchased from Sigma Aldrich (Castle Hill, Australia). Inhibitors were removed by passage through a packed bed of basic alumina. The initiator 2,2'-azo-bis-isobutyronitrile (AIBN) was obtained from MP Biomedicals (Santa Ana, CA, USA) and purified by recrystallisation with methanol. High

performance liquid chromatography (HPLC) grade methanol was purchased Sigma Aldrich and water was purified with a Milli-Q system (Millipore, Bedford, MA, USA).

Polyethylene (PE) tubing (1.57 mm i.d.) was obtained from SDR Scientific (Chatswood, Australia). The MEPS cartridge assembly included frits, shank and needle hub components. The particulate MEPS cartridge contained a 2.5 mm PE inner lining and was packed with 85 µm poly(Sty-*co*-DVB); both were provided by SGE Analytical Science (Ringwood, Australia).

3.2.2 Instrumentation

A Spectrolinker XL-1000 UV Crosslinker fitted with six 254 nm bulbs was employed for photografting PE tubing (VWR Scientific, Murarrie, Australia). All polymerisations were undertaken by thermal initiation in a water bath (PolyScience, Niles, IL, USA).

The performance of the SPE adsorbents was assessed using an ICS3000 system (ThermoScientific, Scoresby, Australia) consisting of two quaternary solvent pumps, an autosampler and an Ultraviolet (UV) detector with an 11 µL flow cell. A ProteCol C18 (4.6 mm i.d. × 250 mm) HPLC column was employed to analyse analyte recovery from the off-line SPE extraction (SGE Analytical Science). All MEPS assemblies comprised a cartridge coupled to 100 µL controlled directional flow (CDF)-MEPS syringe driven by a hand held semi automated analytical syringe (SGE Analytical Science). Chromatograms were achieved isocratically using 80:20 methanol:water v/v at a flow rate of 1 mL min^{-1}.

The macroporous properties of the adsorbents were measured using an Autopore IV mercury intrusion porosimeter. The Brunauer–Emmett–Teller (BET) surface area and

microporosity were assessed using a Tristar II analyser for the argon adsorption/desorption at 77 K (Particle and Surface Science, Gosford, Australia). Microporous surface area was determined using t-plots and the pore size was assessed using the non-localised density functional theory (NLDFT), as no specific model is available for large surface area polymer monoliths either a cylindrical or slit pore geometry was assumed and the model was selected based on the goodness of fit of the data.

The surface morphologies of the polymer monoliths were analysed using a Hitachi SU-70 field emission scanning electron microscope (SEM) in the Central Science Laboratory, University of Tasmania. The polymer monoliths were either sputter-coated with platinum or imaged directly.

3.2.3 Preparation of the polymer monolith SPE adsorbents

PE tubing surface was modified using the single step photografting approach described by Rohr *et al.* [17]. Briefly, the PE tubing was filled with a 1:1 w/w mixture of MMA and EDMA with 3% w/w benzophenone. The tubing was then irritated with at 254 nm for 15 min. All residual polymerisation mixture was rinsed from the tube with methanol and air-dried.

The compositions of poly(VBC-*co*-Sty-*co*-DVB) were adapted from Urban and coworkers [15]; polymer monoliths prepared from poly(DVB) were based on an approach described by Sýkora *et al* [4]. Briefly, the poly(VBC-*co*-Sty-*co*-DVB) was prepared from 18% w/w toluene, 42% w/w dodecanol and 24% w/w DVB. The composition of VBC and Sty was varied to provide 8% w/w, 12% w/w and 16% w/w VBC. The poly(DVB) adsorbents were prepared from 8% w/w toluene, 52% w/w

dodecanol and 40% w/w DVB. All polymerisation mixtures were prepared in glass vials and sonicated for 2 min then purged with nitrogen for 10 min.

Polymerisations were carried out at a temperature of 60 °C for 20 h for poly(VBC-*co*-Sty-*co*-DVB). For the poly(DVB) adsobent 70°C was employed and the polymerization was terminated at 90, 180 and 360 mins. Soxhlet extraction with acetone for 12 h was employed to remove any residual polymerisation mixture from all formed polymer monoliths, whether prepared in glass vials or in PE tubing. The polymers were then dried under vacuum at 25 °C overnight.

The post-polymerisation hypercrosslinking reaction of the poly(VBC-*co*-Sty-*co*-DVB) has been previously described by Urban *et al* [15]. The bulk polymer monolith was swollen in 10 mL of DCE for 2 h and the PE tubes containing polymer monolith were flushed with DCE for 2 h at a flow rate of 120 µL h^{-1}. A saturated solution of $FeCl_3$ (1 g) was prepared in 10 mL of DCE. A 250 µL aliquot was flushed over the polymer monoliths in PE tube for 2 h at a flow rate of 120 µL h^{-1}. The solution of swollen bulk polymer monolith was placed in an ice bath and the $FeCl_3$ solution was added and left for 2 h. Both the bulk and the polymer monoliths in tubes were reacted at 80 °C for 20 h. The products were Soxhlet extracted with acetone for 12 h and dried under vacuum overnight.

For testing in the MEPS format, the MEPS cartridges were filled with polymer monolith sections weighing 2 ± 0.2 mg and once assembled the cartridges were flushed with 8 mL of 95:5 methanol:water v/v to remove any residual polymerisation mixture.

3.2.4 Adsorbent performance

Frontal analysis was employed to determine breakthrough times, adsorption behavior and capacities of the polymer monolith SPE adsorbents. The MEPS cartridge was inserted between the dual quaternary pump and the UV detector. Pump 1 delivered the solvent solutions while Pump 2 delivered the aqueous analyte solution. Unless otherwise stated, a methanol solution refers to methanol:water (95:5 v/v) and aqueous solution refers to water:methanol (95:5 v/v). The adsorbent was first conditioned with methanol solution using a continuous flow of 2.5 mL at 1 mL min^{-1} then equilibrated with 2.5 mL aqueous solution at the same flow rate. The analyte in aqueous solution was continuously pumped over the adsorbent bed and the cartridge effluent was monitored at 254 nm. Uracil was employed as the t_0 marker compound to determine the void volume of the system.

Recovery was determined by off-line extraction. The MEPS cartridge was attached to a 100 µL CDF-MEPS syringe which was driven by a digital syringe drive (see **Appendix B**). Sample and solvent were aspirated into the syringe barrel with the valve in position 2 and dispensed with the syringe valve in position 1 *via* the modified MEPS needle [18]. The flow rate to aspirate was 3.5 mL min^{-1} (the highest programmable speed, 1.2 second aspiration) and dispense was achieved at 0.428 mL min^{-1} (66 second total extraction time) and 1.0 mL min^{-1} (36 second total extraction time). The flow rates for dispense were selected to replicate flow rates for frontal analysis. The extraction workflow involved first preconditioning with 100 µL of methanol and then 100 µL water. Next, a 100 µL aliquot of the 400 mg L^{-1} anisole in aqueous solution was applied to the adsorbent, any unretained compounds were removed with 100 µL water. The analyte was eluted with 100 µL methanol. The amount recovered was determined by

comparing the peak area for an extracted anisole solution with a non-extracted anisole solution.

3.3. Results and discussion

3.3.1 Large surface area polymer monoliths

Three categories of adsorbents were selected to investigate the suitability of polymer monoliths as SPE adsorbents. Polymer monoliths were prepared in bulk as well as *in situ* for characterisation. **Category I** comprised poly(VBC-*co*-Sty-*co*-DVB) precursor adsorbents that contained 8, 12, or 16% VBC. These polymer monoliths provided a small surface area performance benchmark. **Category II** adsorbents were prepared by swelling the poly(VBC-*co*-Sty-*co*-DVB) adsorbents in DCE followed by reaction with $FeCl_3$ at 80°C for 20 h to introduce external crosslinking to the adsorbent. **Category III** polymer monoliths were prepared from poly(DVB) to achieve an extensive internally crosslinked polymer network. As the highest grade DVB is only 80% (the rest is predominately ethyl styrene), termination of the polymerisation reaction at 90 min, 180 min and 360 min was investigated to prevent the formation of a lightly crosslinked monovinyl surface layer which may block the analyte access to any micro- and mesopores [19].

3.2 Frontal analysis

Frontal analysis was employed to evaluate both analyte adsorption and capacity of the adsorbent using anisole as a probe molecule, to provide a comparison between all polymer monolith adsorbents, and to aid selection of the best performing adsorbent from each class. The void volume of the system was determined to be approximately 80

µL. Analyte breakthrough (V_B) is defined as the volume corresponding to 1% of the maximum signal, calculated from **Equation 3.1**,

$$V_B = V_R - 2\sigma_v \quad (3.1)$$

where V_R is the retention volume determined from the inflection point of the curve and σ_v is the standard deviation of the derivative curve as described by Bielicka-Daszkiewicz and coworkers [20]. **Figure 3.1** shows the breakthrough curves for all investigated adsorbents using 400 mg L^{-1} of anisole in aqueous solution and a flow rate of 0.5 mL min^{-1}.

For all small surface area precursor adsorbents the breakthrough curve for anisole mirrored the breakthrough of the unretained uracil (80 µL) (**Figure 3.1A**), highlighting the necessity of a large available surface area for analyte interaction. These small surface area polymer monoliths were considered unsuitable for SPE and were not assessed further. Following the hypercrosslinking reaction of poly(VBC-*co*-Sty-*co*-DVB) materials, breakthrough did not occur until approximately 700 µL of the aqueous anisole solution had been passed through the cartridge. Interestingly, all hypercrosslinked poly(VBC-*co*-Sty-*co*-DVB) polymer monoliths yielded the same breakthrough time for anisole (**Figure 3.1B**). To confirm this result the analyte concentration was reduced to 40 mg L^{-1} and the assay was repeated for hypercrosslinked poly(VBC-*co*-Sty-*co*-DVB) with 12 and 16%. Again, for the two adsorbents, the breakthrough occurred at very similar times 7.32 mL and 7.43 mL respectively. Urban *et al.* have reported that the dry state surface area increases as the content of VBC is raised in the polymerisation mixture from 8% to 16% (300 m^2g^{-1} to 600 m^2g^{-1}) and our results reveal the same trend (see **Appendix C**) [15]. Given that the increase in the analyte loading capacity was not equivalent with the increase in dry state surface area only the hypercrosslinked poly(VBC-*co*-Sty-*co*-DVB) adsorbent containing 16% VBC

is discussed further. Poly(DVB) adsorbents displayed increasing anisole V_B with longer polymerisation times (**Figure 3.1C**). This is likely due to an increased amount of small voids between forming microglobules that may provide additional sites for interaction. The 360 min polymerised poly(DVB) adsorbent had the best performance of all assessed adsorbents with an anisole V_B = 1.15 mL.

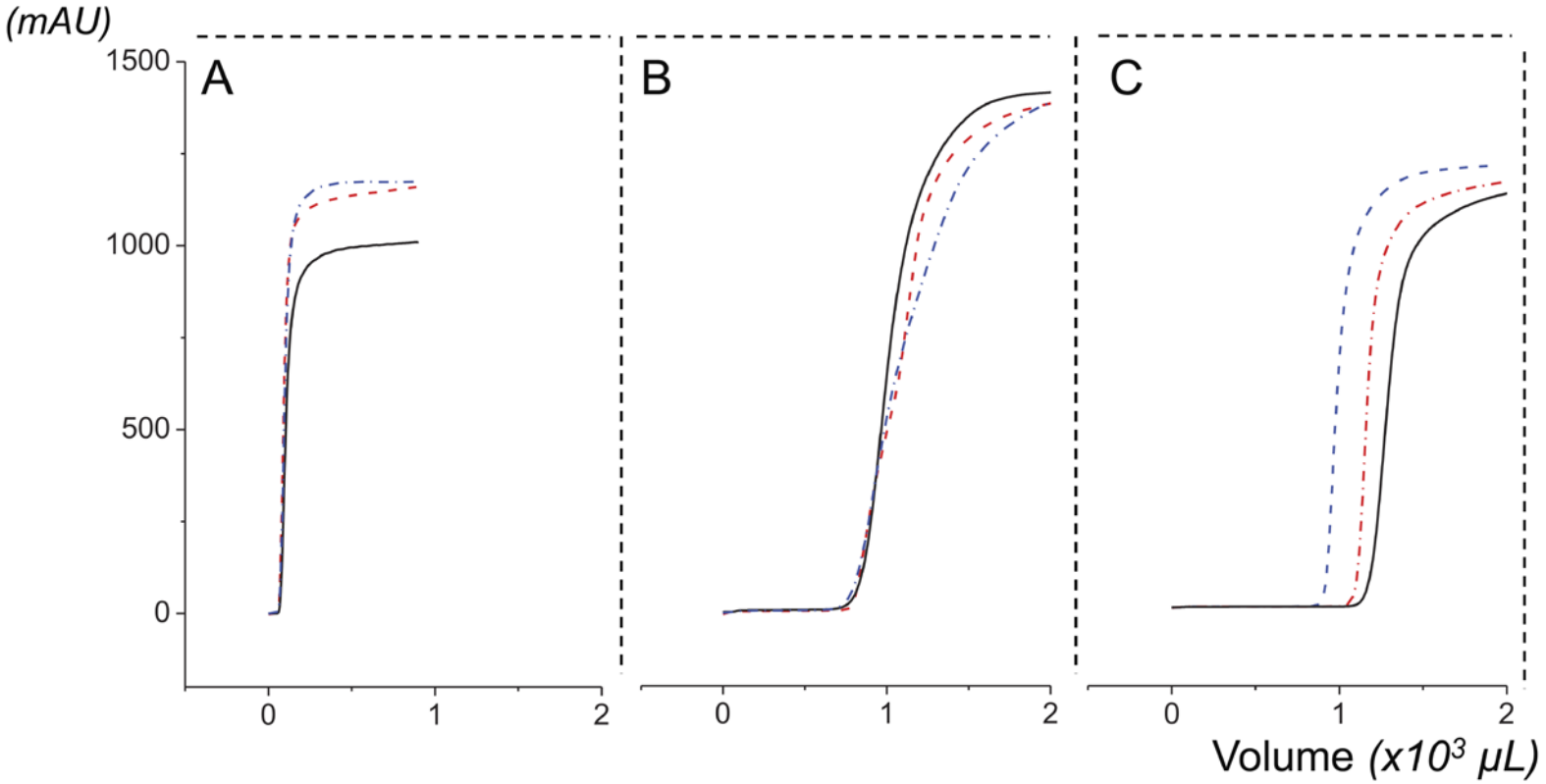

Figure 3.1. The anisole (400 mg L^{-1}) breakthrough curves with adsorbents from each of the three categories. A) Small surface area precursors 8% (---), 12% (—)and 16% (-·-) VBC. B) Hypercrosslinked poly(VBC-*co*-Sty-*co*-DVB) adsorbents 8 (---), 12 (—) and 16 (-·-) % VBC. C) poly(DVB) - polymerization terminated at 90 (---), 180 (-·-) and 360 min (—).

The best performing polymer monoliths hypercrosslinked poly(VBC-*co*-Sty-*co*-DVB) with 16% VBC and poly(DVB) polymerised for 360 mins were further probed using anisole adsorption. The time of retention (t_R) was obtained for anisole concentrations of 400, 300, 200, 100 and 40 mg L^{-1} in aqueous solution and used to determine the amount of analyte adsorbed (q_c),

$$q_c = (t_R - t_0) f C \quad (3.2)$$

where t_0 is the void time, f is flow rate and C is analyte concentration. The adsorption isotherm for each adsorbent was constructed and can be seen in **Figure 3.2**. The semi-reciprocal plot was employed to linearise the data and validate the applicability of the Langmuir equation (**Equation 3.3**),

$$q_c = \frac{q_m K_a C}{1 + K_a C} \quad (3.3)$$

where q_m is maximum capacity, and K_a is binding constant. The high correlation coefficients of the linearised data indicate that adsorption of anisole on all adsorbents can be expressed by the Langmuir isotherm (**Table 3.1**).

In the case of poly(DVB) the lower model fit may be due to textural surface heterogeneity. The maximum capacity (q_m) of the polymer monoliths and the binding constant (K_a) were determined from a direct least squares analysis of the adsorption data. The hypercrosslinked poly(VBC-*co*-Sty-*co*-DVB) displays a steeper initial slope of the adsorption isotherm for the anisole probe (**Figure 3.2**) which is expressed by the higher K_a. The enhanced affinity is connected to the large surface area and the subsequent high volume of small micro and mesopores which lead to intensified π- π interactions [21, 22]. Despite the greater the analyte affinity (K_a) for the hypercrosslinked poly(VBC-*co*-Sty-*co*-DVB) this adsorbent displayed a lower maximum adsorption capacity than the poly(DVB) adsorbent.

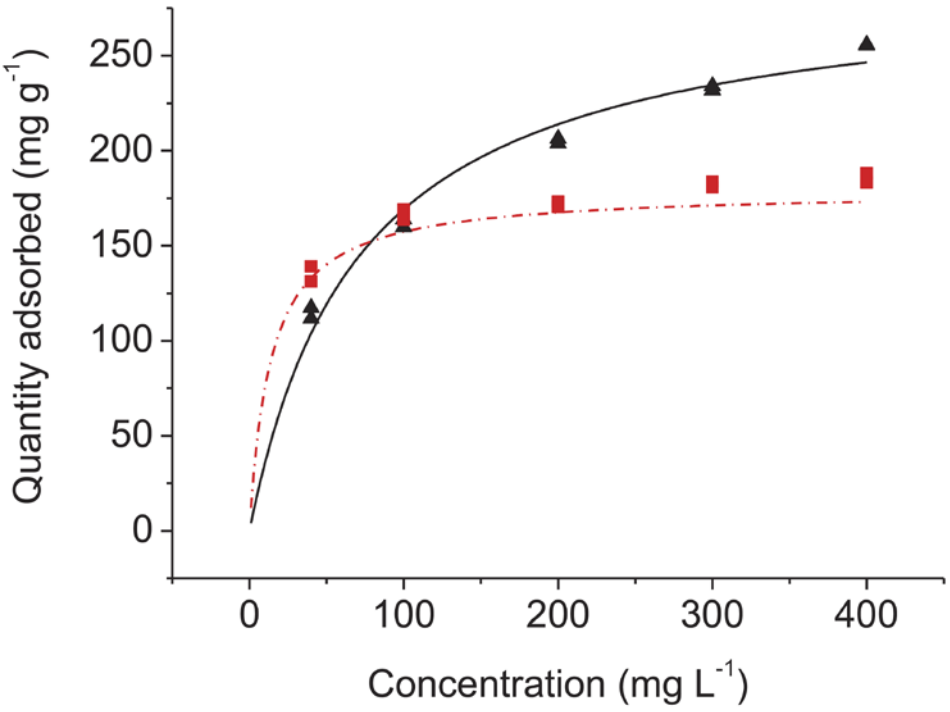

Figure 3.2. A) Langmuir isotherms of anisole on hypercrosslinked poly(VBC-*co*-Sty-*co*-DVB) (■), and poly(DVB) (▲).

The specific surface area (S) of each adsorbent was calculated by,

$$SSA = \frac{q_m/_{MW}}{\alpha_{anisole} N_{Avo}} \qquad (3.4)$$

where *MW* is the molecular weight of the well retained probe molecule (anisole), $\alpha_{anisole}$ is the occupied surface area of one anisole molecule (0.32 nm^2, assuming the anisole molecule is lying flat on the adsorbent surface, 6.84 × 4.67 = 32 $Å^2$) and N_{Avo} is the Avogadro number (6.023 × 10^{23} mol^{-1}). The poly(DVB) revealed a surface area substantially greater than for the hypercrosslinked poly(VBC-*co*-Sty-*co*-DVB) (**Table 3.1**).

Table 3.1. The parameters of the Langmuir equation and calculated specific surface area determined from the adsorption of anisole on adsorbents solvated in an aqueous environment.

Adsorbent	r^2	q_m (mg g^{-1})	K_a (L mg^{-1})	SSA (m^2 g^{-1})
Hypercrosslinked	0.998	191	60.97	341
$DVB_{monolith}$	0.993	298	13.91	518

The ability for an adsorbent to effectively extract an analyte from an aqueous solution significantly depends on both the chemical structure of the analyte and the adsorbent phase itself. Therefore, a broader study of the adsorbent suitability was conducted using a range of analytes. Retention factor (*k'*), V_B and V_R as well as the q_c were investigated. The performance was evaluated for both polymer monoliths and compared with a conventional SPE particulate adsorbent, 85 µm poly(Sty-*co*-DVB). The adsorption data for 100 mg L^{-1} anisole (0.23 – 0.42 nm^2), phenol (0.20 – 0.36 nm^2) and cortisone (0.47-0.97 nm^2) in aqueous solutions is provided in **Table 3.2**. Both polymer monolith adsorbents, displayed a high V_R for the small aromatic's, anisole and phenol. However, the V_R of the higher molecular weight analyte, cortisone, was very low. By reducing the cortisone concentration to 10 mg L^{-1} the V_R was improved to 832 µL and 980 µL for poly(VBC-*co*-Sty-*co*-DVB) and poly(DVB) respectively. This indicates that the surface area available to cortisone was saturated at the higher analyte concentration. In contrast, the retention of cortisone from the 100 mg L^{-1} solution was substantially higher for the particulate poly(Sty-*co*-DVB) adsorbent. This highlights that a greater understanding into the pore structure of large surface area polymer monoliths is necessary to fully understand their utility for SPE.

Table 3.2. Capacity factor, breakthrough volume and retention volume and amount of analyte adsorbed for adsorbents.

Adsorbent	***k′***	**V_B (µL)**	**V_R (µL)**	**q_c (mg g^{-1})**
Hypercrosslinked				
Anisole	39	1937	3127	142
Phenol	12	332	951	43
Cortisone	0	0	18	1
$DVB_{monolith}$				
Anisole	35	2450	2828	127
Phenol	6	285	442	20
Cortisone	1	25	78	3
Sty-co-$DVB_{particle}$				
Anisole	33	0	2793	139
Phenol	4	0	327	16
Cortisone	12	0	992	49

3.3.3 Characterisation of pore structure

The porous morphology of the large surface area polymer monoliths was investigated with mercury intrusion porosimetry, SEM and argon adsorption/desorption. Low resistance to flow is an essential criterion for SPE to ensure high flow rates can be employed without exceeding the backpressure limitations of the extraction device. Mercury intrusion porosimetry was employed to characterise the macroporous porous properties of the adsorbent. **Table 3.3** lists the median pore size of both the adsorbents investigated; both have a pore size greater than 5 µm to facilitate fast operational fluid flow.

Table 3.3. Characteristics of adsorbents in the dry state obtained from argon adsorption/desorption at 77K and mercury intrusion porosimetry.

Adsorbent	**S_{BET} (m^2g^{-1})**	**$S_{Micropore}$ (m^2g^{-1})**	**Pore volume (cm^3g^{-1})**	**Micropore volume (cm^3g^{-1})**	**Macropore size (µm)**
Hypercrosslinked	817	810	0.381	0.368	12
$DVB_{monolith}$	531	505	0.295	0.252	7
Sty-*co*-$DVB_{particle}$	969	234	1.463	0.101	

Scanning electron micrographs display the clustered globule morphology typical of organic polymer monoliths. Both materials are made up of interconnected globules of approximately 5 µm in diameter (**top Figure 3.3**). At higher magnification the surface of the hypercrosslinked poly(VBC-*co*-Sty-*co*-DVB) polymer monolith appears smooth and homogenous (**Figure 3.3A**). In contrast, the surface morphology of poly(DVB) appears considerably textured, with small polymeric microspheres on the order of 5 – 10 nm agglomerating to provide a rough surface to the globular structure (**Figure 3.3B**). These textural voids between the polymeric microspheres could be considered as heterogeneous mesoporosity. As the platinum coating can mask these small features the differences between the adsorbents was confirmed by imaging without the platinum coating. The bottom micrograph in **Figure 3.3A-B** confirm that the surface of the poly(DVB) is considerably more textured.

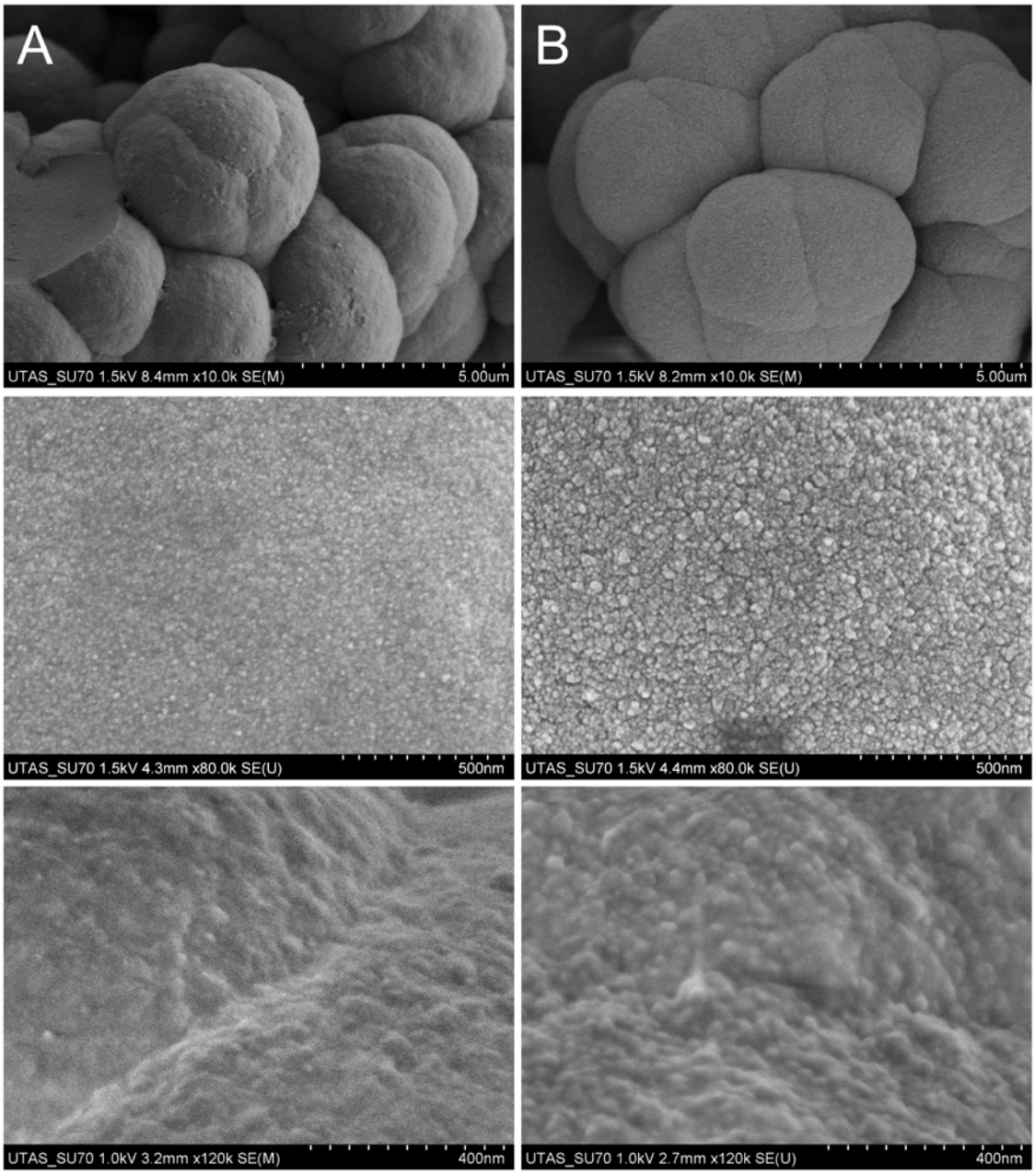

Figure 3.3. The SEM images of polymer monoliths prepared from A) hypercrosslinked poly(VBC-*co*-Sty-*co*-DVB) and B) poly(DVB). In the top (10 000 x magnification) and middle micrographs (80 000 x magnification) the adsorbents have been platinum coated. In the bottom (1200 000 x magnification) micrographs the adsorbents were imaged directly without a platinum coating.

The dry state surface area of the polymer monoliths was measured by BET for comparison with anisole's Langmuir adsorption isotherm measured in the solvated state. **Figure 3.4** compares argon adsorption/desorption isotherms of the hypercrosslinked poly(VBC-*co*-Sty-*co*-DVB) and poly(DVB) polymer monolith and identifies the observable similarities and differences with the conventional particulate poly(Sty-*co*-DVB) adsorbent. The isotherm for hypercrosslinked poly(VBC-*co*-Sty-*co*-DVB) can be classified as *Type I*, indicative of micropores, with *Type H4* hysteresis that is characteristic of narrow slit pores in the micropore region. Further analysis of the pore size by NLDFT indicates a homogenous pore size distribution with pores of approximately 1 nm. The pore structure of hypercrosslinked adsorbents has been likened to a microporous netting [23]. The isotherm for poly(DVB) is also classified by a *Type I* isotherms. However, following the micropore saturation, the knee of the isotherm is wide and no clear plateau attained. This hysteresis loop can be classified as a *Type H2*, indicating the presence of disordered mesopores with a broad size distribution and no distinguishable shape [24]. Pore size analysis by NLDFT indicated more heterogeneous pore size distribution with pores ranging from 1 to 6 nm. This supports the data visually obtained by SEM.

The isotherm of the particulate poly(Sty-*co*-DVB) adsorbent is in stark contrast to the polymer monolith adsorbents. **Figure 3.4C** is described as a *Type IV* isotherm typical of an adsorbent consisting of both meso- and micropores. This isotherm possesses two sharp inclines, the first at low relative pressures (P/P_0) highlights the substantial amount of micropores. The second distinct incline near saturation pressure indicates a high density of mesopores. The hysteresis loop can also be classified as *Type H2* suggesting a wide distribution in mesopore size, further analysis by NLDFT reveals a substantial

portion of microposity at 1-2 nm along with a dominant portion of mesopores ranging from 2 nm to 100 nm.

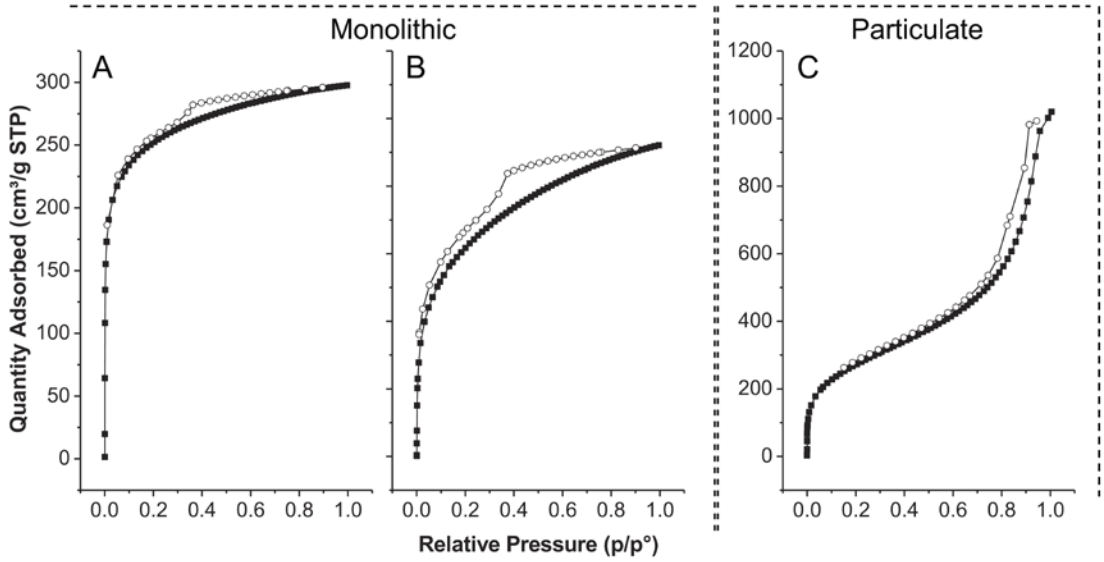

Figure 3.4. Argon adsorption/desorption isotherms of argon at 77 K for adsorbents A) hypercrosslinked poly(VBC-*co*-Sty-*co*-DVB), B) poly(DVB) and for comparison C) poly(Sty-*co*-DVB) particulate.

An elevated surface area of large surface area polymer monoliths is often attributed to the presence of mesoporous. In this study, the vast majority of the surface area of polymer monoliths is in fact recognised as micropores (**Table 3.3**). The microporous structure of the large surface area polymer monoliths provides a key insight to the reduced V_R of the higher molecular weight analtye, cortisone seen in **Table 3.2**. The results suggest a size exclusion mechanism prevents cortisone from penetrating the microporous structure, which accounts for the vast majority of the surface area. To gain a precise insight into the molecular weight limitations of these large surface area

polymer monoliths in the aqueous environment a detailed assessment using aqueous inverse size exclusion chromatography (ISEC) is necessary. This was avoided in this study due to the innate difficulties of microscale ISEC [25]. However, these results presented herein suggest that polymer monoliths with a permanent mesoporous structure are yet to be successfully fabricated.

Table 3.3 summarises the physical properties of both polymer monoliths, hypercrosslinked poly(VBC-*co*-Sty-*co*-DVB) and poly(DVB), as well as the particulate poly(Sty-*co*-DVB). The measured dry state surface area of the poly(DVB) is similar to the estimated surface area in the solvated state measured from anisole adsorption (**Table 3.1**). Previous studied have provided compelling evidence to suggest that the dry state characteristics of polymers does not directly translate to the behaviors observed when the polymer is in a solvated environment due to the appearance gel-type micropores [26-28]. Loosely crosslinked polymer chains on the outer surface of the polymer microglobule swell in a good solvent promoting the formation of a permeable layer. However, here we find the surface area of poly(DVB) in the dry state is very similar to the surface area estimated in the aqueous environment. This is not unexpected as the wettability of the hydrophobic poly(DVB) surface is poor thus the adsorbent is unlikely to swell.

Contrary, the BET surface area of the hypercrosslinked poly(VBC-*co*-Sty-*co*-DVB) adsorbent is approximately 2.5 times greater than the surface area estimated in the solvated state by the Langmuir adsorption isotherm of anisole (**Table 3.1 & 3.3**). It is well known that hypercrosslinked materials swell in all solvents, including water to reduce the inner strain induced through the formation of the methylene bridges [29]. When solvated, a conformational rearrangement of the hypercrosslinked network may

occur blocking pores that may be otherwise accessible in the dry state [23]. As such, the solvated surface area does not correspond to values measured in the dry state. This testifies that a measure of dry state surface area alone is not adequate to determine an adsorbent's suitability for SPE.

3.3.4 Polymer monoliths for SPE

Despite the molecular weight limitations of the polymer monoliths both the poly(DVB) and hypercrosslinked poly(VBC-*co*-Sty-*co*-DVB) adsorbents displayed exciting potentials for the SPE of small aromatic analytes. The SPE performance of the poly(DVB) was benchmarked against the particulate 85 µm poly(Sty-*co*-DVB). Anisole was employed as the probe analyte at a concentration of 400 mg L^{-1} in aqueous solution. The shape of the breakthrough curve was compared for both the polymer monolith and particles at three flow rates, 1 mL min^{-1}, 0.5 mL min^{-1} and 0.1 mL min^{-1} (**Figure 3.5**). For the particulate poly(Sty-*co*-DVB), at a flow rate of 1 mL min^{-1} anisole is immediately detected at the cartridge outlet, passing through the cartridge without interaction as most of the interactable surface is inside the porous particle. The shallow breakthrough curve is due to poor analyte diffusion-driven mass transfer, it takes considerable time for the analyte to partition in and out of the 85 µm particles. Saturation of the adsorbent occurs after 6 min. A similar curve can be seen for the flow rate of 0.5 mL min^{-1}. A decrease in flow rate to 0.1 mL min^{-1} improves the analyte/adsorbent interactions, as slower flow rates provide sufficient time for the analyte to reach equilibrium with the particulate adsorbent, as such the analyte is not seen at the column outlet until 2.5 min. These results highlight that slow operational flow rates are necessary to achieve the highest extraction performance of the particulate poly(Sty-*co*-DVB) materials. Therefore, these materials are not suitable for rapid SPE

workflows as the use of fast flow rates leads to low extraction recoveries and high sample carryover.

Regardless of the operational flow rate (0.1 - 1 mL min^{-1}) the analyte is well retained on the poly(DVB) polymer monolith adsorbent and a sharp breakthrough curve is observed when the adsorbent reaches saturation (**Figure 3.5A-C**). These observations indicate fast mass transfer, and suggest adsorption is neither mass transfer limited nor flow rate dependent. The porous morphology of large surface area polymer monoliths visualised in **Figure 3.3** supports these empirical observations. The fused interconnected globules are composed of agglomerated microspheres, which possess a compact non-porous core. The polymer monolith has an approximate globule size of only 5 μm and unlike the deeply penetrating pores of particulate adsorbent the micro- and mesoporous structure of large surface area polymer monoliths is represented by the series of shallow voids formed between the agglomerated microspheres. Any interactable surface is accessible by a small diffusion distance and this enables the use of fast flow rates without compromising efficiency. These vastly different characteristics have important implications on the development and use of SPE workflows, since the need to optimise the speed of extraction to maximise analyte recovery and minimise carryover is largely eliminated. This represents a significant breakthrough for the use of polymer monoliths for SPE.

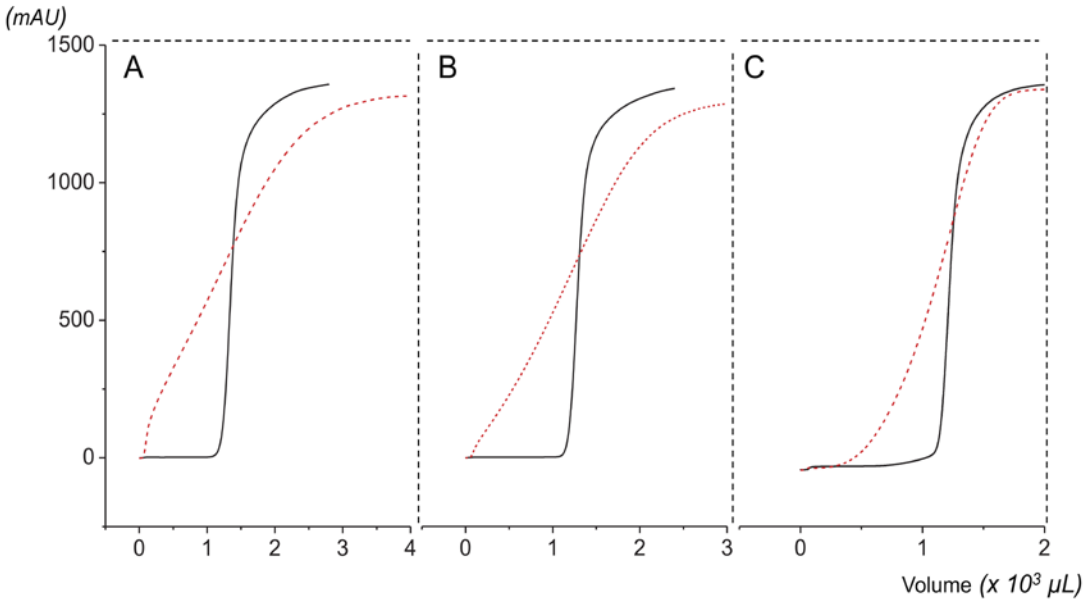

Figure 3.5. Breakthrough curves obtained by frontal analysis for poly(DVB) monolith (—), poly(Sty-*co*-DVB) 85 µm particulate (---). A) 1 mL min^{-1} B) 0.5 mL min^{-1} C) 0.1 mL min^{-1}.

To further corroborate observations of enhanced suitability of polymer monoliths for SPE, a comparative study of recovery was undertaken. Analyte recovery is perhaps the most important performance characteristic of SPE. Recovery of 400 mg L^{-1} anisole using both materials was compared at two different extraction flow rates of 1 mL min^{-1} and 0.5 mL min^{-1}. The off-line SPE was achieved by attaching the MEPS cartridge to a 100 µL CDF syringe and the extraction was driven by the digital syringe drive. Sample and solvent were applied to the adsorbent bed from above *via* the syringe barrel. With an extraction flow rate of approximately 0.5 mL min^{-1} similar recoveries of 88% ± 0.03 and 90% ± 0.10 was achieved for the polymer monolith poly(DVB) and the particulate poly(Sty-*co*-DVB) respectively. An increase in extraction flow rate to 1 mL min^{-1} reduced analtye recovery to 80% ± 0.08 when using the particulate poly(Sty-*co*-DVB) adsorbent. The extraction efficiency of the polymer monolith poly(DVB) remained stable at 89% ± 0.05. This again confirms that polymer monolith are superior adsorbents

for SPE of low molecular weight analytes, as the need to optimise flow rates becomes obsolete facilitating both rapid and efficient sample preparation.

3.4. Concluding remarks

Polymer monoliths with enhanced micro- and mesoporosity displayed a high analyte capacity and have been shown to be suitable for SPE. However, while an enhanced surface area is important, a detailed characterisation of the physical properties is essential to adequately demonstrate utility and to advance this technology by unraveling the key physical characteristics which provide the observed advantages over alternative adsorbents. Despite assumptions that the pore structure of large surface area polymer monoliths is mesoporous it has been demonstrated that in aqueous environments surface is are almost exclusively composed of micropores. As the vast majority of the surface area is within the porous network the utility of large surface area polymer monoliths is limited to analytes that can penetrate these small pores. This work highlights that there is still considerable need to gain a broader understanding of polymer monolith morphologies to avoid assumptions of their suitability. Further, the physical limitations of large surface area polymer monoliths described in this work provide an insight that is crucial for future developments in appropriately tailoring adsorbents for the SPE of analytes over a broader molecular weight range.

Large surface area polymer monoliths have excellent properties as adsorbents for the SPE of low molecular weight species. While the extraction performance of the poly(Sty-*co*-DVB) particulate adsorbent was highly dependent on the extraction flow rate, the performance of the polymer monolith was independent of flow rate due to its open porous structure that provides improved analyte mass transfer. The fast mass

transfer properties improve extraction efficiency without the need to optimise extraction flow rates demonstrating that these polymer monoliths are superior adsorbents for SPE of small molecules.

3.5. References

[1] Svec, F., Tennikova, T. B., Deyl, Z. *Monolithic Materials*; Elsevier, 2003.

[2] Guiochon, G. *J. Chromatogr. A* 2007, *1168*, 101–168.

[3] Buchmeiser, M. R. *Polymer* 2007, *48*, 2187–2198.

[4] Sýkora, D., Peters, E. C., Svec, F. *Macromol. Mater. Eng.* 2000, *275*, 42–47.

[5] Li, Y., Tolley, H. D., Lee, M. L. *J. Chromatogr. A* 2010, *1217*, 4934–4945.

[6] Lubbad, S. H., Buchmeiser, M. R. *J. Chromatogr. A* 2010, *1217*, 3223–3230.

[7] Trojer, L., Bisjak, C. P., Wieder, W., Bonn, G. K. *J. Chromatogr. A* 2009, *1216*, 6303–6309.

[8] Greiderer, A., Trojer, L., Huck, C. W., Bonn, G. K. *J. Chromatogr. A* 2009, *1216*, 7747–7754.

[9] Nischang, I., Teasdale, I., Brüggemann, O. *J. Chromatogr. A* 2010, *1217*, 7514–7522.

[10] Smirnov, K. N., Dyatchkov, I. A., Telnov, M. V., Pirogov, A. V., Shpigun, O. A. *J. Chromatogr. A* 2011, *1218*, 5010–5019.

[11] Davankov, V. A., Tsyurupa, M. P. *React. Polym.* 1990, *13*, 27–42.

[12] Veverka, P., Jerabek, K. *React. Funct. Polym.* 1999, *41*, 21–25.

[13] Ahn, J.-H., Jang, J.-E., Oh, C.-G., Ihm, S.-K., Cortez, J., Sherrington, D. C. *Macromolecules* 2006, *39*, 627–632.

[14] Urban, J., Svec, F., Fréchet, J. M. J. *Anal. Chem.* 2010, *82*, 1621–1623.

[15] Urban, J., Svec, F., Fréchet, J. M. J. *J. Chromatogr. A* 2010, *1217*, 8212–8221.

[16] Maya, F., Svec, F. *Polymer* 2013, 1–7.

[17] Rohr, T., Hilder, E. F., Donovan, J. J., Svec, F., Frechet, J. M. *Macromolecules* 2003, *36*, 1677–1684.

[18] Candish, E., Gooley, A., Wirth, H.-J., Dawes, P. A., Shellie, R. A., Hilder, E. F. *J. Sep. Sci.* 2012, *35*, 2399–2406.

[19] Okay, O. *Prog. Polym. Sci.* 2000, *25*, 711–779.

[20] Bielicka-Daszkiewicz, K., Voelkel, A. *Talanta* 2009, *80*, 614–621.

[21] Jerabek, K., Hankova, L., Prokop, Z. *React. Polym.* 1994, *23*, 107–112.

[22] Fontanals, N., Galià, M., Cormack, P. A. G., Marcé, R. M., Sherrington, D. C., Borrull, F. *J. Chromatogr. A* 2005, *1075*, 51–56.

[23] Davankov, V. A., Tsyurupa, M. P. *Hypercrosslinked Polymeric Networks and Adsorbing Materials*; Elsevier, 2010.

[24] Lowell, S. *Characterization of Porous Solids and Powders: Surface Area, Pore Size and Density*; Springer, 2004.

[25] Jarmalavičienė, R., Kornyšova, O., Westerlund, D., Maruška, A. *Anal. Bioanal. Chem.* 2003, *377*, 902–908.

[26] Jerabek, K. *Anal. Chem.* 1985, *57*, 1598–1602.

[27] Nevejans, F., Verzele, M. *J. Chromatogr. A* 1987, *406*, 325–342.

[28] Nischang, I., Teasdale, I., Brüggemann, O. *Anal. Bioanal. Chem.* 2010, *400*, 2289–2304.

[29] Zhang, X., Shen, S., Fan, L. *J Mater Sci* 2007, *42*, 7621–7629.

4. Hydrophilic monolithic poly(divinyl benzene) restricted access adsorbents and their application for miniaturised solid phase extraction

4.1. Introduction

Highly selective and sensitive analysis of drugs and metabolites by mass spectrometry (MS) has emerged as an essential tool for clinical chemistry, forensic toxicology and pharmaceutical research. Blood, plasma and serum are among the most difficult samples to analyse as they are poorly compatible with MS [1]. Matrix components, including cellular material, proteins and non-volatile lower molecular weight solutes, can severely reduce assay sensitivity. Non-volatile solutes can impede analyte ionisation and the highly abundant protein fraction can substantially suppress the signal of lower molecular weight target analytes [2]. Furthermore, matrix components complicate data and foul the instrument. The key to achieving highly sensitive and accurate analysis is to present a purified sample to the MS.

Adsorbents based on hydrophobicity and ion-exchange are extremely efficient for removal of salts and non-adsorbed matrix compounds but protein rich matrices remain problematic. Proteins and peptides exhibit both hydrophobic and ionic interactions resulting in their non-specific surface adsorption and precipitation [3]. Non-specific adsorption can diminish the extraction performance, block the SPE cartridge, complicate data, and reduce assay sensitivity [3, 4]. To circumvent, multi-step sample pretreatment procedures including centrifugation, protein precipitation and filtration are routinely introduced into the workflow prior to SPE. Multistep procedures nullify the

benefits of the miniaturised SPE formats, since the additional processes are labour intensive, and time and sample/solvent consuming. Alternatively, the morphology and chemistry of the SPE adsorbent can be engineered for reduced protein adsorption.

Restricted access materials (RAMs) facilitate rapid and efficient purification of biological materials; non-adsorbed low molecular weight matrix compounds and the protein rich matrix can be eliminated using a single adsorbent [5, 6]. Whereas small molecules are retained, a diffusion barrier limits the accessibility of proteins to the adsorbent's surface. RAMs are classified according to the mechanism for protein exclusion, a physical barrier of small pores prevents proteins from interacting with the adsorbent by a size exclusion mechanism [7]. Hagestam and Pinkerton used 6 nm porous silica particles to prevent protein interaction, here the silica surface was grafted with a hydrophobic tripeptide (glycine-l-phenylalanine-l-phenylalanine) [5, 8-10]. The external surface was rendered hydrophilic by an enzymatic cleavage of the peptide at the glycine unit to completely eliminate protein interaction. Similarly, adsorbents with more traditional C18, C8 and C4 internal pore functionalities are common [7, 11]. Adsorbents with a hydrophilic chemical mesh barrier based on poly(ethylene glycol) (PEG) make up the second category of RAMs. PEG is well known to inhibit protein interaction, demonstrated approaches have embed hydrophobic functionality within the hydrophilic mesh itself [12, 13]. Alternatively, the underlying hydrophobic C18 and C8 particulate can be shielded by a PEG mesh layer [14].

Widespread adoption of RAMs remains limited, despite their introduction 30 years ago. RAMs are almost exclusively employed as pre-columns for on-line sample purification. Unfortunately, substantial skills are necessary for operation, on-line formats of sample preparation can require highly complicated systems, expensive instrumentation and

intensive method development [15]. Off-line tools for sample preparation are generally considered a more realistic approach for routine laboratory use. A marriage between miniaturised SPE devices and RAMs for analyte purification from biological materials affords considerable potential. Unfortunately, RAMs are almost exclusively based around particulate adsorbents, which is problematic for the operation of miniaturised SPE devices. To adopt RAMs for fast and efficient sample preparation the morphologies of the adsorbent must be amended to suit miniaturised SPE devices.

The unique structural morphologies of porous polymer monoliths present a number of desirable attributes for miniaturised SPE. First, the macroporous structure can be highly permeable, enabling fast fluid flows while maintaining low backpressures. Second, the highly crosslinked non-porous core of the polymeric microglobules means that any interactable internal surface area is accessible by a small diffusion distance for improved solute mass transfer kinetics [16]. To date, the few examples of polymeric monolithic RAMs are limited to on-line sample clean up. The hydrophobic polyacrylamide RAMs described by Maruška and co-workers possessed a hydrophilic dextran coating to prevent protein binding [17, 18]. Dong *et al.* also described a hydrophobic poly(ethylhexyl methacrylate-*co*-ethylene dimethacrylate) polymer monolith column grafted with a hydrophilic glycerol monomethacrylate film [19]. In both examples, the hydrophilic chemical shield successfully reduced the non-specific protein adsorption. However, the aforementioned polymer monoliths possess the typical morphology largely absent of micro (0.2-2 nm) and mesoporosity (2-50 nm) and this limits the analyte capacity. For a highly sensitive miniaturised SPE assay the adsorbent must possesses a permanent large surface area for high capacity analyte interaction.

High capacity large surface area polymer monoliths can be fabricated by increasing the internal crosslinking density [20, 21]. Using this approach to fabricate the typical

globular structure of a polymer monolith presents a textured surface of aggregated microglobules, voids between the microglobules deliver permanent micro- and mesoporosity to the structure [22]. In Chapter 3 it is demonstrated that large surface area polymer monoliths adsorbents based on poly(divinyl benzene) (DVB) are highly promising for the SPE extraction of small molecules. The inherent structural morphology may be exploited to determine if the adsorbents possess a physical mechanism for protein exclusion and in this Chapter suitability of polymer monolith poly(DVB) adsorbents as RAMs is explored. A hydrophilic coating is introduced to the poly(DVB) by anchoring poly(ethylene glycol) methacrylate to the surface. The density of the surface layer was delicately balanced to prevent proteins from accessing to hydrophobic surface while preserving hydrophobic capacity and fast analyte mass transfer. The structural properties, extraction performance and non-specific protein binding are then extensively evaluated before and after the introduction of the hydrophilic chemical barrier. The suitability of the resultant RAMs was demonstrated for the miniaturised SPE purification of highly complex, protein rich biological samples.

4.2. Experimental section

4.2.1 Chemicals and materials

DVB (containing 80% 1,3-DVB + 1,4-DVB and 20% 1-ethyl-3-vinyl benzene + 1-ethyl-4-vinyl benzene), poly(ethylene glycol) methyl ether methacrylate average M_n 950 ($PEGMA_{950}$), poly(ethylene glycol) methacrylate average M_n 360 ($PEGMA_{360}$), poly(ethylene glycol) diacrylate average M_n 258 ($PEGDA_{258}$), ethylene glycol dimethacrlyate (EDMA) (98%), methyl methacrylate (MMA) (99%), anisole, 1-dodecanol, benzophenone (99%), ibuprofen, human serum albumin lyophilized powder

≥97% (HSA), fluorescamine, ammonium hydroxide and sodium tetraborate were all purchased from Sigma Aldrich (Castle Hill, Australia). Monomer inhibitors were removed by passage through a packed bed of basic alumina. The initiator 2,2'-azo-bis-isobutyronitrile (AIBN) was obtained from MP Biomedicals (Santa Ana, CA, USA) and purified by recrystallisation with methanol. High performance liquid chromatography (HPLC) grade, acetone, acetonitrile, methanol and toluene were purchased from Sigma Aldrich and water was purified with a Milli-Q system (Millipore, Bedford, MA, USA).

Polyethylene (PE) tubing (1.57 mm i.d.) was obtained from SDR Scientific (Chatswood, Australia). The MEPS cartridge assembly included frits, shank and needle hub components (SGE Analytical Science, Ringwood, Australia).

4.2.2 Sample collection

Blood samples were obtained by finger lancet (Acc-Chek Softclix, Roche Diagostics, Castle Hill, Australia) from a healthy female volunteer and stored in EDTA MiniCollect tubes (ThermoScientific, Scoresby, Australia). All blood samples were centrifuged to obtain the plasma fraction. The plasma was diluted with water (20% v/v) and spiked with 50 ng mL^{-1} ibuprofen.

4.2.3 Instrumentation

A Spectrolinker XL-1000 UV Crosslinker fitted with six 254 nm bulbs was employed for photografting (VWR Scientific, Murarrie, Australia). All polymerisations were undertaken by thermal initiation in a water bath (PolyScience, Niles, IL, USA). An inverted fluorescence microscope (Nikon, Eclipse Ti-U, Japan) was employed to determine protein binding with violet pass excitation (lex at 380-420 nm) and emission

(lem at 450 nm) filters (Semrock, Rochester, NY, USA) operated with NIS-Elements BR 3.10 software (Melville, NY, USA).

The Brunauer–Emmett–Teller (BET) surface area and microporosity were assessed using a Tristar II analyzer for the argon adsorption/desorption at 77 K (Particle and Surface Science, Gosford, Australia). Microporous surface area was determined using t-plots and the pore size was assessed using the non-localised density functional theory (NLDFT). The macroporous properties of the adsorbent materials were measured using an Autopore IV mercury intrusion porosimeter. The surface morphologies of the adsorbents were analyzed using a Hitachi SU-70 field emission scanning electron microscope (SEM); the polymer monoliths were sputter-coated with platinum.

Chemical functionality of the adsorbents was determined using solid-state ^{13}C cross-polarisation magic angle spinning nuclear magnetic resonance (CP-MAS NMR) spectroscopy and attenuated total reflectance Fourier transform infrared (ATR-FTIR) spectroscopy. ^{13}C CP-MAS NMR was carried out to determine the presence of vinyl groups on the poly(DVB) using a Bruker DPX 200 spectrometer (Bruker, Alexandria, Australia) operating at 50 MHz Larmor frequency for ^{13}C, with a 4 mm solid-state MAS NMR probehead and at a MAS rotational frequency of 10 kHz. Spectra were recorded using a 4 μs 90° pulse, a 4 ms contact time, a 3 s repetition delay, and 15360 transients. The ^{1}H and ^{13}C pulses were calibrated with adamantane and a mixture of 3 singly ^{13}C labelled alanines. The ^{13}C chemical shift scale was externally referenced to tetramethylsilane (TMS) at 0.0 ppm using adamantane by setting the CH resonance to 38.5 ppm [23]. All data was collected using Topspin software (Bruker, Alexandria, Australia). ATR-FTIR spectroscopy was used to determine the functional groups on the adsorbents surface. The spectra were recorded on Vertex 70 (Bruker Optic, Ettlingen,

Germany) spectrometer in 500–4000 cm^{-1} region, 32 scans were signal-averaged with a spectral resolution of 4 cm^{-1} using a single reflection diamond ATR attachment, Platinum ATR (Bruker Ettlingen, Germany).

SPE adsorbent performance was assessed using an ICS3000 system (ThermoScientific, Scoresby, Australia) consisting of two quaternary solvent pumps, an autosampler and an ultraviolet (UV) detector with an 11 µL flow cell. Analyte recovery and protein adsorption from the off-line SPE extraction was analysed using a ProteCol C8 (3 µm particles and 1000 Å pores, 4.6 mm i.d. × 250 mm) HPLC column (SGE Analytical Science) using gradient elution with mobile phase A (95:5 0.1% trifluoroacetic acid:methanol v/v) and mobile phase B (95:5 methanol: 0.1% trifluoroacetic acid v/v). The elution involved ramping from 60% mobile phase A to 100% mobile phase B in 10 min using a flow rate of 0.6 mL min^{-1}. All MEPS assemblies comprised a cartridge coupled to 100 µL or 50 µL controlled directional flow (CDF)-MEPS syringe driven by an eVol hand held semi automated analytical syringe (SGE Analytical Science, Australia).

MS experiments were performed using a micrOTOF-Q mass spectrometer (Bruker Daltonics, Brenman, Australia) equipped with an electrospray ionisation (ESI) source. The instrument was operated as follows: +3.5 kV capillary potential (negative ion mode), nitrogen nebuliser gas at 1.7 bar, nitrogen dry gas at 220°C and a flow rate of 4 L min^{-1}. Calibration of the time of flight (TOF)-MS was carried out prior to each analysis by direct infusion of multimode tune mix low concentration (Agilent Technologies, Mulgrave, Australia) at 5 µL min^{-1}. Data were collected between 100-600 m/z at an acquisition rate of 0.5 Hz, using micrOTOF control 2.2. Ibuprofen was monitored using a single extracted ion: 205.12 ±0.01 m/z. The analyte identity was

confirmed using standard addition. All ion traces were processed using Compass Data Analysis 4.0 (Bruker, Preston, Australia) and smoothed using the Gauss smoothing algorithm at 2.003 s.

4.2.4 Preparation of the polymer monolith SPE adsorbents

PE tubing surface was modified using the single step photografting approach described by Rohr *et al.* [24]. Briefly, the PE tubing was filled with a 1:1 w/w mixture of MMA and EDMA with 3% w/w benzophenone. The tubing was then irradiated with 254 nm for 15 min. All residual polymerisation mixture was rinsed from the tube with methanol and air-dried.

The poly(DVB) polymer monoliths were based on an approach described by Sýkora *et al*. [20]. Briefly, the composition included 40% w/w DVB, 8% w/w toluene, 52% w/w dodecanol and 1% w/w AIBN with respect to monomers. All polymerisation mixtures were prepared in glass vials and sonicated for 2 min then purged with nitrogen for 10 min. Polymerisation reactions were carried out at 70 °C for 180 min. Residual polymerisation mixture was removed by Soxhlet extraction with methanol for 24 h for all monoliths, whether prepared in glass vials or in PE tubing. The polymers were then dried under vacuum at 25 °C overnight.

The post-polymerisation thermal grafting reaction was developed from an approach described by Tripp *et al.* [25]. The grafting mixture was prepared in toluene containing 5-20% w/w functional monomer ($PEGMA_{360}$ or $PEGMA_{950}$), 1% w/w $PEGDA_{258}$ and 1% AIBN w/w with respect to the functional monomer. The bulk polymer monolith was submerged in the grafting mixture. The grafting mixture was manually flushed through the PE tubes containing polymer monolith with a syringe, the PE tubes were then

submerged in the grafting solution. The mixture was polymerised at 65°C for 20 h. The products were Soxhlet extracted with methanol for 24 h and dried under vacuum overnight. To completely ensure that any graft solution was not retained in the PE tube-containing polymer monolith, this was further flushed with 20 mL of methanol at 1 mL min^{-1}

For testing in the MEPS format, the MEPS cartridges were filled with polymer monolith sections weighing 2 ± 0.2 mg and once assembled the cartridges were flushed with 20 mL of 95:5 methanol:water v/v.

4.2.5 Adsorbent performance

Breakthrough times and adsorption behavior for the polymer monolith SPE adsorbents were determined using frontal analysis. The MEPS cartridge was inserted between the dual quaternary pump and the UV detector. Pump 1 delivered the solvent solutions while Pump 2 delivered the aqueous analyte solution. The adsorbent was first conditioned with methanol:water (95:5 v/v) using a continuous flow of 2.5 mL at 1 mL min^{-1} then equilibrated with 2.5 mL water:methanol (95:5 v/v) at the same flow rate. The analyte in aqueous solution was continuously pumped over the adsorbent bed and the cartridge effluent was monitored at 254 nm. Uracil was employed as the t_0 marker compound to determine the void volume of the system.

4.2.6 Fluorescence assay of protein adsorption

To determine the adsorption of HSA on the polymer monolith adsorbents a stock solution of the protein was prepared at 1 mg mL^{-1} in 10 mM sodium tetraborate buffer. A 3 mg mL^{-1} solution of fluorescamine in acetone was prepared. A final protein

concentration of 50 µg mL^{-1} was achieved by combining 5% HSA solution and 15% fluorescamine solution in a 10 mM sodium tetraborate solution. Adsorbents were first conditioned with 250 µL of methanol and equilibrated with 250 µL of water at 50 µL min^{-1}. A 400 µL aliquot of the protein solution was passed over the polymer monolith adsorbent and any unretained protein was flushed out with 250 µL of water both at a flow rate of 50 µL min^{-1}. The adsorbents were left to dry at room temperature then the fluorescence intensity of the cross-section of the polymer monolith adsorbent was analysed. Images were compared with the cross-section of the polymer monolith adsorbents taken prior to the protein-binding assay.

4.2.7 RAM polymer monoliths for SPE

Analyte protein adsorption and recovery were determined by off-line extraction and analysed by HPLC. The SPE cartridge was attached to a 100 µL CDF-MEPS syringe which was driven by a digital syringe drive (see **Appendix B**). Sample and solvent were aspirated into the syringe barrel with the valve in Position 2 and dispensed with the syringe valve in Position 1 *via* the modified MEPS needle [26]. The flow rate to aspirate was 3.5 mL min^{-1} (the highest programmable speed, 1.2 second aspiration) and dispense was achieved at 1.0 mL min^{-1} (36 second total extraction time). To determine protein adsorption the extraction workflow involved first preconditioning with 100 µL of methanol and then 100 µL water. Next, a 1 00 µL aliquot of an aqueous 1 mg mL^{-1} solution of HSA was passed over the adsorbent bed. This sample was collected and compared with a non-extracted HSA solution to assess depletion of the HSA. To determine analyte recovery the adsorbent was conditioned and equilibrated with methanol and water respectively. Next, a 100 µL aliquot of the 10 mg L^{-1} ibuprofen in aqueous solution was applied to the adsorbent, any unretained compounds were removed with 100 µL water. The analyte was eluted with 100 µL methanol and

analysed by HPLC. The amount recovered was determined by comparing the peak area for an extracted ibuprofen solution with a non-extracted ibuprofen solution. For MS analysis the 50 µL CDF syringe was employed. The sample was processed by modification of the aforementioned conditions, where the elution solvent employed acetonitrile with 0.3% v/v ammonium hydroxide and the clean sample was delivered directly to the ESI source at a rate of 20 µL min^{-1} (2.6 min total analysis time) (see **Appendix D**). Following the first elution a second 50 µL elution was performed using 1% formic acid:isopropanol (60:40 v/v) to clean the bed prior to the next extraction cycle.

4.3. Results and discussion

4.3.1 Characterisation of large surface area polymer monolith

For rapid and efficient sample preparation of complex biological samples the SPE adsorbent must adhere to a number of essential morphology requirements. Foremost, for a sensitive assay a large surface area is desirable. The capacity of an adsorbent bed is strongly related to the surface area available for interaction. Argon adsorption/desorption determined the specific surface area of the poly(DVB) adsorbent to be 497 mg g^{-1}. As demonstrated in Chapter 3 the dry state surface area of poly(DVB) adsorbents is equivalent to their surface area under aqueous conditions, as determined from the Langmuir adsorption of a well retained analyte. This preliminary measure suggests the extraction capacity may prove equivalent to particulate silica based RAMs where surface areas ranging from 100-400 m^2g^{-1} are common [8, 11]. Further probing of the poly(DVB) BET isotherm and the t-plot indicate that the adsorbent's microporosity (0.2-2 nm) accounts for the majority of the surface area. In fact, the slope of the t-plot reveals that the external surface area was only 16 m^2 g^{-1} and that 93% of the total pore volume (0.30 cm^3 g^{-1}) is attributed to the micropores (0.28 cm^3 g^{-1}). NLDFT was

employed to gain insight into the adsorbent's pore size, assuming cylindrical pore geometry. The large surface area of the poly(DVB) polymer monolith possesses a heterogeneous pore size distribution with pores ranging from 1 to 6 nm (**Figure 4.1**). The innate process of fabricating poly(DVB) polymer monoliths creates a physical size exclusion barrier that inhibits proteins from gaining access to the large internal surface.

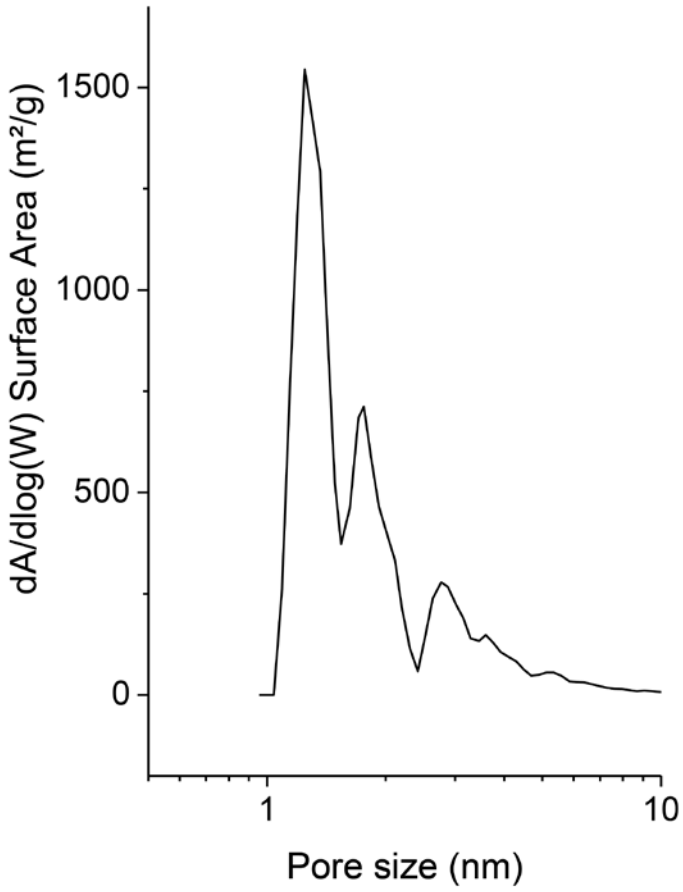

Figure 4.1. Pore size data determined by NLDFT with argon adsorption/desorption isotherms at 77 K for the poly(DVB) adsorbent.

4.3.2 Hydrophilic functionalisation of poly(DVB) adsorbents

A more effective and complete sample purification may be possible using poly(DVB) as there is little external surface area is available for protein interaction. Unfortunately, the

hydrophobic nature of the external surface remains problematic for protein-rich sample. Non-specific protein adsorption will foul the cartridge and complicate the data. Thus a hydrophilic external surface must be incorporated to render the poly(DVB) adsorbent compatible with biological samples. Introducing hydrophilic functionality into poly(DVB) polymer monoliths can be achieved using a number of approaches. Commonly explored approaches involve the co-polymerisation with either a hydrophilic monomer or a reactive monomer followed by a post-polymerisation reaction to reveal hydrophilic functionality. These fabrication approaches would ultimately diminish the surface area and hence the applicability for SPE since the structural morphology of the large surface area poly(DVB) is dependent on a high concentration of crosslinking monomer in the polymerisation mixture [22, 27]. Approaches to introduce surface hydophilicity are limited to a post-polymerisation reaction whereby a hydrophilic layer is grafted to the adsorbent surface. It is well established that grafting hydrophilic poly(ethylene glycol) (PEG) and its structural analogues onto a polymer surface results in a reduction of the non-specific surface adhesion of proteins. The hydrophilic monomer PEGMA was selected for grafting as it can be crosslinked to the adsorbent's surface [28, 3].

Previous demonstrations for $PEGMA_{360}$ introduction to the surface of hydrophobic polymer monoliths predominantly involves the UV photografting of the hydrophilic monomer onto a precursor polymer monolith based on methacrylate chemistry [29, 30, 24]. This rapid and highly efficient grafting reaction is not compatible with the poly(DVB) as the aromatic ring absorbs the 254 nm UV light. Commonly, thermal grafting polymerisation reactions exploit the reactive initiator used for living or controlled polymerisations, post-polymerisation the functional monomer can be grafted to the residual initiator [31, 32, 19]. Unfortunately, this synthesis necessitates

specialised initiators and in order to leave initiating groups intact the conditions of polymerisation can be limited. It has been demonstrated that following the polymerisation of poly(DVB) particulate 39-43% of the vinyl groups remain uncrosslinked and available for further functionalisation [33, 34]. This 39-43% does not include the vinyl groups that are trapped within the particle and not available for further grafting [33]. Tripp *et al.* exhibited an approach to crosslink a gel layer of glycidyl methacrylate to the surface of a preformed poly(styrene-*co*-DVB) monolith by manipulating the pendant vinyl groups [25]. As the poly(DVB) monolith presents a higher degree of crosslinking than the poly(styrene-*co*-DVB) equivalent solid state ^{13}C-NMR was employed to confirm the presence of residual vinyl groups in the polymer monolith poly(DVB). Spectroscopic characterisation reveals signals at 138 and 113 ppm (signals A and B) corresponding to vinyl carbons adjacent and non-adjacent to the aromatic ring and confirming the suitability of the polymer monolith poly(DVB) adsorbent for further modification (**Figure 4.2**) [33]

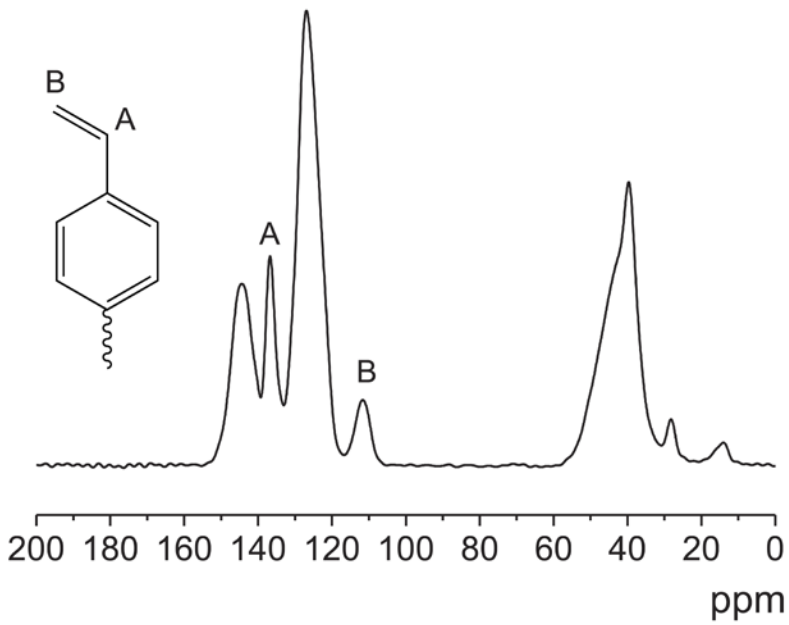

Figure 4.2. ^{13}C solid-state NMR confirming the presence of residual vinyl groups for grafting to poly(DVB).

Two different PEGMA monomers with glycol chain lengths of M_n 360 and 950 to compare the effect on the target analytes' resistance to mass transfer following the grafting of the poly(DVB) adsorbent with the hydrophilic layer. The hydrophilic layer should be appropriately dense to prevent proteins from access to the hydrophobic surface, although it also must remain sufficiently thin and permeable to ensure efficient mass transfer [35-37]. Given the small pore size of the poly(DVB) adsorbent the PEGMA monomers may be sufficiently large to exploit the size exclusion character of the poly(DVB) coating only the external surface with the hydrophilic functional monomer while preserving the hydrophobic pore surface. For grafting, the preformed poly(DVB) polymer monolith was submerged in a mixture containing 5-20% of the PEGMA monomer in toluene and thermally polymerised for 24 h. For the higher concentrations of $PEGMA_{360}$ the grafting reaction yielded a sticky transparent gel whereas the graft solution for the $PEGMA_{950}$ remained a liquid. To remove any unattached PEGMA chains the polymers were extensively washed using Soxhlet extraction. Assessment of the grafted adsorbents was undertaken on the materials prepared from 20% functional monomer in the graft solution unless otherwise stated.

A highly permeable adsorbent bed is a necessity for miniaturised SPE devices, thus the macroporous properties of the grafted polymers were investigated using mercury intrusion porosimetry. In the dry state, the grafting reaction did not appear to significantly influence the macropore (flow through pore) size of the poly(DVB)-*g*-PEGMA adsorbents. Adsorbents grafted with the $PEGMA_{360}$ and $PEGMA_{950}$ presented a macropore size of 6.7 µm which mirrored that of the precursor poly(DVB). By maintaining large macropore size both poly(DVB)-*g*-PEGMA materials present highly permeable morphology a second qualifying criteria for miniaturised SPE.

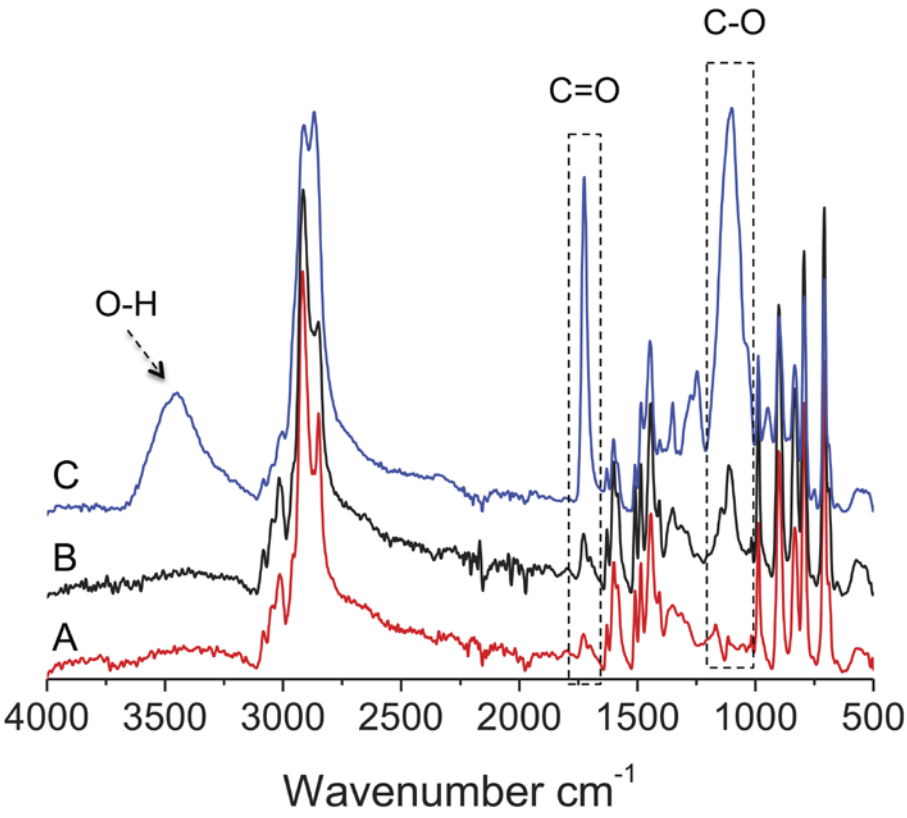

Figure 4.3. ATR-FTIR spectra of A) poly(DVB) B) poly(DVB)-*g*-$PEGMA_{950}$ and C) poly(DVB)-*g*-$PEGMA_{360}$

The functionality of both poly(DVB)-*g*-PEGMA adsorbents was compared to the precursor poly(DVB) using ATR-FTIR. The overlaid FTIR spectra revealed distinct changes in the chemical functionality (**Figure 4.3**). The spectra corresponding to

poly(DVB)-*g*-PEGMA$_{360}$ exposed a very distinct band at 1000 cm^{-1} which can be attributed to the ether functionality and bands at 1724 cm^{-1} and 1247 cm^{-1} can be credited to the ester functionality of the PEGMA monomer. Lastly, the wide band at 3449 cm^{-1} is indicative of the terminal hydroxyl group on the PEGMA$_{360}$ chain. The spectral changes are more subtle for the poly(DVB)-*g*-PEGMA$_{950}$, a band at 1000 cm^{-1} (ether functional group) is the dominate change. Relative intensity of this band is expected due to the large number of the repeating glycol units. In contrast, only a very small band is seen at 1724 cm^{-1} relating to the single ester group on each of the attached monomer chains. **Figure 4.3** infers a higher density of grafting was achieved for the shorter chain length PEGMA$_{360}$.

Grafting density observations were further reinforced visually by SEM (**Figure 4.4**). The poly(DVB) displayed both the clustered globule morphology typical of an organic polymer monolith and the characteristic textured surface morphology unique to polymer monoliths with a high degree of internal crosslinking (**Figure 4.4A**). The grafted layer of the PEGMA$_{360}$ was clearly evident for the poly(DVB)-*g*-PEGMA$_{360}$ by the sheet like layer that drapes the polymer globules (**Figure 4.4B**). In contrast, the poly(DVB)-*g*-PEGMA$_{950}$ appeared identical to the poly(DVB) precursor. This cast doubt over the success of the PEGMA$_{950}$ grafting. The poly(DVB)-*g*-PEGMA$_{950}$ was further probed using a crude assay that involved dropping an aqueous solution of green food dye on the surface of both the poly(DVB) and the poly(DVB)-*g*-PEGMA$_{950}$.

Figure 4.5 demonstrates the change in surface chemistry; here the aqueous dye solution was repelled from the hydrophobic the poly(DVB) beading on the surface, whereas the surface of the poly(DVB)-*g*-PEGMA$_{950}$ is wet by the dye solution following the grafting reaction, enabling penetration of the adsorbent. It is clear that the grafting of

PEGMA$_{950}$ was successful, but the density of grafting to the surface of the poly(DVB) is much lower than for the PEGMA$_{360}$. The reason for the lower observed grafting density was not investigated further but possible reasons may be a lower reactivity of the PEGMA$_{950}$ monomer or a steric hindrance due to the longer glycol chain limiting access to the surface.

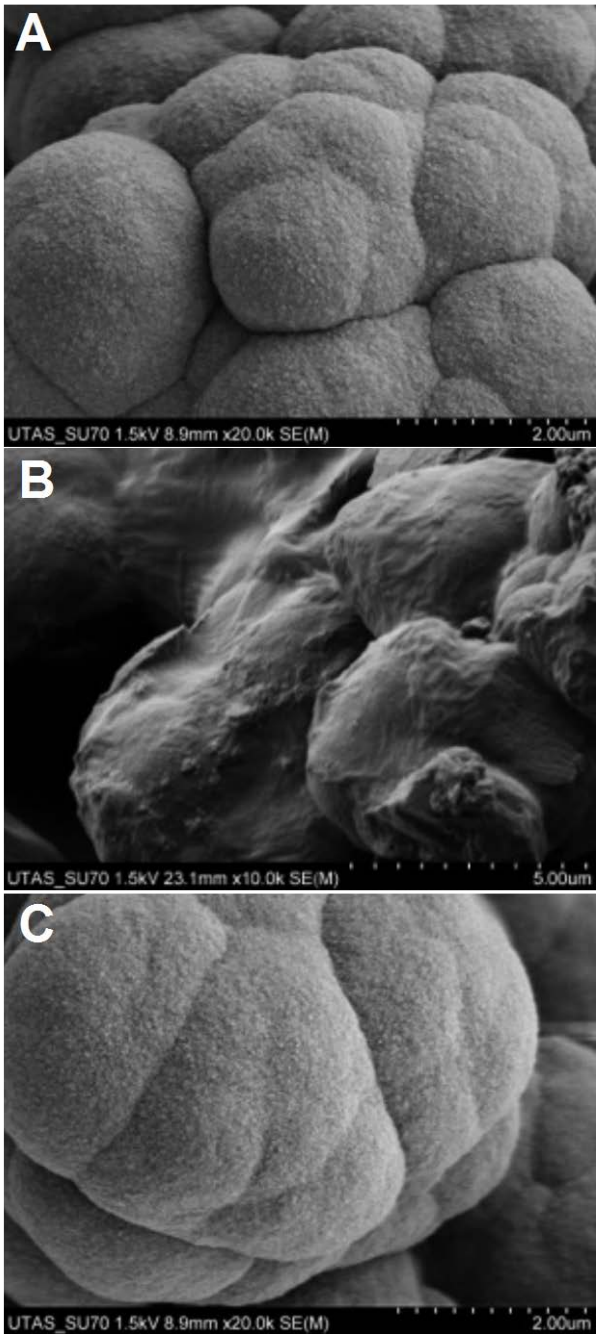

Figure 4.4. SEM images of the surface of A) poly(DVB), B) poly(DVB)-*g*-PEGMA$_{360}$ and C) poly(DVB)-*g*-PEGMA$_{950}$.

Figure 4.5. An aqueous solution of green food dye spotted on the poly(DVB) and the poly(DVB)-*g*-PEGMA$_{950}$ adsorbents.

4.3.3 Frontal analysis

All three adsorbents were prepared in MEPS cartridges to determine their suitability for SPE. This format was explored as it could be seamlessly interfaced with HPLC to determine analyte breakthrough curves. Analyte adsorption was compared for all polymer monolith adsorbents using anisole and ibuprofen as probe molecules and a comparison of analyte breakthrough times was made. Results of anisole adsorption reveal only a small reduction in the anisole breakthrough time for both poly(DVB)-*g*-PEGMA$_{360}$ and poly(DVB)-*g*-PEGMA$_{950}$ (**Figure 4.6A**). Despite of the hydrophilic layer, hydrophobic capacity of the adsorbent has largely been preserved. The second point to note from **Figure 4.6A** is that poly(DVB)-*g*-PEGMA$_{360}$ exhibits a shallow breakthrough curve suggesting that the thick hydrophilic coating leads to considerably slow partition kinetics. The poor analyte diffusion-driven mass transfer indicates this adsorbent is unsuitable for rapid miniaturised SPE workflows. Low extraction recoveries and high sample carryovers will result, since the analyte is unable to achieve equilibrium with the adsorbent bed when fast flow rates are employed. Therefore, poly(DVB)-*g*-PEGMA$_{360}$ was not investigated further. In contrast, the anisole

breakthrough curve for poly(DVB)-*g*-PEGMA$_{950}$ layer remains sharp, indicating that fast mass transfer is maintained in spite of the grafted hydrophilic layer being present. Analyte breakthrough was investigated to further corroborate these observations. Here ibuprofen was selected as an application representative analyte. Breakthrough times were compared for the precursor poly(DVB) and the poly(DVB)-*g*-PEGMA$_{950}$ (**Figure 4.6B**). Again a small reduction in breakthrough time was observed but the sharp breakthrough curve was maintained. The practical implication of this outcome is that the protocols to optimise extraction speed for maximum analyte recovery and low sample carryover can be eliminated. The poly(DVB)-*g*-PEGMA$_{950}$ adsorbent affords a high extraction performance independent of operational flow rate, this is rarely exhibited by the alternative technologies.

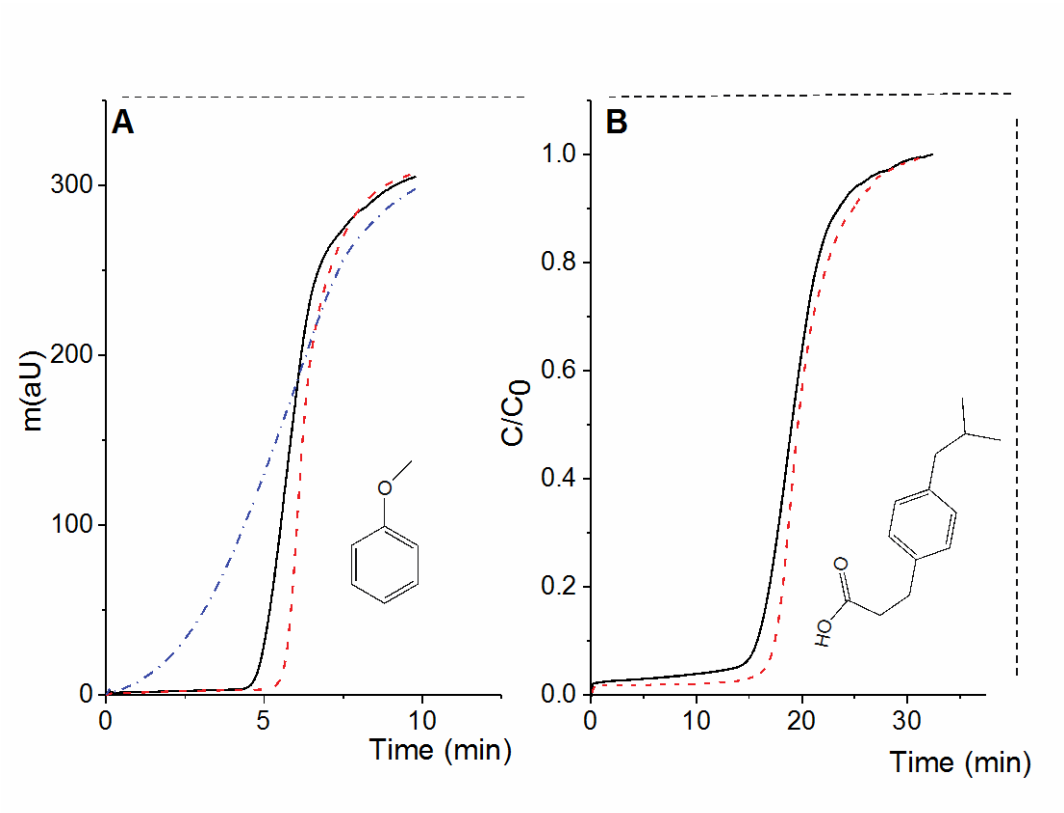

Figure 4.6. A) Anisole breakthrough for poly(DVB) (---), poly(DVB)-*g*-PEGMA$_{360}$ (-·-) and poly(DVB)-*g*-PEGMA$_{950}$ (——). B) Ibuprofen breakthrough for poly(DVB) (---) and poly(DVB)-*g*-PEGMA$_{950}$ (—).

4.3.4 Protein adsorption

HSA is the most abundant human plasma protein so it is suitable to investigate whether the grafted $PEGMA_{950}$ layer reduces HSA binding. It is widely reported that grafting density is a key factor to prevent protein binding to hydrophobic surfaces. Polymers prepared from grafting solutions containing 20, 10 and 5% w/w $PEGMA_{950}$ were explored. Following a typical SPE workflow, the adsorbent bed was conditioned with methanol then equilibrated in water, next fluorescent HSA was flushed through the adsorbent bed. Any residual protein could be removed by flushing with water. The poly(DVB) presents a substantial fluorescent signal, despite the small pores limiting access to the large internal surface area. It appears a considerable amount of HSA has been adsorbed on the hydrophobic surface (**Figure 4.7**). The grafting solution containing 5% $PEGMA_{950}$ did not yield a hydrophilic layer sufficient to prevent protein interaction with a lower degree of protein binding observed by increasing the concentration of $PEGMA_{950}$ in the graft solution to 10%. The poly(DVB)-*g*-$PEGMA_{950}$ (20%) displayed a very low fluorescent response that was equivalent to the signal exhibited prior to protein binding. This adsorbent is compatible with complex biological samples as the hydrophilic layer is sufficiently dense to substantially reduce protein binding. The potential exists to yield superior analyte purification from complex biological samples.

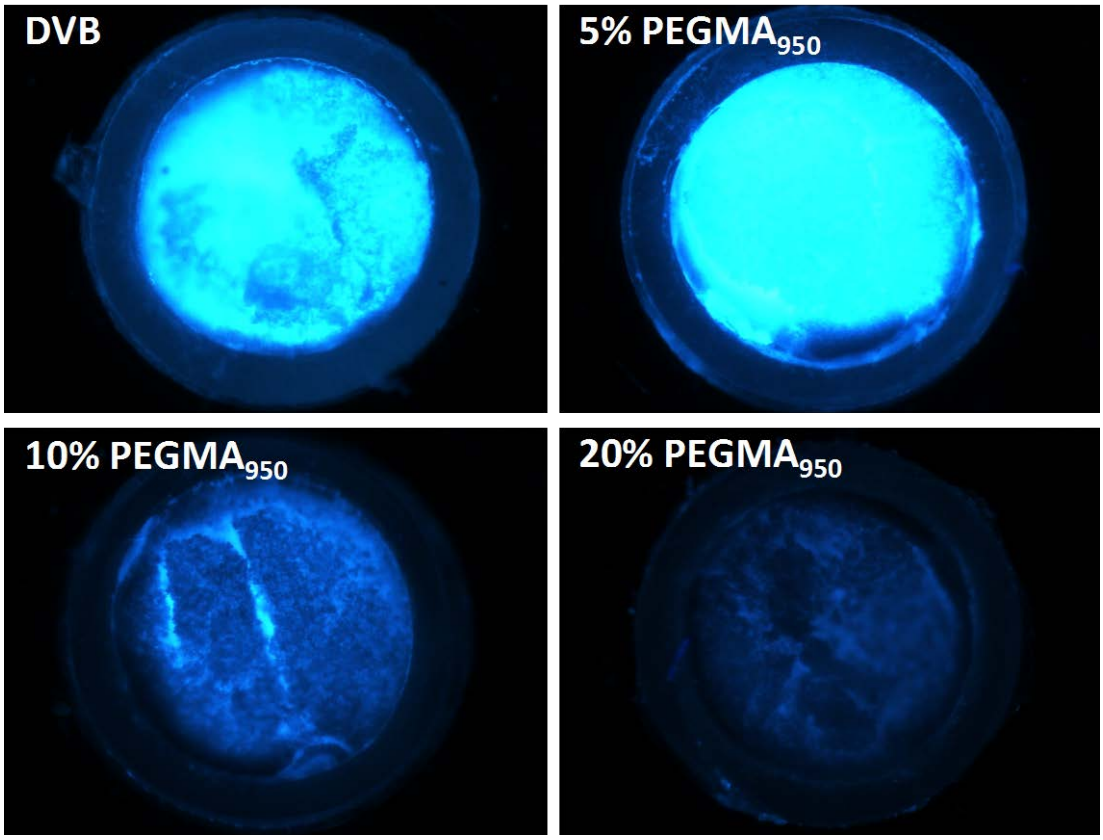

Figure 4.7. Optical microscopy images of protein binding fluorescently labeled HSA on poly(DVB) and poly(DVB) grafted with increasing percentages of $PEGMA_{950}$.

4.3.5 RAM polymer monoliths for SPE

To broaden the validation of biocompatibility the degree of protein binding was quantitated chromatographically. The amount of HSA adsorbed was measured for both the poly(DVB) and the poly(DVB)-*g*-$PEGMA_{950}$ using off-line SPE. Off-line SPE was achieved by attaching the MEPS cartridge to a 100 µL CDF syringe. Sample and solvent were applied to the adsorbent bed from above *via* the CDF syringe barrel [26]. An aliquot of HSA was passed through the adsorbent bed and any reduction in peak area of the effluent corresponded to non-specific protein binding. The poly(DVB) adsorbed 31% ± 2.41 of the HSA sample. Given that only a very small external surface area is available for interaction the amount of HSA adsorbed was substantial. While not

completely eliminated, the amount of HSA adsorbed onto the poly(DVB)-*g*-PEGMA$_{950}$ was reduced to 12% ± 0.49. A further increase in the amount of PEGMA$_{950}$ in the grafting polymerisation solution may aid the complete elimination of protein binding. The protein recovery (inverse of amount adsorbed) reported herein yields similar values to both particulate and polymer monolith RAMs which range from 88-100% [8, 14, 19, 36].

The final performance qualifier of these adsorbents is analyte recovery; which is a critically important performance characteristic of miniaturised SPE. A comparative study of recovery was undertaken to benchmark the performance of the poly(DVB)-*g*-PEGMA$_{950}$ against the poly(DVB) adsorbent. Recovery of 50 ng mL^{-1} ibuprofen was determined for the two materials. The poly(DVB) offered an analyte recovery of 92% ± 0.30 compared to 78% ± 0.93 using poly(DVB)-*g*-PEGMA$_{950}$. The high recovery of ibuprofen indicates that despite the microporous structure of the poly(DVB) adsorbent the analyte interactions occur rapidly. Reduced analyte recovery was expected given the reduced breakthrough times seen in **Figure 4.6**. Regardless, of this small reduction in analyte recovery, 78% is still considered extremely high value for analyte recovery. This qualifies the poly(DVB)-*g*-PEGMA$_{950}$ as a highly suitable biocompatible RAM for miniaturised SPE.

At-line ESI-MS was employed to finalise the assessment of poly(DVB)-*g*-PEGMA$_{950}$ for the miniaturised SPE clean up of human plasma. By infusing the processed sample directly from the adsorbent bed into the ESI-MS using the at-line approach developed in Chapter 2 an impression of the effectiveness of the sample clean up can be obtained [26]. A diluted (20% v/v) plasma sample spiked with ibuprofen was processed using both the poly(DVB) and the poly(DVB)-*g*-PEGMA$_{950}$ adsorbents. The extracted ion

chromatogram of the elution profiles were compared between the poly(DVB) and the poly(DVB)-*g*-PEGMA$_{950}$ (**Figure 4.8**). To this end, the peak area of the ibuprofen elution profile from the poly(DVB)-*g*-PEGMA$_{950}$ was twice as large as the profile obtained using hydrophobic poly(DVB). Here we see that the poly(DVB) assay was crippled by the hydrophobic surface chemistry, the adsorbed protein matrix contaminants led to a dramatic reduction in assay sensitivity. The biocompatibility of the poly(DVB)-*g*-PEGMA$_{950}$ adsorbent has been clearly demonstrated for fast and efficient purification of analytes in highly complex biological samples.

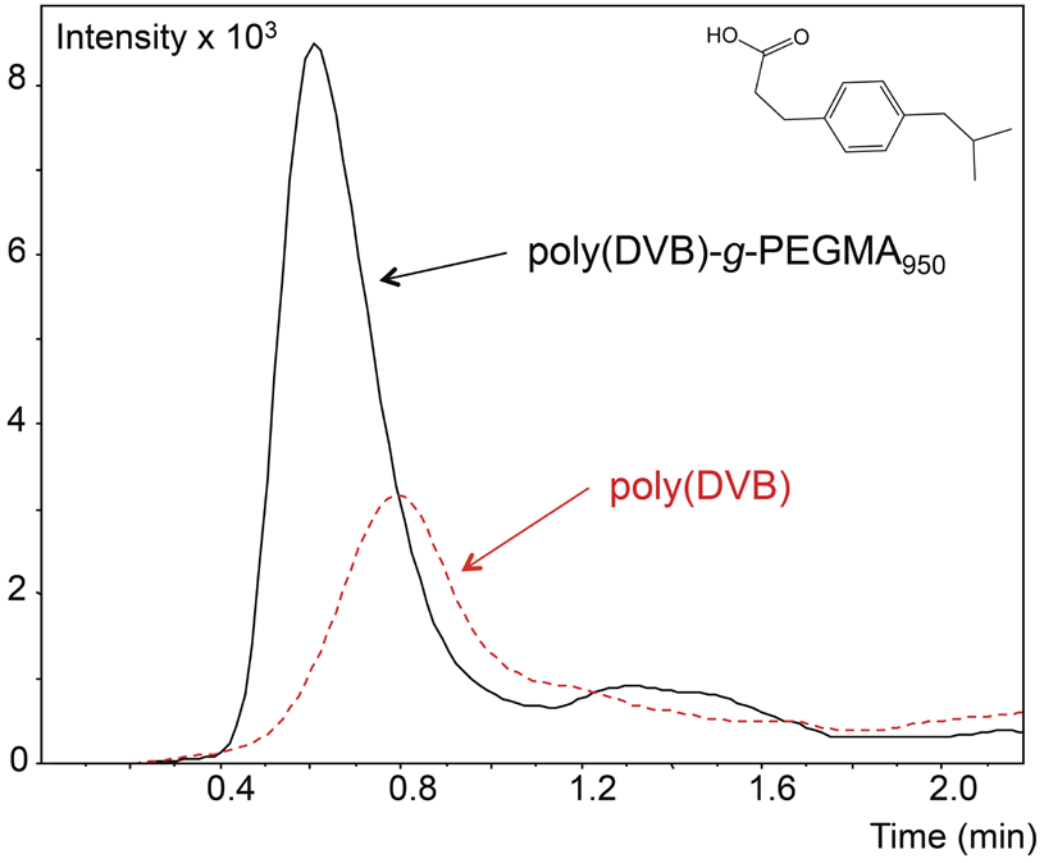

Figure 4.8. Comparison of sample clean up of ibuprofen (205 m/z) in a dilute plasma sample (20% v/v) using poly(DVB) and poly(DVB)-*g*-PEGMA$_{950}$ adsorbents. The processed samples were eluted directly from the adsorbent at-line into the ESI-MS (see Chapter 2). The extracted ion chromatogram of the poly(DVB)-*g*-PEGMA$_{950}$ is represented in black while poly(DVB) is in red.

4.4. Concluding remarks

A number of essential morphological criteria are necessary for miniaturised SPE. First, the adsorbent bed must be highly permeable to circumvent the backpressure limitations of the miniaturised device. Second, to achieve a highly sensitive assay the adsorbent bed must possess a large surface area for analyte interaction. The morphology of poly(DVB) polymer monoliths makes them highly appealing for miniaturised SPE. These adsorbents are both highly permeable and present a large surface area for analyte interaction. Despite the desirable morphological attributes of polymer monolith poly(DVB), use with highly complex biological samples can be problematic due to non-specific protein adsorption to the hydrophobic surface. To improve the suitability of poly(DVB) adsorbents for the preparation of biological samples the hydrophilic monomers $PEGMA_{360}$ and $PEGMA_{950}$ were crosslinked to the hydrophobic surface to provide a biocompatible RAMs.

It was essential to carefully evaluate the adsorbent performance for both poly(DVB)-*g*-$PEGMA_{360}$ and poly(DVB)-*g*-$PEGMA_{950}$ as a hydrophilic coating can be a double-edged sword. While the coating may prevent proteins from accessing the hydrophobic surface, it may also diminish the adsorbent's suitability for miniaturised SPE as longer time is required for the analyte to penetrate for interaction with the hydrophobic surface. Frontal analyses of anisole and ibuprofen were employed to compare the breakthrough curves of the two grafted adsorbents with the ungrafted precursor. Poly(DVB)-*g*-$PEGMA_{360}$ exhibited a shallow breakthrough curve which is not conducive with rapid miniaturised SPE workflows as it becomes necessary to optimise operational flow rates to achieve high analyte recoveries. The presence of the $PEGMA_{950}$ layer did not dramatically affect the adsorptive properties of the poly(DVB)-*g*-$PEGMA_{950}$, only a small reduction in hydrophobic capacity was observed and the analyte mass transfer

was not noticeable affected. It is demonstrated here that the poly(DVB)-*g*-PEGMA$_{950}$ adsorbent affords a high extraction performance independent to operational flow rate, which is a highly desirable characteristic of a miniaturised SPE adsorbent. Furthermore, protein adsorption was substantially restricted by the grafted a layer of PEGMA$_{950}$ qualifying that the poly(DVB)-*g*-PEGMA$_{950}$ is a high surface area biocompatible RAM exceedingly suited towards miniaturised SPE. The poly(DVB)-*g*-PEGMA$_{950}$ RAM was demonstrated to produce cleaner extracts for a more sensitive ESI-MS assay. The superiority of the poly(DVB)-*g*-PEGMA$_{950}$ adsorbent morphology is extremely beneficial for rapid and efficient miniaturised SPE purification of analytes in highly complex biological samples.

4.5 References

[1] Westerlund, D. *Chromatographia* 1987, *24*, 155–164.

[2] Annesley, T. M. *Clin. Chem.* 2003, *49*, 1041–1044.

[3] Li, Y., Lee, M. L. *J. Sep. Sci.* 2009, *32*, 3369–3378.

[4] Georgi, K., Boos, K. S. *LC GC Eur.* 2004, *17*, 21–24.

[5] Cassiano, N. M., Lima, V. V., Oliveira, R. V., de Pietro, A. C., Cass, Q. B. *Anal. Bioanal. Chem.* 2006, *384*, 1462–1469.

[6] Souverain, S., Rudaz, S., Veuthey, J.-L. *J. Chromatogr. B* 2004, *801*, 141–156.

[7] Unger, K. K. *Chromatographia* 1991, *31*, 507–511.

[8] Hagestam, I. H., Pinkerton, T. C. *Anal. Chem.* 1985, *57*, 1757–1763.

[9] Souverain, S., Rudaz, S., Veuthey, J.-L. *J. Chromatogr. B* 2004, *801*, 141–156.

[10] Cook, S. E., Pinkerton, T. C. *J. Chromatogr. A* 1986, *368*, 233–248.

[11] Boos, K.-S., Rudolphi, A., Vielhauer, S., Walfort, A., Lubda, D., Eisenbeiß, F. *Fresenius J. Anal. Chem.* 1995, *352*, 684–690.

[12] Gisch, D. J., Hunter, B. T., Feibush, B. *J. Chromatogr. A* 1988, *433*, 264–268.

[13] Kanda, T., Shirota, O., Ohtsu, Y., Yamaguchi, M. *J. Chromatogr. A* 1996, *722*, 115–121.

[14] Desilets, C. P., Rounds, M. A., Regnier, F. E. *J. Chromatogr. A* 1991, *544*, 25–39.

[15] Liska, I. *J. Chromatogr. A* 1993, *655*, 163–176.

[16] Svec, F., Tennikova, T. B., Deyl, Z. *Monolithic Materials*; Elsevier, 2003.

[17] Jarmalavičienė, R., Kornyšova, O., Westerlund, D., Maruška, A. *Anal. Bioanal. Chem.* 2003, *377*, 902–908.

[18] Jarmalavičienė, R., Szumski, M., Kornyšova, O., Kłodzińska, E., Westerlund, D., Krawczyk, S., Mickevičius, D., Buszewski, B., Maruška, A. *Electrophoresis* 2008, *29*, 1753–1760.

[19] Turson, M., Zhou, M., Jiang, P., Dong, X. *J. Sep. Sci.* 2011, *34*, 127–134.

[20] Sýkora, D., Peters, E. C., Svec, F. *Macromol. Mater. Eng.* 2000, *275*, 42–47.

[21] Lubbad, S. H., Buchmeiser, M. R. *J. Chromatogr. A* 2010, *1217*, 3223–3230.

[22] Buchmeiser, M. R. *Polymer* 2007, *48*, 2187–2198.

[23] Morcombe, C. R., Zilm, K. W. *J. Magn. Reson.* 2003, *162*, 479–486.

[24] Rohr, T., Hilder, E. F., Donovan, J. J., Svec, F., Frechet, J. M. *Macromolecules* 2003, *36*, 1677–1684.

[25] Tripp, J. A., Needham, T. P., Ripp, E. M., Konzman, B. G., Homnick, P. J. *React. Funct. Polym.* 2010, *70*, 414–418.

[26] Candish, E., Gooley, A., Wirth, H.-J., Dawes, P. A., Shellie, R. A., Hilder, E. F. *J. Sep. Sci.* 2012, *35*, 2399–2406.

[27] Smirnov, K. N., Dyatchkov, I. A., Telnov, M. V., Pirogov, A. V., Shpigun, O. A. *J. Chromatogr. A* 2011, *1218*, 5010–5019.

[28] Gu, B., Armenta, J. M., Lee, M. L. *J. Chromatogr. A* 2005, *1079*, 382–391.

[29] Krenkova, J., Lacher, N. A., Svec, F. *Anal. Chem.* 2009, *81*, 2004–2012.

[30] Stachowiak, T. B., Svec, F., Fréchet, J. M. J. *Chem. Mater.* 2006, *18*, 5950–5957.

[31] Barlow, K. J., Hao, X., Hughes, T. C., Hutt, O. E., Polyzos, A., Turner, K. A., Moad, G. *Polym. Chem.* 2014, *5*, 722–732.

[32] Peters, E. C., Svec, F., Fréchet, J. M. J., Viklund, C., Irgum, K. *Macromolecules* 1999, *32*, 6377–6379.

[33] Gaborieau, M., Nebhani, L., Graf, R., Barner, L., Barner-Kowollik, C. *Macromolecules* 2010, *43*, 3868–3875.

[34] Hubbard, K. L., Finch, J. A., Darling, G. D. *React. Funct. Polym.* 1999, *42*, 279–289.

[35] Jarmalavičienė, R., Kornyšova, O., Westerlund, D., Maruška, A. *Anal. Bioanal. Chem.* 2003, *377*, 902–908.

[36] Jarmalavičienė, R., Kornyšova, O., Bendokas, V., Westerlund, D., Buszewski, B., Maruška, A. *Anal. Bioanal. Chem.* 2008, *391*, 2323–2328.

[37] D'Sa, R. A., Meenan, B. J. *Langmuir* 2010, *26*, 1894–1903.

5. General conclusions and future perspectives

The following general conclusions summarise the main findings of this thesis exploring improved miniaturised solid phase extraction (SPE) technologies for rapid sample preparation assays.

5.1 Controlled directional flow miniaturised solid phase extraction

5.1.1 Conclusions

The inherent nature of the microextraction by packed sorbent (MEPS) dictates that both sample and solvent must pass the adsorbent twice. First, upon aspiration then again when the fluid is expelled from the syringe barrel. This bi-directional fluid flow was shown to be problematic for two reasons; first the analyte is diluted and mixed in the entire volume of elution solvent to yield a broad, unfocused elution band that subsequently leads to reduced assay sensitivity. Second, to dispense, the analyte must pass back through the adsorbent bed where normal partitioning equilibria dictates diminished recoveries and increased sample carryover. In the example demonstrated in this thesis the signal for MEPS carryover (second elution) of codeine was shown to be 65% of the first elution. Previous investigations into this technology have developed rigorous adsorbent wash protocols to solve this problem. This is an unfavourable solution as it necessitates lengthy optimisation protocols and introduces additional steps to the workflow, increasing the time required for sample preparation.

The alternative approach is to improve the MEPS technology to circumvent the bi-directional fluid flow path. A two-way valve was integrated into the barrel of the syringe to control the direction that fluid is introduced to the device. Sample and solvent could be apirated *via* a side arm into the syringe barrel then dispensed over the

adsorbent bed. In the modified approach, the fluid makes a single pass of the adsorbent bed. The advantage of controlled directional flow (CDF)-MEPS is that the sample can be eluted without dilution, which eliminates the need to optimise the elution volumes. The direct carryover of codeine was reduced from 65% for conventional MEPS to only 1% for CDF-MEPS, which removes the need for extensive wash cycles and aids in the realisation of rapid miniaturised SPE workflows. The CDF-MEPS technology was interfaced directly with electrospray ionisation mass spectrometry (ESI-MS). A rapid and sensitive analysis was accomplished, as sharp, concentrated sample bands were eluted directly from the adsorbent into the ESI-MS. The at-line ESI-MS analysis of a range of opiates and urinary codeine metabolites was demonstrated using CDF-MEPS. This demonstrated that the developed technology affords a flexible, fast and sensitive approach to screen for target analytes (existing over a dynamic concentration range) in biological matrices.

5.1.2 Future work

Traditional bi-directional miniaturised SPE devices necessitate a highly permeable bed to facilitate the aspiration of fluid. While dispensing fluid over an adsorbent bed is not generally problematic, fluid aspiration is challenging due to the restriction created by the adsorbent bed. Thus, traditional miniaturised SPE devices' are limited to short bed lengths and large particulate SPE adsorbents (in the order of 40-100 µm). The CDF valve removes these limitations as sample and solvent can be applied from above the adsorbent bed. CDF-MEPS format reveals exciting possibilities to further develop the device for more efficient sample preparation and at-line MS analysis. Preliminary work with a disposable format of CDF-MEPS highlights that packing the cartridge with smaller particles (3 - 20 µm) can deliver an increased assay sensitivity (**Figure 5.1**) [1]. In addition, longer bed lengths can also be investigated (2.5 mm – 100 mm). The

procedures and benefits of a "in-syringe separation" hyphenated directly with MS can be explored. A preliminary scoping study was undertaken for the at-line analysis of a tryptic digest of cytochrome c using a 100 mm long adsorbent bed (10 µm C18 particulate) (**Figure 5.2**). A crude separation that reduces peak overlap can result in a cleaner mass spectrum for increased assay sensitivity. However, the use of smaller particles and longer adsorption bed lengths uncovers additional operational/engineering challenges that must be addressed as increasing demand is placed on the syringe drivers to dispense fluid over a well-packed adsorbent bed.

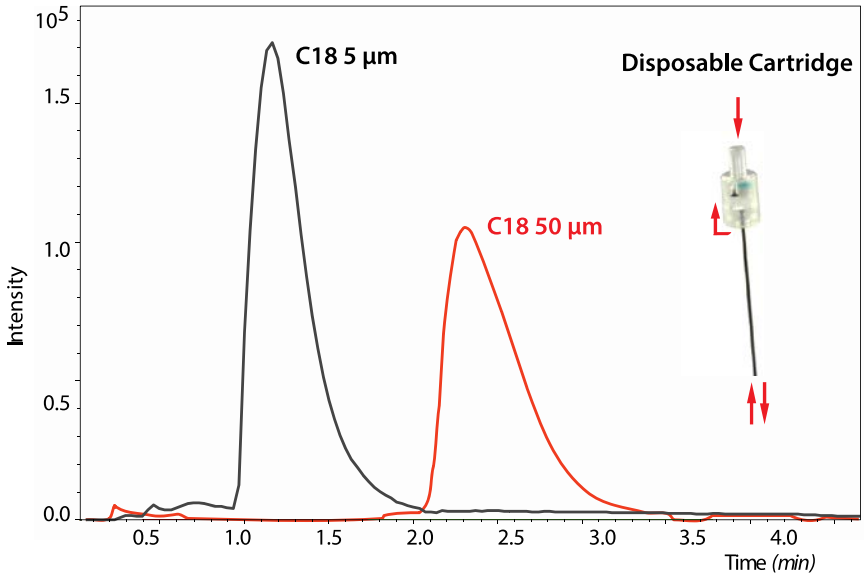

Figure 5.1. Extracted ion chromatogram of codeine-6-glucuronide in urine (10% v/v) prepared at-line with 5 µm C18 particles (black) and 50 µm C18 particles (red). Insert: Disposable SPE cartridge with an integrated CDF valve. The disposable format integrates the valve into the cartridge body, the restriction created by the adsorbent bed means fluid bypasses the bed on aspiration. During the dispense cycle the valve seals and liquid penetrates through the packed bed.

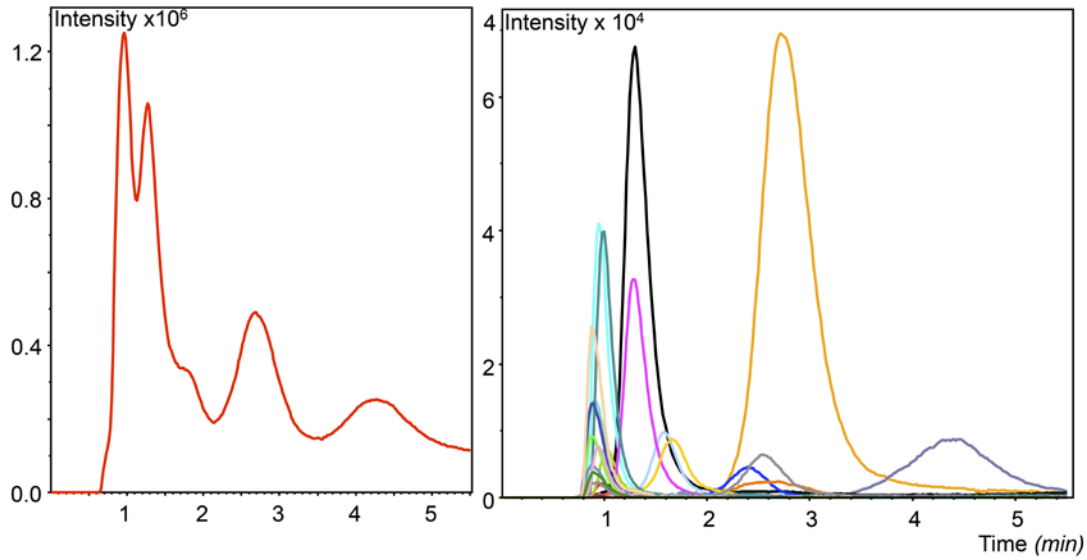

Figure 5.2. Right) The total ion chromatogram of an at-line elution of the tryptic peptides of cytochrome c eluted from the 100 mm long 10 µm C18 adsorbent bed with 40:60 methanol:water v/v. Left) The extracted ion chromatogram corresponding to the tryptic peptides of cytochrome c with zero and one missed cleavage.

Alternatively, coupling together MEPS adsorbent (2.5 mm) of complementing chemistries for a "two-dimensional" miniaturised SPE could provide a more efficient sample clean up. Fractions from the first extraction could be further purified on the second adsorbent bed. Exciting possibilities exist to explore the at-line MS analysis of drugs of abuse by coupling a strong cation exchange extraction with a hydrophobic extraction.

Finally, the rapid analysis and reduced solvent consumption of the CDF-MEPS approach represents a new era of sample preparation with the exciting capability of

coupling MEPS with miniaturised portable and fieldable MS technologies for point-of-collection analysis.

5.2 Polymer monoliths for solid phase extraction

5.2.1 Conclusions

Adsorbents for miniaturised SPE necessitate a number of essential morphological criteria; first the adsorbent bed must be highly permeable to circumvent any backpressure limitations of the device. Second, to achieve a highly sensitive assay the adsorbent bed must possess a large surface area for a high capacity of analyte interactions. Adsorbent fabricated from poly(divinyl benzene) (DVB) and hypercrosslinked poly(4-vinylbenzyl chloride-*co*-styrene -*co*-DVB) (VBC-*co*-Sty-*co*-DVB) displayed both a highly permeable macroporous structure with an enhanced quantity of micro- and mesopores. The permanent highly porous morphology of large surface area polymer monoliths made them highly appealing to investigate for SPE.

The polymeric microglobules possess non-porous highly crosslinked cores and any interactable surface of polymer monolith adsorbents was accessible by a small diffusion distance. Thus, the polymer monolith structure provides improved solute mass transfer kinetics. Both frontal analysis and off-line SPE with anisole and phenol as the probe analytes demonstrated the structural superiority of the poly(DVB) polymer monolith over a conventional 85 µm poly(Sty-*co*-DVB) particulate. As a result of the polymer monolith architecture the extraction efficiency of the poly(DVB) polymer monolith is largely independent of the operational flow rate. This is highly attractive as lengthy protocols to optimise operational flow rate to achieve a high analyte recovery can largely be eliminated. In contrast, the extraction performance of the 85 µm poly(Sty-*co*-

DVB) particulate adsorbent was found to be highly dependent on the flow rate of extraction, not conducive with rapid SPE workflows.

However, an in depth probing into the structure of large surface area polymer monoliths revealed some fundamental physical characteristics that could limit their suitability for SPE. In aqueous environments the surface structure is almost exclusively composed of micropores (< 2 nm). Therefore, the utility of large surface area polymer monoliths is limited to analytes that can penetrate these small pores. While analytes such as anisole and phenol could freely access the micropores, a size exclusion mechanism prevented the larger probe analyte, cortisone, from penetrating the microporous structure, as evident by the small analyte capacity.

The size exclusion mechanism of the poly(DVB) adsorbents was exploited to provide a selective extraction of low molecular weight analytes in complex biological matrices. Unfortunately, complex biological samples rich in proteins are problematic as proteins adsorb non-specifically on the hydrophobic surfaces. This fouls the adsorbent and complicates the “clean” processed sample. To improve the suitability of the poly(DVB) adsorbents for the preparation of protein rich biological samples the hydrophilic monomers poly(ethylene glycol) methacrylate M_n 360 ($PEGMA_{360}$) and poly(ethylene glycol) methylether methacrylate M_n 950 ($PEGMA_{950}$) were crosslinked to the pendant vinyl groups of the hydrophobic poly(DVB). These materials were investigated to assess their suitability as large surface area biocompatible adsorbent.

Careful optimisation of the hydrophilic layer was essential, this layer must prevent proteins fouling but must not diminish the hydrophobic capacity or reduce the efficiency of the interaction between the analyte and the hydrophobic surface. The

breakthrough curve of the poly(DVB)-*g*-PEGMA$_{360}$ demonstrated that a thick hydrophilic layer prevented rapid analyte mass transfer which is undesirable for miniaturised SPE. In contrast, the thin layer of the PEGMA$_{950}$ did not dramatically effect the hydrophobic adsorptive properties of the poly(DVB)-*g*-PEGMA$_{950}$, only a small reduction in hydrophobic capacity was observed for both anisole and ibuprofen. The poly(DVB)-*g*-PEGMA$_{950}$ was demonstrated to produce cleaner extracts for a more sensitive at-line ESI-MS assay. The superiority of the poly(DVB)-*g*-PEGMA$_{950}$ adsorbent provides a powerful tool to yield cleaner sample extracts for MS analysis.

5.2.2 Future work

This work highlights that there is still a considerable need to gain a broader understanding of polymer monolith morphologies to avoid assumptions of their suitability for SPE applications. Further work is necessary to gain a precise insight into the molecular weight limitations of large surface area polymer monoliths. A detailed assessment using aqueous inverse size exclusion chromatography (ISEC) would provide a greater understanding of these materials and assist with the further development of adsorbents for SPE. To date, little work has been undertaken to identify and optimise the exact characteristics of pore structure that could provide improved capacities for SPE.

The macroporous properties of the larger surface area polymer monolith are one of the simplest parameter that can be tuned to improve interactions between the adsorbent and the analyte. The design of miniaturised SPE devices often necessitate that the fluid is aspirated through the adsorbent bed. Thus the polymer monoliths investigated in this work were specifically explored because of their large macropores (> 5 µm). However, the adoption of the CDF syringe has removed this limitation enabling the fluid to be

aspirated directly into the barrel of the syringe and applied to the adsorbent bed from above. Scope now exists to explore polymer monoliths that present macropores over a broader range (as low as 0.5 µm). Tuning the porogenic solvent to favour solubilisation of the growing polymer chain will provide a larger number of smaller globules. This ultimately increases the surface area producing a greater number of interaction points for more efficient interactions between the analyte and the adsorbent as the sample is forced through the smaller macropores.

Developing polymer monoliths with improved mesoporous structural characteristics and a high density of functionality remains a practical challenge and innovation is required to drive this technology forward. Recent works by Zhang *et al.* and Sterchele *et al.* has described a refreshingly novel approach to synthesise polymer monoliths based on a ‘‘solvothermal’’ synthetic method. A polymerisation of poly(DVB) using a mixture of tetrahydrofuran and water as the porogenic solvent was undertaken at a relatively high polymerisation temperature (100°C) in an autoclave. The unusual polymerisation conditions led to materials with very high specific surface areas of 700 m^2 g^{-1} provided by mesopores of 22 nm [3, 4]. Exciting possibilities exist to investigate these materials and apply them as adsorbents for miniaturised SPE.

Further scope exists to investigate the thermal grafting of a variety of functional monomers to large surface area adsorbents. The possibility to extend this work to the thermal grafting of ion exchange monomers may facilitate the fabrication of mixed mode polymer monolith with possess both a high hydrophobic capacity *and* a high ion exchange capacity. In addition, a comprehensive study into PEGMA monomers with increasing glycol chain length could enable the complete elimination of protein fouling of hydrophobic surfaces.

Finally, these biocompatible polymer monolith restricted access adsorbents could provide an ideal structural morphology for the at-line MS analysis of drugs of abuse, particularly the low molecular weight amphetamines, methamphetamine and their structural analogs in biological fluids. Further investigation could assist in the realisation of miniaturised portable analytical laboratories for confirmatory road side drug testing.

5.3 References

[1] Candish, E., Gooley, A. A., Shellie, R. A., Hilder, E. F. *G.I.T. Laboratory Journal* 2012, *18*, 32–34.

[2] Candish. E. Hon, W. B., Gooley, A. A., Wirth, H-J., Shellie, R. A. & Hilder, E. F. *Microsample preparation devices for filtration, digestion and extraction of whole blood (poster presentation).* 62nd ASMS Conference on Mass Spectrometry and Allied Topics. Baltimore. USA. 2014.

[3] Zhang, Y., Wei, S., Liu, F., Du, Y., Liu, S., Ji, Y., Yokoi, T., Tatsumi, T., Xiao, F.-S. *Nano Today* 2009, *4*, 135–142.

[4] Sterchele, S., Centomo, P., Zecca, M., Hanková, L., Jerabek, K. *Microporous Mesoporous Mater.* 2014, *185*, 26–29.

Appendix

Appendix A

Table 1. The program for the digital analytical syringe for the digital at-line CDF-MEPS ESI-MSI workflow in Chapter 2

Step	Aspirate (µL)	Dispence (µL)	Speed (µL/min)	Valve Position
Condition				
Aspirate - Methanol	50		400	1
Dispense		50	400	1
Equilibrate				
Aspirate - Water	50		400	1
Dispense		50	400	1
Sample load				
Aspirate - Urine (10% v/v)	50		300	1
Dispense		50	300	1
Wash				
Aspirate - Water	50		400	1
Dispense		50	400	1
Elute				
Aspirate - Methanol	50		400	2
Dispense		50	20	1

*Note: All solvents and samples contained 0.1% v/v formic acid

Appendix

Appendix B

Table 2. The program for the digital analytical syringe for SPE workflow for HPLC analysis in Chapter 3 and 4.

Step	Aspirate (µL)	Dispence (µL)	Speed (µL/min)	Valve Position
Condition				
Aspirate - Methanol	100		3500	2
Dispense		100	1000 or 500	1
Equilibrate				
Aspirate - Water	100		3500	2
Dispense		100	1000 or 500	1
Sample load				
Aspirate – Aqueous solution	100		3500	2
Dispense		100	1000 or 500	1
Wash				
Aspirate - Water	100		3500	2
Dispense		100	1000 or 500	1
Elute				
Aspirate - Methanol	100		3500	2
Dispense		100	1000 or 500	1

Appendix

Appendix C

Table 3. Characteristics of hypercrosslinked poly(VBC-*co*-Sty-*co*-DVB) polymer monoliths in the dry state obtained from argon adsorption/desorption at 77K and mercury intrusion porosimetry

Adsorbent	**S_{BET} (m^2g^{-1})**	**$S_{Micropore}$ (m^2g^{-1})**	**Pore volume (cm^3g^{-1})**	**Micropore volume (cm^3g^{-1})**	**Macropore size (μm)**
Hypercrosslinked					
16% VBC	817	810	0.381	0.368	12
12% VBC	737	719	0.353	0.324	11
8% VBC	686	675	0.327	0.308	7

Appendix

Appendix D

Table 4. The program for the digital analytical syringe for the digital at-line CDF-MEPS ESI-MSI workflow in Chapter 4

Step	Aspirate (µL)	Dispence (µL)	Speed (µL/min)	Valve Position
Condition				
Aspirate - Acetonitrile	50		3500	1
Dispense		50	1000	1
Equilibrate				
Aspirate - Water	50		3500	1
Dispense		50	1000	1
Sample load				
Aspirate - Plasma (20% v/v)	50		3500	1
Dispense		50	1000	1
Wash				
Aspirate - Water	50		3500	1
Dispense		50	1000	1
Elute				
Aspirate - Acetonitrile	50		3500	2
Dispense		50	20	1

*Note: All solvents and samples contained 0.3% v/v ammonium hydroxide